

# Synthesis of Ammonium, Sodium, and Potassium Fluoroionophores

By

---

Katherine F. Dennen

A Thesis submitted to the Faculty of the  
WORCESTER POLYTECHNIC INSTITUTE

In partial fulfillment of the requirements for the  
Degree of Master of Science

In

Chemistry

September 6, 2002

Approved:

---

Dr. W. Grant McGimpsey, Advisor

---

Dr. James P. Dittami, Department Head

## Abstract

N-(1-methylpyrene) monoaza-15-crown-5 (**P5**), N-(1-methylpyrene) monoaza-18-crown-6 (**P6**), N-(9-anthryl-methyl) monoaza-15-crown-5 (**A5**), N-(9-anthryl-methyl) monoaza-18crown-6 (**A6**), were synthesized and tested as fluoroionophores for potassium and sodium cations. Upon metal ion complexation, fluorescence yields increased dramatically due to an internal photoinduced electron transfer quenching mechanism (an off-on fluorescence switch).

The results for these model compounds led to the design and synthesis of 1,3 alternate calixarene[4]arene-crown-5 (**I**) and bicyclic peptide (**V**). Calixarene **I** was synthesized and found to selectively complex potassium cations as predicted.

The design of bicyclic peptide **V** is directed toward the selective complexation of ammonium cations. The synthesis of **V** involved the preparation of an open chain hexapeptide consisting of two trityl-protected homoserine residues. Addition of an amino methyl pyrene across two homoserine residues was attempted by triflating the alcohols. The cyclization of the peptide ring is expedited to produce a basket-like structure that molecular modeling indicates should have improved selectivity over that of nonactin, the current industry standard.

## Acknowledgements

I would like to thank my Advisor, Dr. W. Grant McGimpsey, for his guidance over the past two years. Providing an enormous amount of support, patience, and concern for his students, I am very grateful for having been a part of this work group.

For their assistance with this project, I would also like to Dr. Stephen Weininger and Dr. James Dittami. Having an enormous amount of knowledge concerning synthetic organic chemistry, their time and effort was greatly appreciated.

Helping me in innumerable ways, I would like to thank Dr. Hubert Nienaber, John Benco, and Christopher Cooper. Over the past two years, they have taught me a great deal both in and out of the lab. Their time, guidance, and patience were truly appreciated.

I would like to thank my friends and colleagues Mustafa Guler, Ernesto Soto, Cheryl Nowak, Nantanit Wanichacheva, and Selman Yavuz. Getting to know all of them and spending time together in and out of the lab has been a great experience.

I'd like to acknowledge and thank Bayer Corporation for their financial support.

And, I'd also like to thank Susan Wade for helping me scan in all the data found in Appendix A.

## Table of Contents

ABSTRACT.....	1
ACKNOWLEDGEMENTS.....	2
TABLE OF CONTENTS.....	3
LIST OF FIGURES .....	4
LIST OF TABLES.....	6
INTRODUCTION .....	9
EXPERIMENTAL.....	19
I. GENERAL MATERIALS .....	19
II. GENERAL METHODS.....	19
III. SYNTHESIS.....	22
RESULTS AND DISCUSSION.....	36
I. AZA-CROWN-ETHERS.....	36
<i>i. Synthesis</i> .....	36
<i>ii. Photo-electron transfer (PET)</i> .....	38
<i>iii. Fluorescence Data</i> .....	39
II. 1,3 ALTERNATE CALIXARENE[4]ARENECROWN-5.....	46
<i>i. Synthesis</i> .....	46
<i>ii. Fluorescence Data</i> .....	47
<i>iii. Solvent Effects</i> .....	50
III. BICYCLIC PEPTIDE V.....	53
<i>i. Design of Synthetic Route</i> .....	53
<i>ii. Preliminary Synthesis</i> .....	56
<i>iii. Synthesis</i> .....	60
APPENDIX A.....	68
REFERENCES .....	89

## List of Figures

**Figure 1:** Model of photo-electron transfer (PET)

**Figure 2:** **A.** Structure of cryptand [2.2.2] **B.** Structure of supercryptand

**Figure 3:** Structure of Nonactin

**Figure 4:** 19-crown-6 ether with decalino subunits

**Figure 5:** Bicyclic peptide structures

**Figure 6:** Fluorescence emission spectra ( $\lambda_{\text{ex}}$  333 nm) of **P5**

**Figure 7:** Fluorescence area increase of **P5**

**Figure 8:** Fluorescence emission spectra ( $\lambda_{\text{ex}}$  333 nm) of **P6**

**Figure 9:** Fluorescence area increase of **P6**

**Figure 10:** Fluorescence emission spectra ( $\lambda_{\text{ex}}$  365 nm) of **A5**

**Figure 11:** Fluorescence area increase of **A5**

**Figure 12:** Fluorescence emission spectra ( $\lambda_{\text{ex}}$  365 nm) of **A6**

**Figure 13:** Fluorescence area increase of **A6**

**Figure 14:** 1,3 alternate calixarene[4]arene-crown-5

**Figure 15:** Fluorescence emission spectra ( $\lambda_{\text{ex}}$  355 nm) of **A6** in DCM

**Figure 16:** Fluorescence area increase of **A6** in DCM

**Figure 17:** Fluorescence emission spectra ( $\lambda_{\text{ex}}$  355 nm) of **I**

**Figure 18:** Open chain unprotected linear peptide

**Figure 18:** Delta fluorescence response to  $\text{K}^+$  of **I**

**Figure 19:** Cyclizations of Fmoc-L-Ser-OH

**Figure 20:** Structures of triflic chloride, triflic anhydride, and tosyl chloride

**Figure 21:** Structure of Bzl-L-Ser-OMe

## List of Schemes

**Scheme 1:** Enzymatic degradation of creatinine and urea

**Scheme 2:** Formation of 1-(Bromomethyl)pyrene

**Scheme 3:** Formation of N-(1-methylpyrene) monoaza-15-crown-5 (**P5**)

**Scheme 4:** Formation of N-(1-methylpyrene) monoaza-18-crown-6 (**P6**)

**Scheme 5:** Formation of N-(9-anthryl-methyl) monoaza-15-crown-5 (**A5**)

**Scheme 6:** Formation of N-(9-anthryl-methyl) monoaza-18-crown-6 (**A5**)

**Scheme 7:** Loading of 2-Chlorotrityl Chloride resin

**Scheme 8:** Deprotection of Fmoc-Ala-Resin

**Scheme 9:** Coupling of Fmoc-D-Hse-OH

**Scheme 10:** Cleavage of peptide from resin

**Scheme 11:** Deprotection of alcohols

**Scheme 12:** Triflation and pyrene addition

**Scheme 13:** Mechanism of pyrene addition to aza crown ether

**Scheme 14:** Retrosynthetic analysis of bicyclic peptide **V**

**Scheme 15:** Solid phase peptide coupling using PyBOP, HOBT, and DIPEA.

**Scheme 16:** 2-Chlorotrityl Chloride resin cleavage using 1% TFA in DCM

**Scheme 17:** Deprotection of alcohol using 1% TFA and 2.5 eq. TIS.

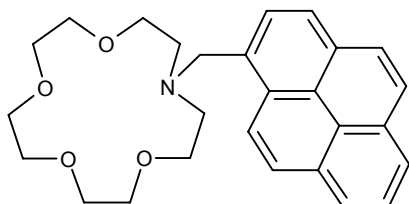
**Scheme 18:** Triflation and pyrene addition mechanism

## List of Tables

**Table 1:** Sample Concentrations of **P5, P6, A5, A6**, in 1:1 DCM:MeOH, **A6** in DCM, and each absorbance at the given wavelength of excitation

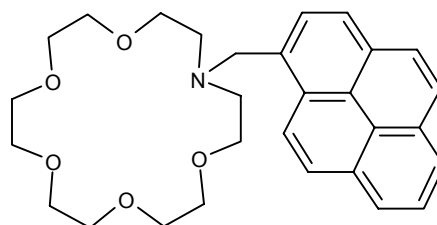
**Table 2:** Molar concentrations of host, base, and cation used for fluorescence testing are shown, along with the fluorescence enhancement, FE, which was calculated based on the increase in fluorescence areas upon cation addition.

## Summary of Compounds



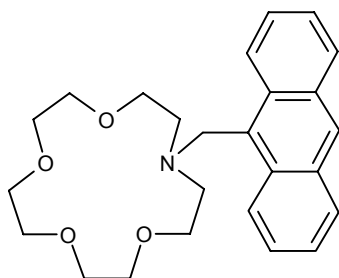
N-(1-methylpyrene) monoaza-15-crown-5

**(P5)**



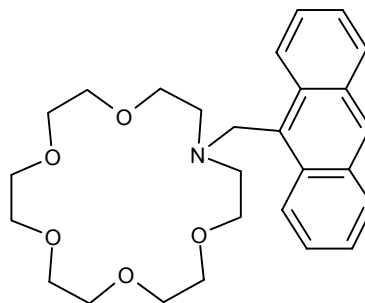
N-(1-methylpyrene) monoaza-18-crown-6

**(P6)**



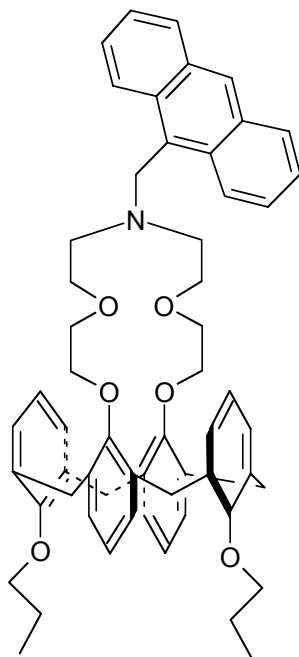
N-(9-anthrylmethyl) monoaza-18-crown-6

**(A5)**



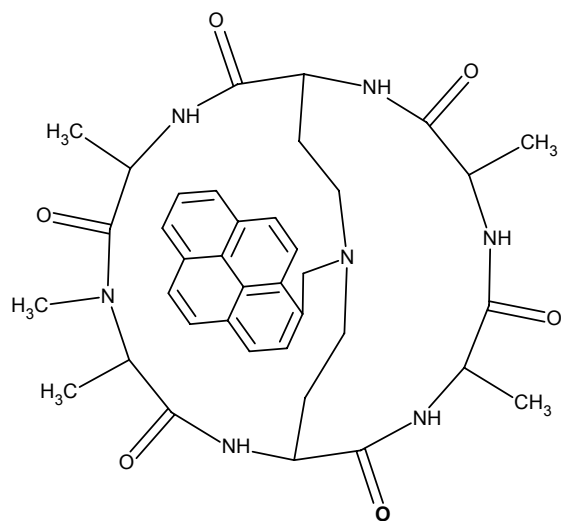
N-(9-anthrylmethyl) monoaza-15-crown-5

**(A6)**



1,3 alternate calixarene[4]arene-crown-5

(I)



*cyclo*-[L-Ala-D-Hse-L-MeAla-D-Ala-L-Hse-D-Ala]

(V)

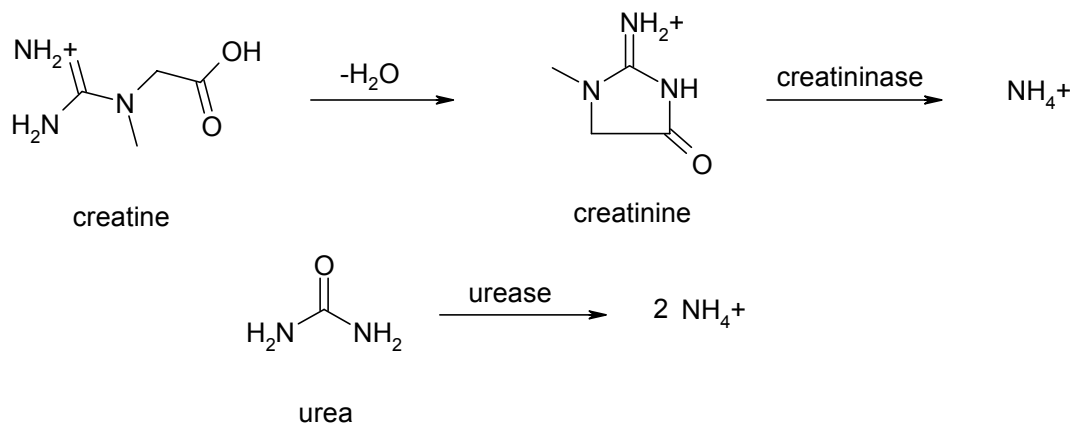
## Introduction

The focus of this research has been toward the synthesis of fluoroionophores for incorporation into bulk optodes for the detection of blood analyte concentrations, such as potassium and ammonium cations. Blood analyte concentrations are important in medical diagnoses because they can indicate problems within the body.<sup>1</sup> The design and synthesis of a fluoroionophore that changes optical properties upon complexation with certain analytes may provide a quick and cost effective method of reliably testing blood analyte concentrations.

Our research is directed toward the synthesis of various fluoroionophores that will ultimately lead to the fabrication of an optical sensor. Preliminary studies included the synthesis and fluorescence testing of four chromophore-containing aza-crown ether compounds, N-(1-methylpyrene) monoaza-15-crown-5, N-(1-methylpyrene) monoaza-18-crown-6, N-(9-anthryl-methyl) monoaza-15-crown-5, N-(9-anthryl-methyl) monoaza-18-crown-6, (**P5**, **P6**, **A5**, **A6**), respectively. These studies led to the novel synthesis of a calixarene covalently linked to an aza crown ether, 1,3 alternate calixarene[4]arene-crown-5, (**I**), that is N-substituted with a fluorescent anthracene group and is tailored for selective potassium complexation. This research has further led to the design and synthesis of bicyclic peptide **V**, which modeling indicates should have better selectivity for ammonium cations than the current industry standard, nonactin.

Biologically, the detection of ammonium cations is important because it is a metabolite of creatinine and urea. Concentrations of creatinine and urea present in the blood can give an indication of kidney, thyroid, and muscle function.<sup>2</sup> Since creatinine

and urea can both be enzymatically degraded into ammonium cation, (**Scheme 1**), bicyclic peptide **V** could potentially be used to test creatinine and urea concentrations.



**Scheme 1:** Enzymatic degradation of creatinine and urea

To synthesize a working fluoroionophore for the detection of cations, several factors were considered. Fluoroionophores should be highly sensitive and selectively complex the desired cation with a high equilibrium constant for complexation. Unwanted complexation with other cations can alter the optical properties of the fluoroionophore and in the process lower reliability of testing. Low sensitivity to the cation desired would also lower the accuracy of detection.

The selectivity of complexation of specific cations over others present is based in part on size-fit factors. The fluoroionophore must possess a sufficient cavity size to complex specific cations. If the cavity is too small, complexation may be impossible. Conversely, if it is too large, complexation may not occur. The electrostatics of the

fluoroionophore also effect the complexation. For complexation of cations to occur, negative charge densities must be present to interact with the positively charged cation.

To optically detect cation concentrations, the molecule must be able to participate in photo-induced electron transfer (PET). PET requires that an electron donor is able to travel to the fluorophore and thus quench fluorescence upon excitation.<sup>3</sup> Cation complexation at the donor site consequently prevents electron transfer, thereby eliminating fluorophore quenching, (as shown in **Figure 1**). This increase in fluorescence is proportional to the amount of complexation and therefore the concentration of cation present.

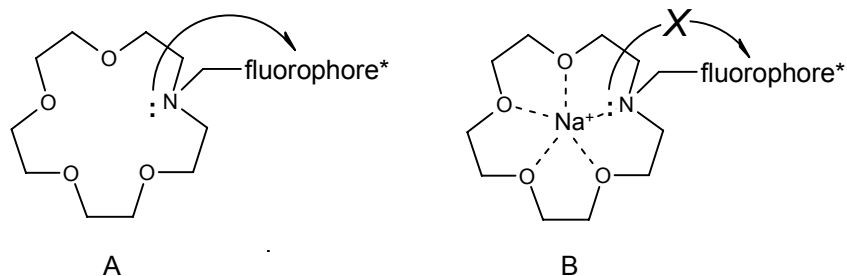


**Figure 1:** A) Model of photo-electron transfer (PET) of the amine lone pair to the excited fluorophore. B) Model of sodium cation complexation of amine lone pair to prevent PET to the fluorophore.

Due to their ability to participate in photoinduced electron transfer (PET), various aspects of N-substituted chromophores onto aza-crown-ether rings have been studied, such as pH dependence,<sup>4</sup> cation selectivity,<sup>5,6</sup> and spacer length effect on PET.<sup>7</sup> The ability of a molecule to signal cation complexation optically is particularly attractive

because this is a highly sensitive method of detection.<sup>3</sup> Yoshida *et. al.* have noted,<sup>8</sup> chromophore containing aza-crown ether compounds maintain their absorption and emission wavelengths and absorption intensity, while their fluorescence intensities are significantly altered upon cation complexation.<sup>1</sup>

Because photo-induced electron transfer (PET) occur over a distance of 10 Å,<sup>6</sup> research has been done by Hai-Feng *et. al.* to determine the magnitude of impact on sensitivity due to spacer length.<sup>7</sup> Pyrene-(CH<sub>2</sub>)<sub>n</sub>-aza-crown ether (n = 1-4) was used to study the effect of spacer length on PET.<sup>12</sup> Results of these studies indicate that maximum efficiency is achieved when n<3 CH<sub>2</sub> linkers,<sup>7</sup> and methyl linked pyrene aza-crown ether, n=1, was found to have higher selectivity for K<sup>+</sup> than all other cations. n=1 methyl linked pyrenyl-aza-crown-6 showed no response to high concentrations of Na<sup>+</sup>, unlike the anthryl substituted counterpart.<sup>9</sup>

Studies done on the effects that different chromophores have on cation complexation have been conducted by Kubo *et. al.*<sup>10</sup> Using an aza-crown-6 with various chromophores attached, this work demonstrated that the size and electronic properties of the aromatic pendants attached to the aza-crown nitrogen may contribute to the selectivity of the host toward metal cations.<sup>10</sup>

Chromophore-containing aza-crown ether compounds are an attractive model, as they complex cations that in turn effectively inhibit PET, thereby making them excellent cation concentration sensors. However, chromophore-containing aza-crown ether compounds do not selectively complex certain cations,<sup>9</sup> making them of little use in blood analyte testing. They also suffer pH dependence problems, where protonation of the amine mimics cation complexation at low pH. In some studies,

benzyltrimethylammonium hydroxide, (BTMAH), is employed to insure deprotonation of the amine.<sup>7,8</sup> To avoid this problem benzo-crown ethers have been used. In these systems, the alkoxy-substituted benzene ring is able to participate in PET rather than the amine. However, in some cases, using a benzo-crown ether lowers the overall fluorescence enhancement, FE, obtained, FE=15 vs. 47.<sup>3</sup>

To help increase crown selectivity, the use of crown ethers covalently-bound to calix[4]arenes have been studied extensively.<sup>11,12,13,14,15,16,17,18,19,20,21,22,23,24</sup> Reinhoudt et al. reported selective binding of potassium ions (relative to sodium or lithium) to calix[4]crown-5 structures, noting that the  $K^+/Na^+$  selectivity was dependent on the calix[4]crown conformation (i.e., cone, partial cone or 1,3-alternate).<sup>9,12</sup>

Since these early reports, studies have expanded to include benzocrown and azacrown structures and their selectivity and sensitivity for binding a wide variety of metal cations and their practical application as sensors. Dabestani et al. reported the synthesis and characterization of an *o*-benzocrown-6-calix[4]arene structure consisting of a 9-cyanoanthracenyl chromophore covalently-linked through a methylenic bridge to the benzo group.<sup>13,15,16</sup> This fluoroionophore acts as an on-off fluorescence switch that is triggered by ion complexation. In the absence of cation, the benzocrown group quenches the cyanoanthracenyl excited singlet state by electron transfer, while in the presence of complexed cation, the electrostatic field of the ion disrupts the electron transfer process. This particular system exhibited high sensitivity for  $Cs^+$  ion, important in the detection of radioactive contamination, and relatively good selectivity for  $Cs^+$  over other alkali metal ions. Similar structures make use of azacrown rings instead of benzocrowns,<sup>17,18,19,20,21,22,23</sup> presumably because the lower oxidation potential of the

amine relative to the benzo group allows greater flexibility in the selection of the fluorophore used in the system, i.e., the amine provides greater driving force for the electron transfer process. Kim et al.<sup>22</sup> have synthesized azacrown-5 calix[4]arenes where the nitrogen of the azacrown is substituted with benzyl or picolyl groups. In the picolyl systems, selectivity for  $\text{Ag}^+$  ions was found to be an order of magnitude higher than for other cations measured. The presence of the pyridinyl ring apparently contributes to the metal ion binding.

Based on the above, we have synthesized **I**, which combines the known optical response of anthryl azacrown-6 to  $\text{K}^+$ , with the expected enhanced selectivity provided by coupling the azacrown to a 1,3-alternate calix[4]arene. Fluorescence testing indicates increased selectivity for  $\text{K}^+$  over  $\text{Na}^+$  and a high sensitivity for  $\text{K}^+$  in the human physiological range.

Considered to be the three-dimensional equivalent of crown ethers, cryptands incorporate N as well as O atoms and show stronger complexation behavior than the crowns.<sup>25</sup> Spherical macrotricycles, also known as supercryptands, have four identical faces each being composed of an 18-membered ring connected at the nitrogen sites.<sup>26</sup>

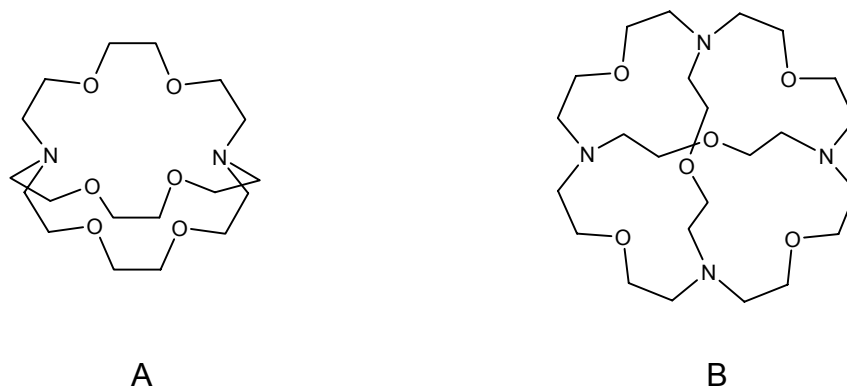


**Figure 2:** A) Structure of cryptand [2.2.2] B) Structure of supercryptand

The macrobicyclic ligand, cryptand [2.2.2], is known to complex with ammonium ions, but the spherical macrotricyclic, supercryptand, forms an even stronger complex.<sup>27</sup> Macrobicyclic ligand [2.2.2] is known to selectively bind  $K^+$  while the spherical macrotricyclic ligand selectively binds  $NH_4^+$ .<sup>27,28,29</sup> The  $NH_4^+ < K^+$  binding selectivity of cryptand [2,2,2] may be related to its O/N ratio and smaller cavity size. The  $K^+ < NH_4^+$  preference of the supercryptand results from a larger number of N sites, a larger cavity size and a tetrahedral arrangement of the four N sites.<sup>27,</sup>

Traditionally, nonactin, shown in **Figure 3**, a natural antibiotic agent, utilizes four ethereal and four carbonyl oxygen atoms to bind  $NH_4^+$ .<sup>30</sup> Because binding of ammonium cation to nonactin is coupled with a proton transport, the dynamic range can be varied by the adjustment of the pH of the ammonium solution. At pH 7, measurements can be achieved in the range from 0.1 to 10 mM ammonium ion.<sup>31</sup>

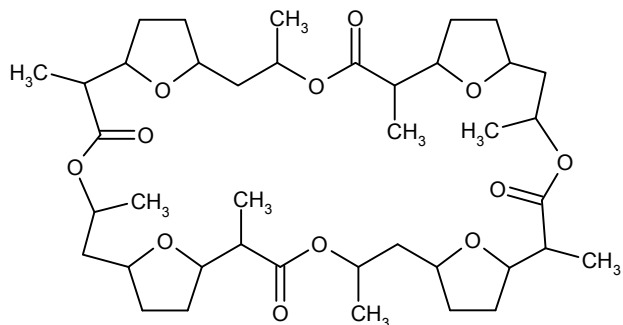


**Figure 3:** Structure of Nonactin

A novel ammonium ionophore that exhibits better selectivity than the natural antibiotic nonactin was successfully designed and synthesized based on a 19-membered crown compound having the decalino subunits in the macrocyclic system shown in **Figure 4**.<sup>32</sup> The use of bulky decalino groups has been employed to provide structure rigidity, and block the complexation of larger ions, while also increasing the lipophilicity of the ionophore molecule. The structural rigidity is thought to decrease the likelihood of complexing smaller ions such as  $\text{Li}^+$ ,  $\text{Na}^+$ , and even  $\text{K}^+$ , while the bulkiness of the groups prevents the complexation of larger ions such as  $\text{Rb}^+$  and  $\text{Cs}^+$ . The 19-membered crown was found to exhibit 10 times the selectivity over  $\text{K}^+$  and 3000 times the selectivity over  $\text{Na}^+$ , thereby making it more selective than nonactin.

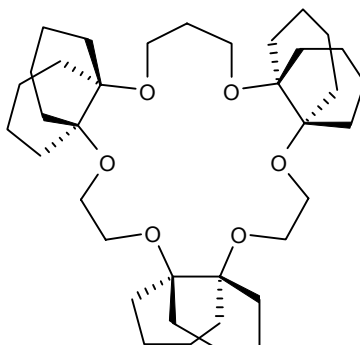


**Figure 4:** 19-crown-6 ether with decalino subunits

Several cyclic peptide systems have also been synthesized for ammonium complexation. Kunik et. al constructed a cyclic peptide composed of L-proline and three amino benzoic acids in an alternating sequence that was able to bind ammonium with stability constants between 11000 and 42000  $M^{-1}$  in chloroform.<sup>33</sup> Bicyclic peptide systems have also been synthesized. Zanotti et al. reported models of bicyclic peptides *cyclo*-(Glu<sup>1</sup>-Leu<sup>2</sup>-Pro<sup>3</sup>-Gly<sup>4</sup>-Ser<sup>5</sup>-Ile<sup>6</sup>-Pro<sup>7</sup>-Ala<sup>8</sup>)-*cyclo*(1-5 $\beta$ ) Phe<sup>9</sup>-Gly<sup>10</sup>, as well as (Glu<sup>1</sup>-X<sup>2</sup>-Pro<sup>3</sup>-Gly<sup>4</sup>-Lys<sup>5</sup>-X<sup>6</sup>-Pro<sup>7</sup>-Gly<sup>8</sup>)-*cyclo*(1 $\gamma$ -5 $\epsilon$ ) where X was Ala or Leu, respectively,<sup>34</sup> shown in **Figure 5**. The most significant deviation found in the ion-binding properties of X=Ala and X=Leu was the fact that stable Na<sup>+</sup>, K<sup>+</sup>, and Ba<sup>2+</sup> complexes were formed with X=Leu and not with X=Ala on the NMR time scale.<sup>35</sup> Another eight-membered bicyclic peptide, *cyclo*-(1,5- $\epsilon$ -succinoyl)(Lys-Gly-Gly-Gly)<sub>2</sub>, has been synthesized by Crusi, et al. demonstrating high selectivity for Sr<sup>2+</sup> cation.<sup>36</sup>

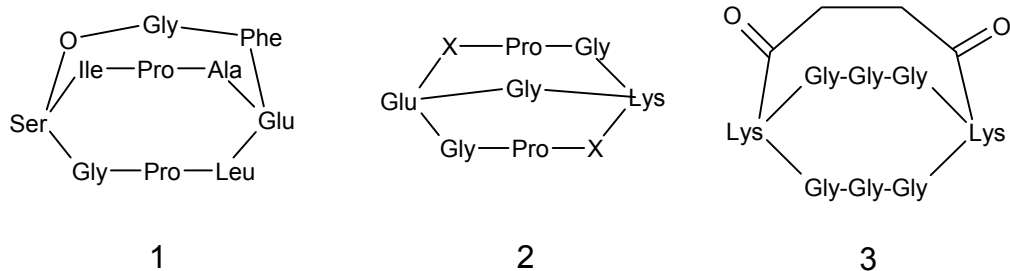


**Figure 5:** Bicyclic peptide structures

- 1)  $cyclo\text{-}(Glu^1\text{-}Leu^2\text{-}Pro^3\text{-}Gly^4\text{-}Ser^5\text{-}Ile^6\text{-}Pro^7\text{-}Ala^8)\text{-}cyclo(1\text{-}5\beta)\text{ Phe}^9\text{-}Gly^{10}$
- 2)  $cyclo\text{-}(Glu^1\text{-}X^2\text{-}Pro^3\text{-}Gly^4\text{-}Lys^5\text{-}X^6\text{-}Pro^7\text{-}Gly^8)\text{-}cyclo(1\gamma\text{-}5\epsilon)$  X = Ala or Leu
- 3)  $cyclo\text{-}(1,5\text{-}\epsilon\text{-succinoyl})(Lys\text{-}Gly\text{-}Gly\text{-}Gly)_2$

Based on these previous studies and on work from our laboratory on ammonium ion complexation<sup>37</sup>, we have designed and undertaken the synthesis of (**V**), a bicyclic peptide that is constructed of a main ring of the sequence  $cyclo\text{-}[L\text{-}Ala\text{-}D\text{-}Hse\text{-}L\text{-}MeAla\text{-}D\text{-}Ala\text{-}L\text{-}Hse\text{-}D\text{-}Ala]$ , with a pyrenyl-methyl-amine bridge across the two homoserine alcohols. Modeling has shown that bicyclic peptide **V** should exhibit high selectivity for ammonium cations.

# Experimental

## I. General Materials

All reagents were used as received without further purification. 1-aza-15-crown-5 (97%), 1-aza-18-crown-6 (95%), 9-chloroanthracene (96%), 1-pyrenemethanol (98%), phosphorus tribromide, benzyltrimethylammoniumhydroxide, potassium acetate, sodium acetate, triethylamine, piperidine, acetonitrile (anhydrous), trifluoromethanesulfonic anhydride, trifluoromethanesulfonic chloride, 1-pyrenemethylamine hydrochloride, ethanol, methanol, and ethyl acetate were all purchased from Aldrich Chemicals. 2-Chlorotriyl Chloride resin (1.0mmol/g loading) 200-400 mesh, 1%DVB, Fmoc-Ala-OH, Fmoc-D-Hse(Trt)-OH, Fmoc-MeAla-OH, Fmoc-D-Ala-OH, 1-hydroxybenzotriazole hydrate (HOBT), and PyBop were purchased from Nova Biochem. Fmoc-Hse(trt)-OH, tBoc-Ala-OH, and trifluoro-acetic acid were purchased from Advanced Chemtech. The Diisopropylethylamine was purchased from Avocado Research Chemicals Ltd; triisopropylsilane 99% from Acros; dimethylformamide from J.T. Baker; dichloromethane and hexane from VWR. Anhydrous magnesium sulfate was purchased from Mallinckrodt.

## II. General Methods

### i. NMR

Proton nuclear magnetic resonance ( $^1\text{H}$  NMR) spectra were obtained on a Bruker AVANCE 400 (400 MHz) NMR spectrometer. Chemical shifts are reported in ppm ( $\delta$ ).

Carbon nuclear magnetic resonance ( $^{13}\text{C}$  NMR) spectra were recorded at 100 MHz on the same instrument mentioned above.

*ii. UV-Visible Spectroscopy*

Ground state absorption spectra were measured in a quartz cuvette (1 cm x 1 cm) with a Shimadzu UV 2100 Spectrophotometer. Samples were measured in single beam mode and compared with a blank obtained with pure solvent. Extinction coefficients were calculated via Beer's law.

*iii. Infrared Spectroscopy*

Infrared spectra were obtained on a Perkin-Elmer Spectrum One FT-IR spectrometer supported in KBr (Aldrich, Standard IR Grade). Samples were prepared with an IR press of 13mm diameter (Z11,241-0) under 10 tons of pressure using a vacuum pump for 10 minutes.

*iv. Fluorescence Spectroscopy*

Fluorescence spectra were obtained at room temperature in a quartz cuvette (1 cm x 1 cm) in air saturated solvent using a Perkin-Elmer LS-50B Spectrofluorimeter.

*v. Mass Spectrometry*

Mass Spectra were performed by SYNPEP Corporation, Dublin, CA. The carrier solvent used was a mixture of  $\text{H}_2\text{O}$  and acetonitrile (1:1). The sample was ionized by

electrospray and injected using compressed air. The mass spectrometer used ultra-grade 5 nitrogen as a curtain gas.

vi. Thin Layer Chromatography (TLC)

Analytical TLC was performed using pre-coated silica gel plates (Whatman 200  $\mu\text{m}$  KCF18 silica gel 60A reverse phase plates or Whatman 250  $\mu\text{m}$  thickness KF6F silica gel 60A normal phase plates), which were illuminated by a UV lamp at 254 nm and 356 nm.

vii. Flash Chromatography

Flash chromatography was performed on a Biotage Flash 12i using KP-Sil 32-63  $\mu\text{m}$  60A silica gel under  $\text{N}_2$  pressure.

viii. Preparative Thin Layer Chromatography

Preparative TLC was performed using precoated silica gel plates (1000  $\mu\text{m}$  Whatman K6F silica gel 60A).

ix. Melting Point Apparatus

All melting points were obtained using a Fisher-Johns Melting point apparatus and are uncorrected.

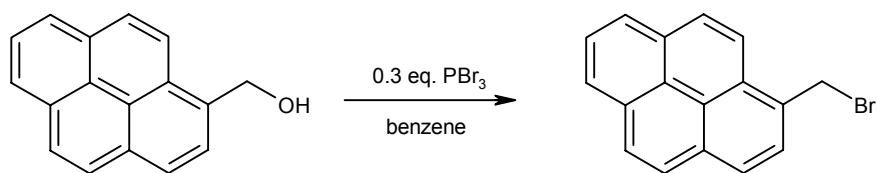
x. Computational studies

Molecular structures were minimized using a SGI 320 running Windows NT. All calculations were performed using the Molecular Operating Environment (MOE), version 2000.02 computing

package (Chemical Computing Group Inc., Montreal, Quebec, Canada.). Dynamics calculations on structures were heated to 400 K, equilibrated at 310 K and cooled to 290 K at a rate of 10 K/ps. The lowest energy structures obtained from these calculations were re-minimized. Electrostatic calculations were performed on these structures using default parameters.

### III. Synthesis

Synthetic details are provided below. All data cited can be found in Appendix A.



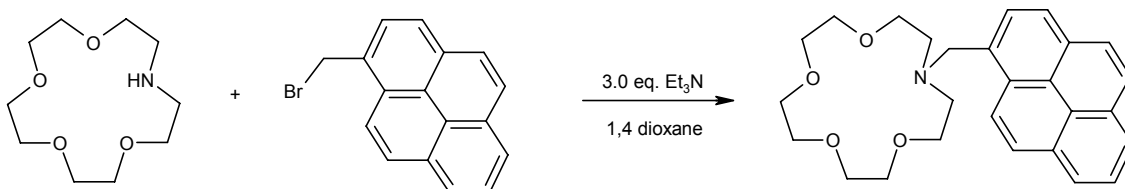
**Scheme 2:** Formation of 1-(Bromomethyl)pyrene

#### *1-(Bromomethyl)pyrene*

1-Pyrene methanol (4.500g, 1.94mmol) and PBr<sub>3</sub> (2.1g, 0.74mL) were refluxed in benzene (250mL) for 4 hrs. The reaction was followed with normal phase TLC with DCM as the mobile phase. The solution was extracted with a 3:2 diethyl ether: water (60mL: 40mL) mixture, rinsed with water twice, and dried over anhydrous sodium sulfate. The solvent was then removed under reduced pressure to yield 1-(bromomethyl)pyrene as a yellow solid (95.4% yield) (5.450g, 1.84mmol). <sup>1</sup>H NMR (CDCl<sub>3</sub>). δ 5.28 (s,

2H), 8.0-8.3 (m, 9H)  $^{13}\text{C}$  NMR ( $\text{CDCl}_3$ ).  $\delta$  32.205 ( $\text{CH}_2$ ), 122.818-131.963 (pyrene).

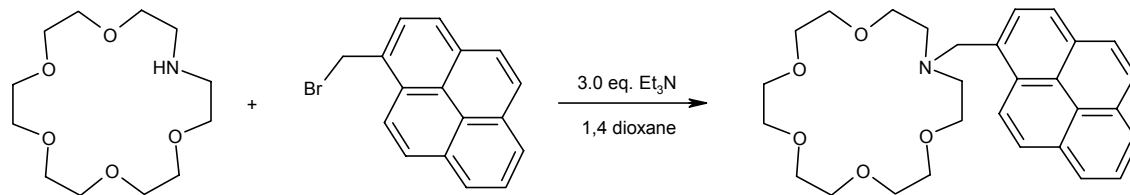
[Scheme 2]



**Scheme 3:** Formation of N-(1-methylpyrene) monoaza-15-crown-5 (**P5**)

*ii. N-(1-methylpyrene) monoaza-15-crown-5 (P5)*

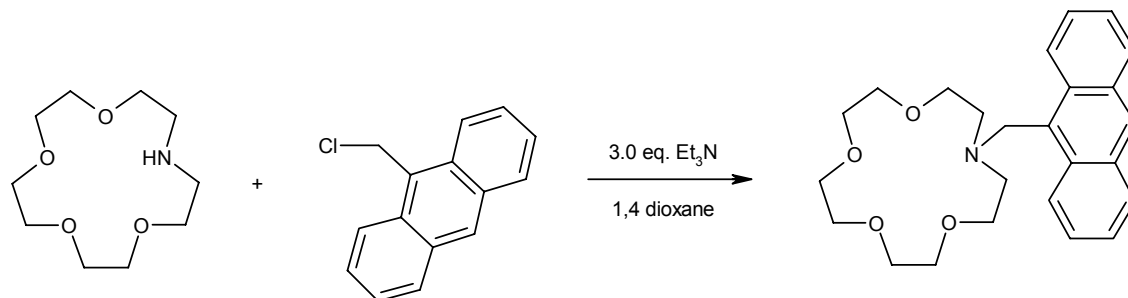
1-aza-18-crown-6 (0.464g, 2.1mmol), 1- (bromomethyl) pyrene (0.520g, 1.76mmol), and triethylamine (0.526g, 0.74mL) were refluxed in 1,4-dioxane (200mL) for 48 hrs. The solvent was evaporated, and the product extracted with  $\text{DCM}:\text{H}_2\text{O}$  (2:3). The organic phase was rinsed three times with water and then dried over anhydrous magnesium sulfate. The crude product was purified using prep-TLC plates in the absence of ambient light. ( $\text{DCM}:\text{EtOH}$  17:1 as eluent), to yield N-(1-methylpyrene) monoaza-15-crown-5 (0.412 g, 0.95mmol) as an oil (45.25% yield overall).  $R_f$  0.13  $\text{DCM}:\text{EtoAc}$  (17:1).  $^1\text{H}$  NMR ( $\text{CDCl}_3$ ).  $\delta$  8.1-7.9 (m, 9H), 4.3 (s, 2H), 3.7-3.5 (m, 20H), 2.9 (t, 4H).  $^{13}\text{C}$  NMR ( $\text{CDCl}_3$ ).  $\delta$  54.9 ( $\text{CH}_2$ ), 59.5 ( $\text{CH}_2$ ), 71.4-70.4 ( $\text{CH}_2$  crown), 133.6-123.8 (pyrene). MS  $m/z$  ( $\text{M}^+$ ) calcd. 434.54 found 434.2. [Scheme 3]



**Scheme 4:** Formation of N-(1-methylpyrene) monoaza-18-crown-6 (**P6**)

*iii. N-(1-methylpyrene) monoaza-18-crown-5 (P5)*

1-aza-18-crown-6 (0.553g, 2.10mmol), 1- (Bromomethyl) Pyrene (0.520g, 1.76mmol), and triethylamine (0.526g, 0.74mL) were refluxed in 1,4-dioxane (200mL) for 24 hrs. The solvent was evaporated, and the product extracted with DCM:H<sub>2</sub>O (2:3). The organic phase was rinsed three times with water and then dried over anhydrous magnesium sulfate. Further purification was done using preparative TLC in the absence of ambient light. (DCM:EtOH 17:1 as eluent), to yield N-(1-methylpyrene) monoaza-18-crown-6. (0.0601g, 0.138mmol) as an oil (6.8% yield overall). *R<sub>f</sub>* 0.03 DCM: EtOAc (17:1). <sup>1</sup>H NMR (CDCl<sub>3</sub>). δ 8.5-7.9 (m, 9H), 4.3 (s, 2H), 3.6-3.4 (m, 20H), 2.9 (t, 4H). <sup>13</sup>C NMR (CDCl<sub>3</sub>). δ 54.9 (CH<sub>2</sub>), 58.77 (CH<sub>2</sub>), 71.1-70.2 (CH<sub>2</sub> crown), 133.6-123.8 (pyrene). MS *m/z* (M<sup>+</sup>) calcd. with Na<sup>+</sup> 500.59 found 500.2. [**Scheme 4**]



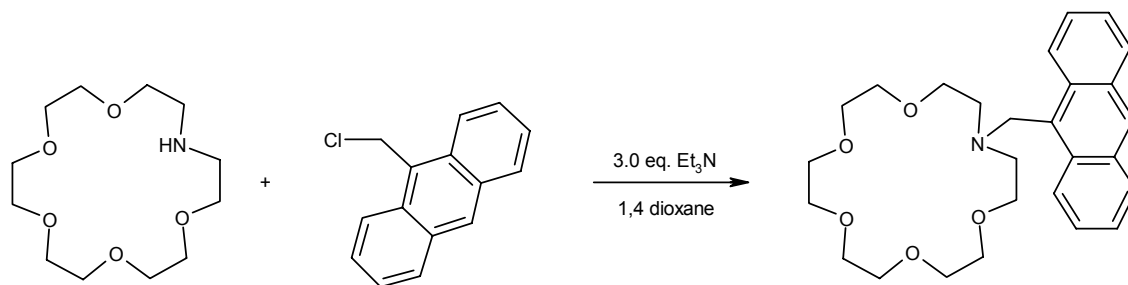
**Scheme 5:** Formation of N-(9-anthryl-methyl) monoaza-15-crown-5 (**A5**)

*iv. N-(9-anthryl-methyl) monoaza-15-crown-5 (A5)*

1-aza-15-crown-5 (0.464g, 2.10mmol), 9-chloromethylanthracene (0.400g, 1.76mmol), and triethylamine (0.526g, 0.74mL) were refluxed in 1,4-dioxane (200mL) for 48 hrs.

The solvent was evaporated, and the product extracted with DCM:H<sub>2</sub>O (2:3). The organic phase was rinsed three times with water and then dried over anhydrous magnesium sulfate. Further purification was done using preparative TLC in the absence of ambient light. (DCM:EtOH 17:1 as eluent), to yield N-(9-Anthryl-methyl) monoaza-15-crown-5 (0.440g, 1.07mmol) as yellow oil (60.8% yield overall). R<sub>f</sub> 0.03 DCM: EtoAc (17:1). <sup>1</sup>H NMR (CDCl<sub>3</sub>). δ 9.0-7.5 (m, 9H), 4.6 (s, 2H), 3.7-3.5 (m, 20H), 2.9 (t, 4H). <sup>13</sup>C NMR (CDCl<sub>3</sub>). δ 52.9 (CH<sub>2</sub>), 54.5 (CH<sub>2</sub>), 71.4-70.4 (CH<sub>2</sub> crown), 131.8-125.2 (anthryl).

[Scheme 5]



**Scheme 6:** Formation of *N*-(9-anthryl-methyl) monoaza-18-crown-6 (**A6**)

*v. N*-(9-anthryl-methyl) monoaza-18-crown-6 (**A6**)

1-aza-18-crown-6 (0.515g, 1.95mmol), 9-chloromethylanthracene (0.400g, 1.76mmol), and triethylamine (0.526g, 0.74mL) were refluxed in 1,4-dioxane (200mL) for 24 hrs.

The solvent was evaporated, and the product extracted with DCM:H<sub>2</sub>O (2:3). The organic phase was rinsed three times with water and dried over anhydrous magnesium sulfate.

Further purification was done using preparative TLC in the absence of ambient light.

(DCM:EtOH 17:1 as eluent), to yield *N*-(9-anthryl-methyl) monoaza-18-crown-6

(0.176g, 0.388mmol). The product was then recrystallized with dichloromethane and ether

to yield a yellow solid (22% yield overall). mp.80°-82°C, *R*<sub>f</sub>0.05 DCM: EtoAc (17:1).

<sup>1</sup>H NMR (CDCl<sub>3</sub>). δ 8.6-7.4 (m, 9H), 4.6 (s, 2H), 3.7-3.5 (m, 20H), 2.9 (t, 4H). <sup>13</sup>C NMR

(CDCl<sub>3</sub>). δ 52.4 (CH<sub>2</sub>), 54.3 (CH<sub>2</sub>), 71.3-70.6 (CH<sub>2</sub> crown), 131.8-124.8 (anthryl). MS

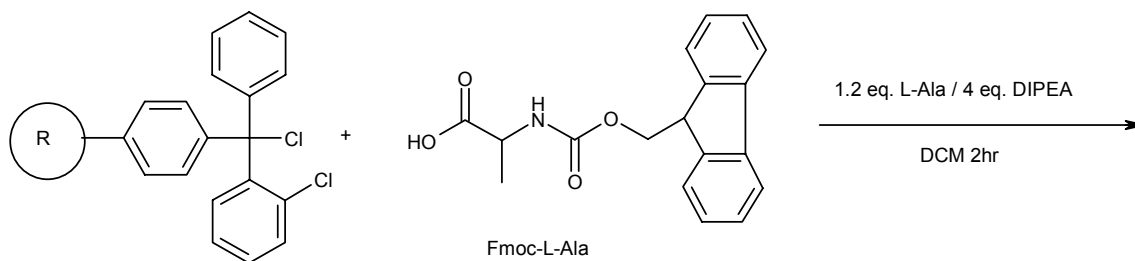
*m/z* (M<sup>+</sup>) calcd. 454.54 found 454.2. [**Scheme 6**]

vi. Synthesis of 1,3 alternate calixarene[4]arene-crown-5 (I)

The synthesis of 1,3 alternate calixarene[4]arene-crown-5 was done by Dr. Hubert Nienaber and the experimental detail can be found in reference 13.<sup>38</sup>

vii. Synthesis of bicyclic peptide (V)

The synthetic pathway used toward the construction of bicyclic peptide V is shown below. An Fmoc solid phase synthesis using a 2-Chlorotrityl Chloride resin was employed along with an N-terminus tBoc protecting group and trityl protected homoserine residues. Upon cleavage, the trityl groups, located on the homoserine side chains, were removed and cyclization of the side chains attempted.

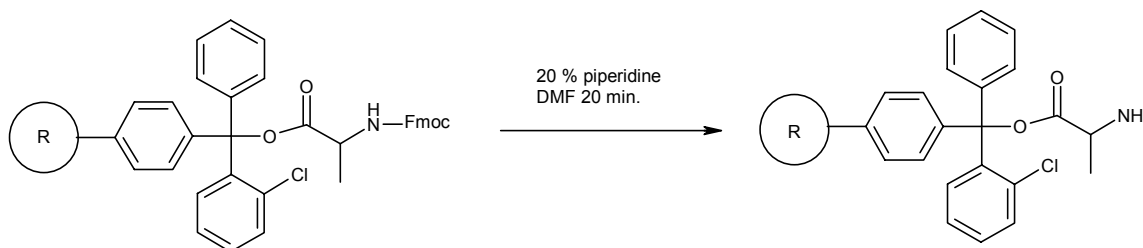


**Scheme 7:** Loading of 2-Chlorotrityl chloride resin

vi. Loading Resin

2-Chlorotrityl Chloride resin (1.0mmol/g, 4.600g) was swelled in a peptide synthesizer (100mL) for 3 minutes by bubbling N<sub>2</sub> through dry DCM. 1.2 eq. of Fmoc-Ala-OH (1.718g, 5.52mmol) and 4.0 eq. of DIPEA (3.21mL, 18.40mmol) were dissolved in dry

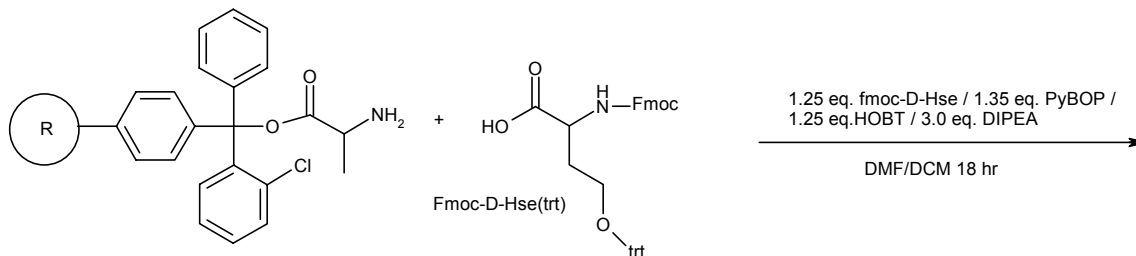
DCM (60mL) and added to the resin. After 2 hours, the mixture was drained and rinsed 2x with 25mL of DCM:MeOH:DIPEA (17:2:1), 3x DCM, 3x DMF, 2x DCM. [Scheme 7]



**Scheme 8:** Deprotection of Fmoc-Ala-Resin

vii. Deprotection of Fmoc-Ala-Resin

The Fmoc-Ala-Resin was deprotected with 20% piperidine in DCM for 20 minutes. The resin was shrunk and reswelled to remove all reagents by rinsing 2x with 40mL DCM, 3x MeOH, 2x EtOH, 3x DCM. A negative Kaiser test was obtained, indicating free amine was present. The Kaiser test was prepared by mixing 2 drops of each solution with the resin and then heating in the oven for 3-5 minutes. The solutions were prepared as indicated in Nova Biochem by: dissolving 5g of ninhydrin in 100mL ethanol; dissolving 80g of liquefied phenol in 20mL ethanol; adding 2mL of a 0.001M aqueous solution of potassium cyanide to 98mL pyridine. A positive test indicates free amine by the presence of blue beads. [Scheme 8]



**Scheme 9:** Coupling of Fmoc-D-Hse-OH

*viii. Coupling Fmoc-D-Hse-OH*

1.25 eq. of Fmoc-D-Hse-OH (3.356g, 5.75mmol), 1.25 eq. HOBT (0.777g, 5.75mmol), 1.35 eq. PyBop (3.231g, 6.21mmol), and 2.5 eq. DIPEA (2.00mL, 11.50mmol) were dissolved in 40mL of DMF and added to the resin-Ala-NH<sub>2</sub>. DCM (40mL) was then added to the peptide synthesizer to facilitate solvation and the reaction was carried out over night. The mixture was then drained and rinsed 2x with 40mL DCM, 3x MeOH, 2x EtOH, and 3x DCM. A positive Kaiser test was obtained, indicating the absence of amine. [Scheme 9]

*ix. Coupling Fmoc-MeAla-OH*

The Fmoc-D-Hse-Ala-resin was deprotected via the procedure above. 1.5 eq. of Fmoc-MeAla-OH (2.245g, 6.90mmol), 1.5 eq. HOBT (0.932g, 6.90mmol), 1.6 eq. PyBop (3.829g, 7.36mmol), and 2.5 eq. DIPEA (2.40mL, 13.80mmol) were dissolved in 40mL of DMF and added to the resin-Ala-D-Hse-NH<sub>2</sub>. DCM (40mL) was then added to the peptide synthesizer to facilitate solvation and the reaction continued for 5 hours. A seemingly positive Kaiser test was obtained 2x, so the mixture was then drained and

rinsed 2x with 40mL DCM, 3x MeOH, 2x EtOH, and 3x DCM and the coupling repeated with 0.3 eq of Fmoc-MeAla-OH (0.440g, 1.35mmol), 0.3 eq. HOBT (0.182g, 1.35mmol), 1.6 eq. PyBop (0.702g, 1.51mmol), and 0.6 eq. DIPEA (0.47mL, 2.70mmol) were dissolved in 40mL DCM and DMF for 4 hours. A positive Kaiser test was obtained.

*x. Coupling Fmoc-D-Ala-OH*

The Fmoc-MeAla-D-Hse-Ala-resin was deprotected via the procedure above. 1.5 eq. of Fmoc-Ala-OH (2.148g, 6.90mmol), 1.5 eq. HOBT (0.932g, 6.90mmol), 1.6 eq. PyBop (3.829g, 7.36mmol), and 2.5 eq. DIPEA (2.40mL, 13.80mmol) were dissolved in 40mL of DMF and added to the resin-Ala-D-Hse-MeAla-NH<sub>2</sub>. DCM (40mL) was then added to the peptide synthesizer to facilitate solvation and the reaction carried out for 6 hours. The mixture was then drained and rinsed 2x with 40mL DCM, 2x MeOH, 1x EtOH, 2x DCM. No reliable secondary amine test was found, so the coupling was repeated with 0.8 eq. of Fmoc-Ala-OH (1.145g, 3.68mmol), 0.8 eq. HOBT (0.497g, 3.68mmol), 0.9 eq. PyBop (2.154g, 4.12mmol), and 1.6 eq. DIPEA (1.28mL, 7.36mmol) to insure complete coupling. The mixture was then drained and rinsed 2x with 40mL DCM, 3x MeOH, 2x EtOH, 3x DCM.

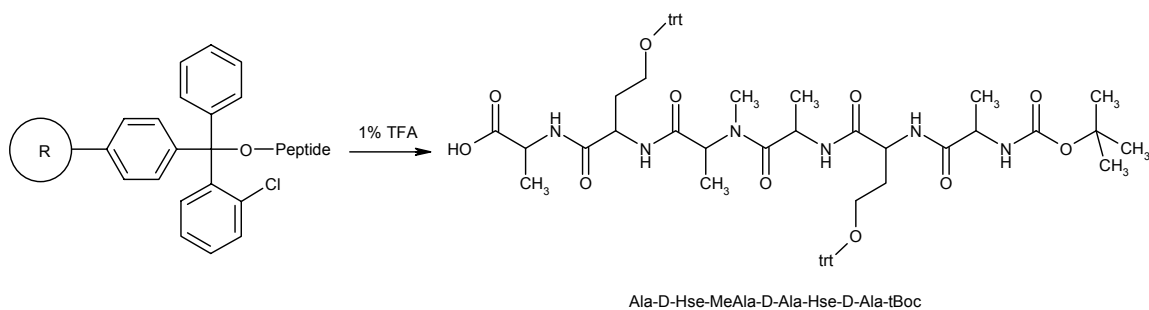
*xi. Coupling Fmoc-Hse-OH*

The Fmoc-D-Ala-MeAla-D-Hse-Ala-resin was deprotected via the procedure above. 1.25 eq. of Fmoc-Hse-OH (3.356g, 5.75mmol), 1.25 eq. HOBT (0.777g, 5.75mmol), 1.35 eq. PyBop (3.231g, 6.21mmol), and 2.5 eq. DIPEA (2.00mL, 11.50mmol) were dissolved in 40mL of DMF and added to the resin-Ala-D-Hse-MeAla-D-Ala-NH<sub>2</sub>. DCM (40mL) was

then added to the peptide synthesizer to facilitate solvation and the reaction was continued for 4 hours. The mixture was then drained and rinsed 2x with 40mL DCM, 3x MeOH, 2x EtOH, and 3x DCM. A positive Kaiser test was obtained, indicating the absence of amine.

### xii. Coupling *t*Boc-Ala-OH

The Fmoc-Hse-D-Ala-MeAla-D-Hse-Ala-resin was deprotected via the procedure above. 1.50eq. *t*Boc-Ala-OH (1.305g, 6.90mmol), 1.5 eq. HOBT (0.932g, 6.90mmol), 1.6 eq. PyBop (3.829g, 7.36mmol), and 2.5 eq. DIPEA (2.40mL, 13.80mmol) were dissolved in 40mL of DMF and added to the resin-Ala-D-Hse-MeAla-NH<sub>2</sub>. DCM (40mL) was then added to the peptide synthesizer to facilitate solvation and the reaction carried out for 3 1/2 hours. The mixture was then drained and rinsed 2x with 40mL DCM, 3x MeOH, 2x EtOH, and 2x MeOH. A positive Kaiser test was obtained, indicating the absence of amine.

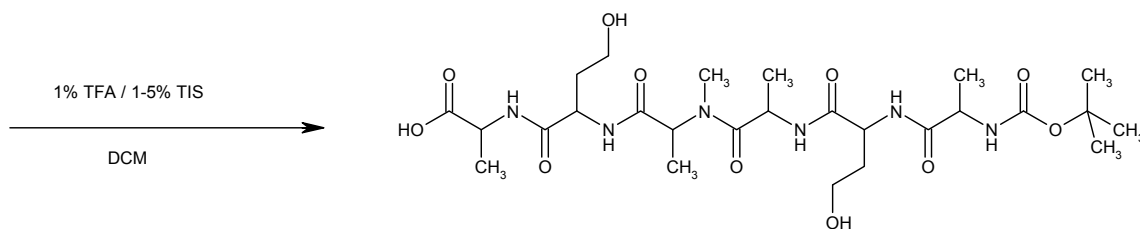


**Scheme 10:** Cleavage of peptide from resin

### xiii. Peptide Cleavage

The shrunken resin was dried using N<sub>2</sub> and cleaved in fractions with 1%TFA in DCM (250mL total) in the peptide synthesizer. The cleavage solution (~42mL) was bubbled

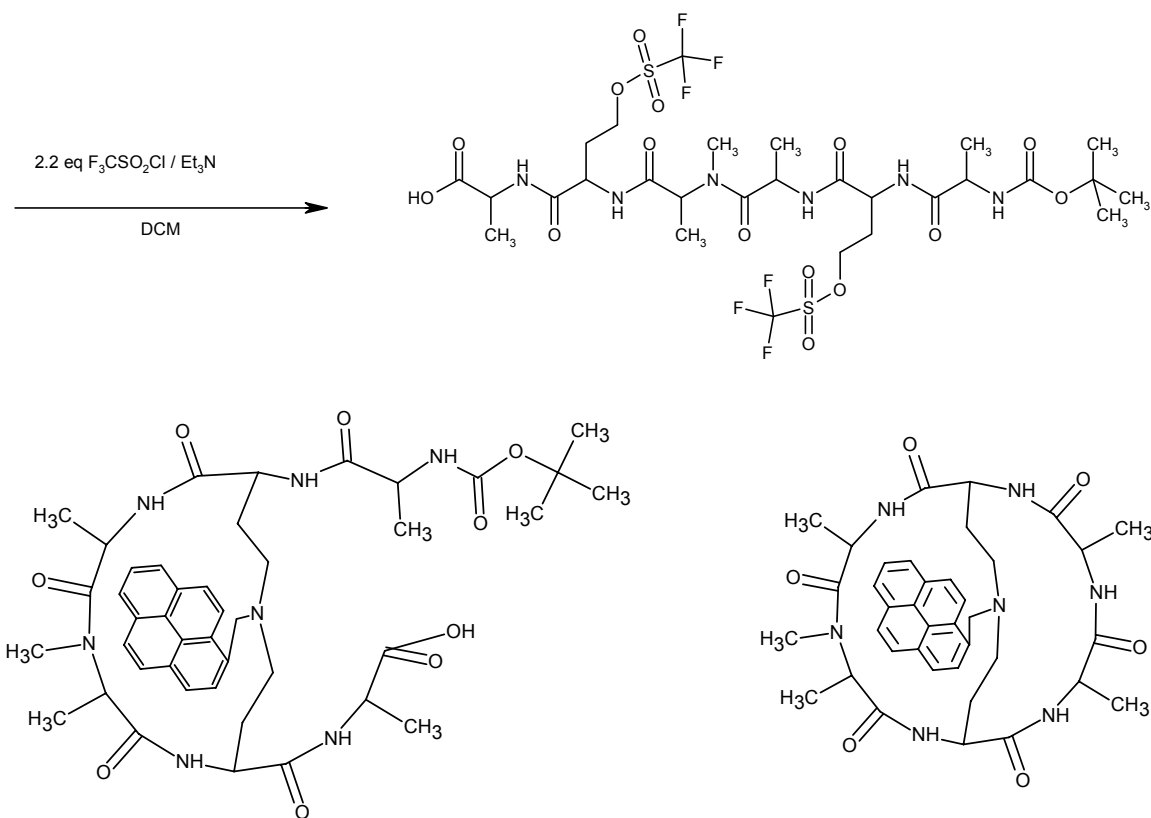
with N<sub>2</sub> for 5 minutes, drained into 10% pyridine in methanol (4.3mL), and collected separately in six 50mL Erlenmeyer flasks. Equivalent molar amounts of TFA and pyridine were used to minimize the amount of excess acid and base. The peptide was then bubbled and rinsed with DCM and MeOH and collected separately. Fractions 1-8 were spotted on a normal phase TLC plate using EtoAc:MeOH (3:1) as an eluent. Fractions 1 and 2 were placed in a 250mL round bottom flask and evaporated to ~5%. Distilled water was added, and the solution was adjusted to a pH of ~7 using pyridine to precipitate the peptide as a white solid (2.100g, 1.90mmol). Fractions 3-8 were combined in a 500mL round bottom flask and evaporated to ~5%. Distilled H<sub>2</sub>O was added and the solution determined to have a pH of ~1; pyridine was added to adjust the pH to ~7 to precipitate the peptide (0.400g, 0.36mmol). mp.72°-74°C, Rf0.43 DCM:MeOH (10:1) (with 2 drops base-piperidine). <sup>1</sup>H NMR (CDCl<sub>3</sub>). δ 9.5-9.4 (**m**, COOH), 8.6 (**s**, 6NH), 7.9-7.2 (**m**, 30H trityl), 4.0-4.6 (**m**, 6CH), 3.1-2.9 (**m**, 1CH<sub>3</sub>N), 2.3-1.8 (**t**, 2CH<sub>2</sub>OH), 1.4-1.2 (**t**, 7CH<sub>3</sub>+2CH<sub>2</sub>). <sup>13</sup>C NMR (CDCl<sub>3</sub>). δ 13.6 (CH<sub>3</sub>), 28.2 (t<sub>boc</sub>-CH<sub>3</sub>), 48.3 (NCH<sub>3</sub>), 53.4 (CH<sub>2</sub>), 59.3 (CH<sub>2</sub>), 86.9-86.4 (CH), 128.6-126.7 (CH trityl), 147.0-143.8 (3C), 155.7 (CONH), 171.5 (COOH) 175.0-173.3 (CO). <sup>135</sup>C NMR (CDCl<sub>3</sub>). δ 14.6 (CH<sub>3</sub>), 29.3 (t<sub>boc</sub>-CH<sub>3</sub>), 53.0 (NCH<sub>3</sub>), 54.5 (CH<sub>2</sub>), 60.0 (CH<sub>2</sub>), 129.7-128.0 (CH trityl), 130.9 (CONH), 146.4-141.6 (COOH). MS *m/z* (M<sup>+</sup>) with Na<sup>+</sup> calcd. 1126.29 found 1126.462. [**Scheme 10**]



**Scheme 11:** Deprotection of alcohols

*xiv. Deprotection of Alcohols*

The protected linear peptide (2.020g, 1.83mmol) was dissolved in 50mL of DCM:TIS:TFA (48:1.5:0.5) for 10 minutes forming a light yellow solution. All solvents were evaporated to yield a slightly crystalline light yellow oil. The trityl groups were precipitated using MeOH. The final amount of trityl groups removed by column chromatography using Hexane:EtoAc (1:1) as eluent and the peptide rinsed through using MeOH to obtain a white solid (1.121g, 1.82mmol) in a 99.4% yield. mp.54°-56°C, R<sub>f</sub> 0.14 EtoAc:DCM:MeOH (2:1:1). <sup>1</sup>H NMR (MeOD). δ 7.4-7.3 (m, 6NH), 3.08-3.07 (s, 2CH<sub>2</sub>OH), 2.9-2.8 (m, 1CH<sub>3</sub>N), 2.5-2.9 (t, 2CH<sub>2</sub>), 1.3-1.0 (t, 7CH<sub>3</sub>). <sup>13</sup>C NMR (MEOD). δ 14.6 (CH<sub>3</sub>), 28.2 (t-boc-CH<sub>3</sub>), 52.4 (CH<sub>2</sub>), 35.7 (CH<sub>2</sub>), 81.1 (CH), 158.3 (CONH), 163.3 (COOH) 176.9-172.7 (CO). <sup>135</sup>C NMR (MeOD). δ 14.6 (CH<sub>3</sub>), 29.2 (t-boc-CH<sub>3</sub>), 53.1 (NCH<sub>3</sub>), 35.5 (CH<sub>2</sub>), 58.0 (CH<sub>2</sub>), 130.9 (CONH). MS *m/z* (M<sup>+</sup>) with Na<sup>+</sup> calcd. 641.66 found 641.32. [Scheme 11]



**Scheme 12:** Triflation and pyrene addition

*xv. Triflation and pyrene addition*

Linear peptide (0.238g, 0.38mmol) and  $\text{Et}_3\text{N}$  (0.18mL, 1.29mmol) were dissolved in 150mL of acetonitrile and cooled to  $0^\circ \text{C}$ . Triflic chloride (.10mL, 0.915mmol) was added dropwise while stirring and then allowed to warm to room temperature for 1 hour. The orange solution was evaporated to yield a yellow oil.

1-Pyrenemethylamine hydrochloride was washed with DCM and 2N NaOH to extract 1-pyrenemethylamine into the organic layer. The organic layer was then dried, and 1-pyrenemethylamine (0.088g, 0.34mmol) was dissolved in acetonitrile with  $\text{Et}_3\text{N}$

(0.21mL, 1.52mmol). This mixture was then added dropwise to the triflated peptide to a volume of 350mL. A low concentration was used (0.95mg/mL) to ensure that the reaction would be intermolecular rather than intramolecular. The solution turned from cloudy orange to clear light orange overnight. <sup>1</sup>H NMR (MeOD). δ 8.2-7.9 (**m**, 9H pyrene), 7.3 (**s**, 6NH), 3.8-4.4 (**m**, 6CH), 3.7 (**m**, CH<sub>2</sub>pyrene), 2.9 (**m**, 1CH<sub>3</sub>N), 2.5 (**t**, 2CH<sub>2</sub>N), 2.0 (**t**, 2CH<sub>2</sub>), 1.3-1.1 (**t**, 21CH<sub>3</sub>). [**Scheme 12**]

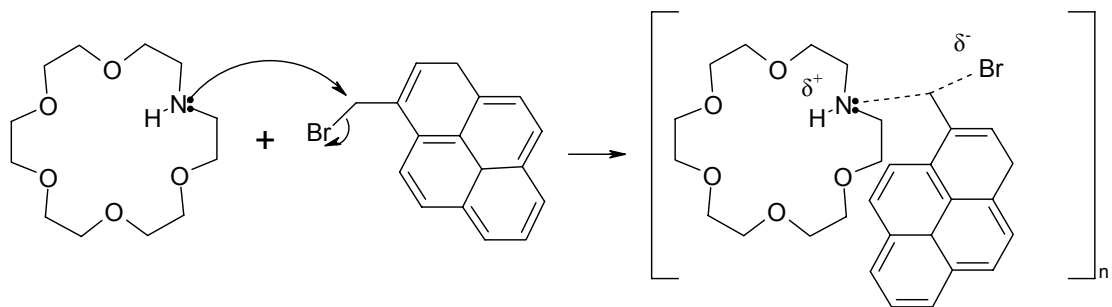
## Results and Discussion

Details of the synthesis and fluorescence testing of the four aza crown ethers, 1,3 alternate calixarene[4]arene-crown-5, and bicyclic peptide **V** are discussed below.

### **I. Aza-crown-ethers**

#### *i. Synthesis*

Chromophore containing aza-crown ether compounds were studied as models for both 1,3 alternate calixarene[4]arene-crown-5 and bicyclic peptide **V**. All four chromophore containing aza-crown ether compounds were synthesized by the same synthetic pathway. Following a literature procedure,<sup>39</sup> 1.0 equivalent of the chromophore, 1.2 equivalents of the aza-crown ether, and 2.5 equivalents of triethylamine were dissolved in 1,4 dioxane. The reaction proceeds via an SN2 mechanism, (see **Scheme 13** below). After 48 hours, the solvent was evaporated and the product extracted into DCM and washed with water. The organic layer was dried over MgSO<sub>4</sub>, rather than NaSO<sub>4</sub>, to prevent any possible contamination or complexation between the sodium cations and the aza-crown ether moiety.



**Scheme 13:** Mechanism of pyrene addition to aza crown ether

Further purification was achieved using preparative thin layer chromatography plates with DCM:EtOH (17:1) as eluent. All plates were run in the dark and the silica removed before the solvent was fully allowed to dry. Initial chromatography done under ambient light conditions caused an apparent decomposition of the product. A literature search concluded that pyrene is known to photo-oxidize on unactivated and activated silica.<sup>40,41,42</sup> Mechanistic studies done by Reyes *et. al.* concluded that the pyrene cation radical forms by an electron transfer from the pyrene excited state to oxygen or by photo-ionization of pyrene and is the precursor to the photoproduct formation. The pyrene cation radical then reacts with physisorbed water on silica to give 1,8-pyrenedione, 1-hydroxypyrene, 1,6-pyrenedione, along with minor products.<sup>41</sup>

Higher product yields were obtained when using 1-aza-15-crown-5 (**P5** 42.5%, **A5** 60.8%). The reason for this result is unclear at this time, but may be due to the fact that the amine 1-aza-15-crown-5 may be more rigid and less sterically hindered than the 1-aza-18-crown-6 (**P6** 6.8%, **A6** 22.0%), enabling it to be more reactive. Adding the anthracene moiety to the aza-crown ethers also proceeded in overall higher yields than

the addition of the 9-methylpyrene and is likely due to the higher reactivity of the 9-chloromethylanthracene moiety.

Characterization of each chromophore-containing aza-crown ether was done primarily with NMR and Mass Spectroscopy. All spectral data can be found in Appendix A.

### ii. Photo-electron transfer (PET)

Chromophore-containing aza-crown ethers are able to participate in photoinduced electron transfer (PET), where, upon excitation an electron of the lone pair on the nitrogen is able to travel to the chromophore, quenching the fluorescence.<sup>7</sup> Upon complexation with a cation, the electrostatic field of the amine is disrupted, thereby preventing PET and causing an increase in fluorescence intensity proportional to the concentration of cations.

The thermodynamics of PET are described by the simplified Rehm-Weller equation (1).  $\Delta G_{\text{PET}}$  is calculated to determine the spontaneity of the PET process for chemosensors with a fluorophore-spacer-receptor system.

$$\Delta G_{\text{PET}} = E_{\text{ox}} - E_{\text{red}} - e^2/\epsilon r - E_{\text{oo}} \quad (1)$$

Here,  $\Delta G_{\text{PET}}$  is the free energy for the PET process,  $E_{\text{ox}}$  is the oxidation potential of the amine,  $E_{\text{red}}$  is the reduction potential of the chromophore, and  $\epsilon$  the dielectric constant of the solvent. The oxidation potential of the aza-crown ether moiety is reported to be +0.84 V vs. Ag/AgCl.<sup>1</sup> Values for the reduction potential of the anthracene and pyrene

were converted from SCE to Ag/AgCl and found to be -1.93 eV and -2.10 eV, respectively.<sup>43</sup> A value of  $e^2/\epsilon r$  was approximated to be -0.1 eV<sup>1</sup> and the singlet-singlet energy was calculated to be 3.28 eV for anthracene and 3.34 eV for pyrene.<sup>43</sup> Using the Rehm-Weller equation,  $\Delta G_{\text{PET}}$  of the anthryl-aza-crown-ethers was calculated to be -0.41 eV and the  $\Delta G_{\text{PET}}$  of the pyrenyl-aza-crown-ethers -0.30 eV. The negative values for PET in these systems indicate that electron transfer quenching is a spontaneous process. The thermodynamic requirement for spontaneity is crucial in the design of cation-sensing systems and is always the first consideration.

### iii. Fluorescence Data

Fluorescence spectra were obtained in air saturated 1:1 DCM: MeOH at concentrations between  $2.0 \times 10^{-4}$  M and  $2.2 \times 10^{-4}$  M by preparing a stock solution of 0.010g, in 100mL of a 1:1 solution. **A6** was also tested in DCM, providing a comparison with 1,3 alternate calixarene[4]arene-crown-5 and determination of solvent effects. The stock solution was then used (0.5mL) to prepare (10mL) a  $1.0 \times 10^{-5}$  M –  $1.2 \times 10^{-5}$  M solution. All fluorescence emission spectra were obtained with the slit widths set at 5.0 nm for the excitation monochromator and 2.5 nm for the emission monochromator on a Perkin-Elmer LS-50B. The samples were prepared as follows with each UV absorbance at the excitation wavelength noted.

Sodium acetate salt (0.01M stock solution) in 1:1 DCM MeOH was used as the sodium cation in experiments with both aza-crown-5 compounds. Potassium acetate salt (0.005M stock solution) in 1:1 DCM: MeOH was used as the potassium cation in experiments with both aza-crown-6 compounds. Benzyltrimethylammonium hydroxide

(0.0055M stock solution) in 1:1 DCM: MeOH was used as a proton scavenger in each of the samples. Data is shown in **Table 1**.

Sample	Concentration [M]	Excitation nm	Abs.
N-(1-methylpyrene) monoaza-15-crown-5 ( <b>P5</b> )	1.15 x10 <sup>-5</sup>	333	0.153
N-(1-methylpyrene) monoaza-18-crown-6 ( <b>P6</b> )	1.00 x10 <sup>-5</sup>	333	0.165
N-(9-anthryl-methyl) monoaza-15-crown-5 ( <b>A5</b> )	1.22 x10 <sup>-5</sup>	355	0.048
N-(9-anthryl-methyl) monoaza-18-crown-6 ( <b>A6</b> )	1.10 x10 <sup>-5</sup>	355	0.040

**Table 1:** Sample Concentrations of **P5**, **P6**, **A5**, **A6**, in 1:1 DCM:MeOH, **A6** in DCM, and each absorbance at the given wavelength of excitation

Fluorescence spectra obtained upon the addition of each cation concentration are shown below along with a plot of the fluorescence area compared to cation concentration. [Figures 6-13] From these plots it can be seen that the complexation of cation is linearly proportional to the fluorescence area obtained. Once all possible complexation has taken place, the plot begins to plateau and the fluorescence area and intensity reach a maximum regardless of the amount of cation added. For **A6** and **P6**, this plateau is observed at a marginally higher concentration of cation than the host molecule, likely due to the value of the complexation constant. A significantly higher concentration of cation is needed for **A5** and **P5** in order to reach a plateau on the complexation plot. This may be due to a lower complexation constant of the host and Na<sup>+</sup>. All four compounds form a 1:1 host-guest complexation based on the data obtained.<sup>9</sup>

DCM:MeOH	[Sensor]	Abs. $\lambda$ 333nm	Abs. $\lambda$ 365nm	[base] x10 <sup>-5</sup> M	[ion] x10 <sup>-5</sup> M	[Cat/Host]	Initial Fl. Area	Final Fl. Area	Fluorescence Enhancement
1:1	x10 <sup>-5</sup> M								
<b>P5</b>	1.15	0.153		0.055	91.5	79	2928	30251	10
<b>P6</b>	1	0.165		0.0935	10.5	10	8013	45965	6
<b>A5</b>	1.22		0.048	0.055	100	82	2875	28034	10
<b>A6</b>	1.1		0.038	0.055	10	9	5	360	68
<b>A6</b> <sub>DCM</sub>	0.55		0.02	0.0875	1.13	2	1035	40629	39

**Table 2:** Molar concentrations of host, base, and cation used for fluorescence testing are shown, along with the fluorescence enhancement, FE, which was calculated based on the increase in fluorescence areas upon cation addition.

**Table 2** shows the calculated enhancement of the fluorescence area upon the addition of the cation indicated. The plateau cation concentration compared to the host concentration is shown along with the total increase in fluorescence upon cation complexation. The amount of fluorescence enhancement upon the addition of the cation shows that PET does in fact take place with fairly high sensitivity.

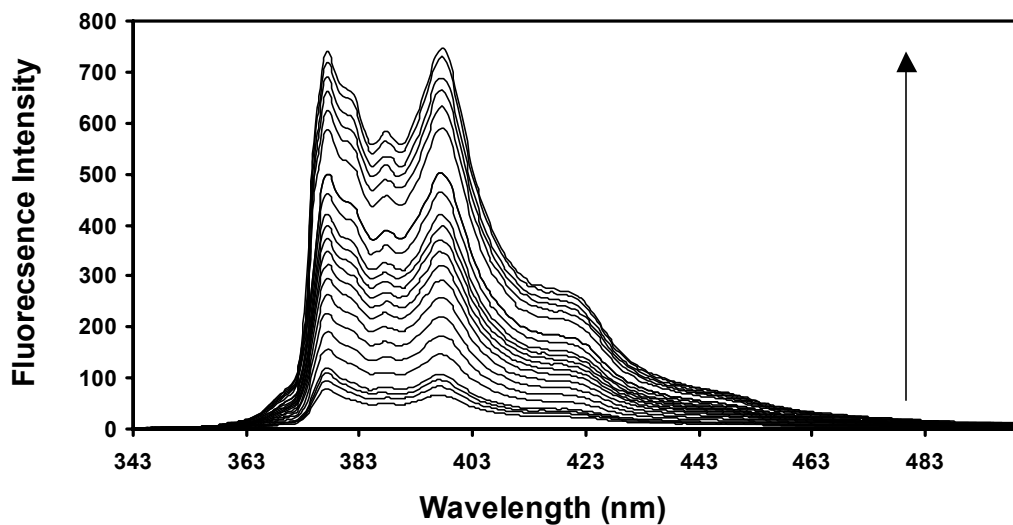


**Figure 6:** Fluorescence emission spectra ( $\lambda_{\text{ex}}$  333 nm) of **P5** ( $1.15 \times 10^{-5}$  M) in DCM: MeOH (1:1) with added BTMAH ( $5.5 \times 10^{-7}$  M) as a function of  $[\text{Na}^+]$ , [0  $\mu\text{M}$  –1000  $\mu\text{M}$ ].

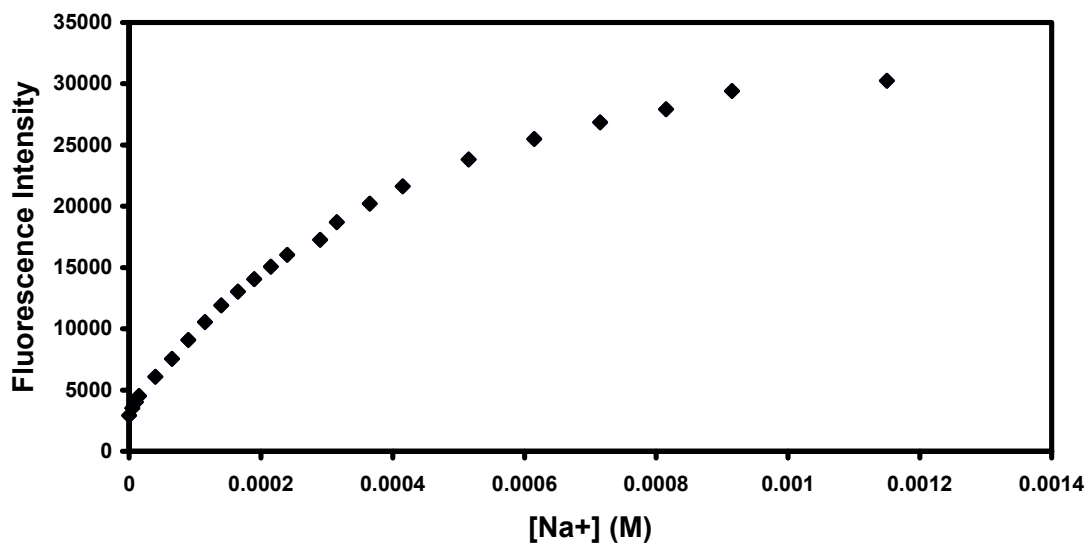


**Figure 7:** Fluorescence area increase of **P5** ( $1.15 \times 10^{-5}$  M) in DCM: MeOH (1:1) with added BTMAH ( $5.5 \times 10^{-7}$  M) as a function of  $[\text{Na}^+]$ , [0  $\mu\text{M}$  –1000  $\mu\text{M}$ ].

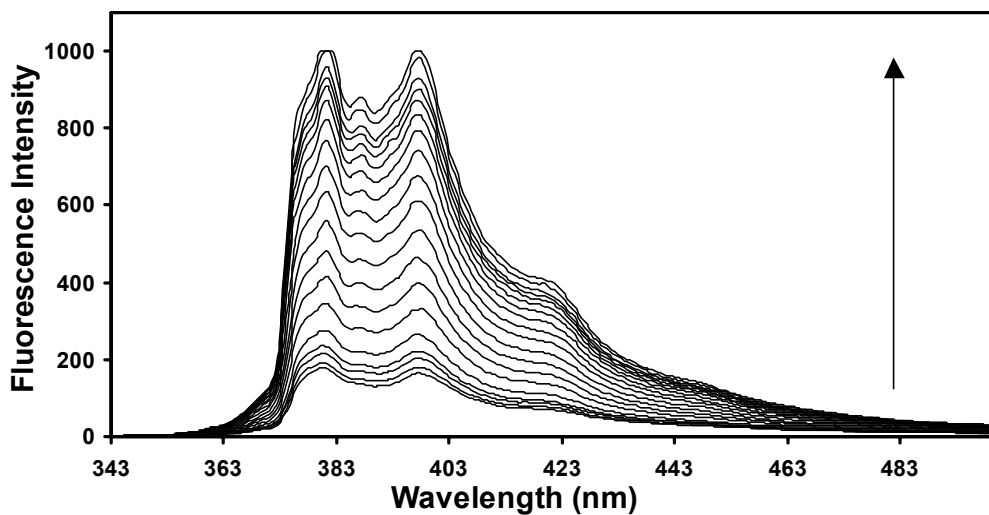


**Figure 8:** Fluorescence emission spectra ( $\lambda_{\text{ex}}$  333 nm) of **P6** ( $1.00 \times 10^{-5}$  M) in DCM: MeOH (1:1) with added BTMAH ( $9.35 \times 10^{-7}$  M) as a function of  $[\text{K}^+]$ , [0  $\mu\text{M}$  –205  $\mu\text{M}$ ].

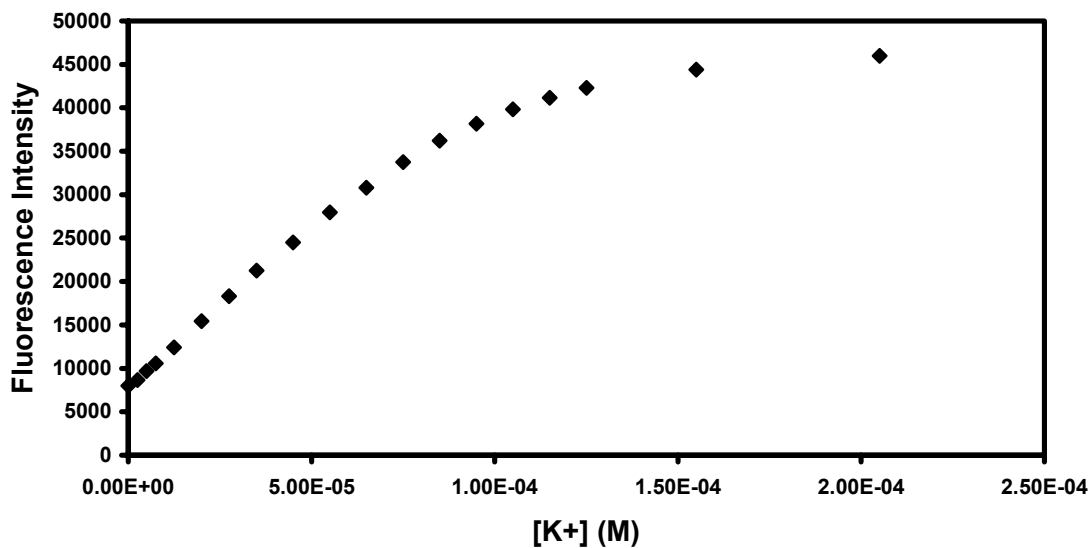


**Figure 9:** Fluorescence area increase of **P6** ( $1.00 \times 10^{-5}$  M) in DCM: MeOH (1:1) with added BTMAH ( $9.35 \times 10^{-7}$  M) as a function of  $[\text{K}^+]$ , [0  $\mu\text{M}$  –205  $\mu\text{M}$ ].

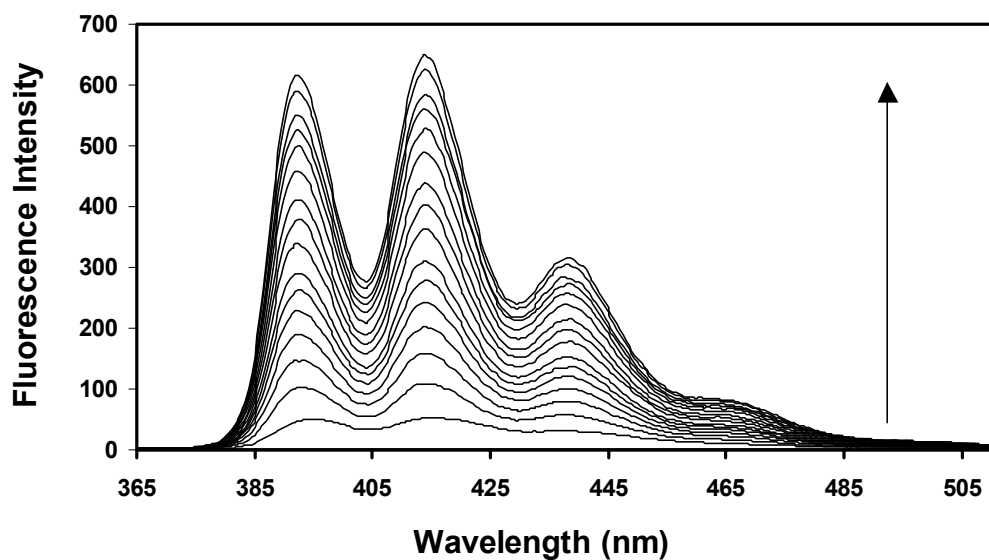


**Figure 10:** Fluorescence emission spectra ( $\lambda_{\text{ex}}$  365 nm) of **A5** ( $1.22 \times 10^{-5}$  M) in DCM: MeOH (1:1) with added BTMAH ( $5.50 \times 10^{-7}$  M) as a function of  $[\text{Na}^+]$ , [0  $\mu\text{M}$  –1400  $\mu\text{M}$ ].

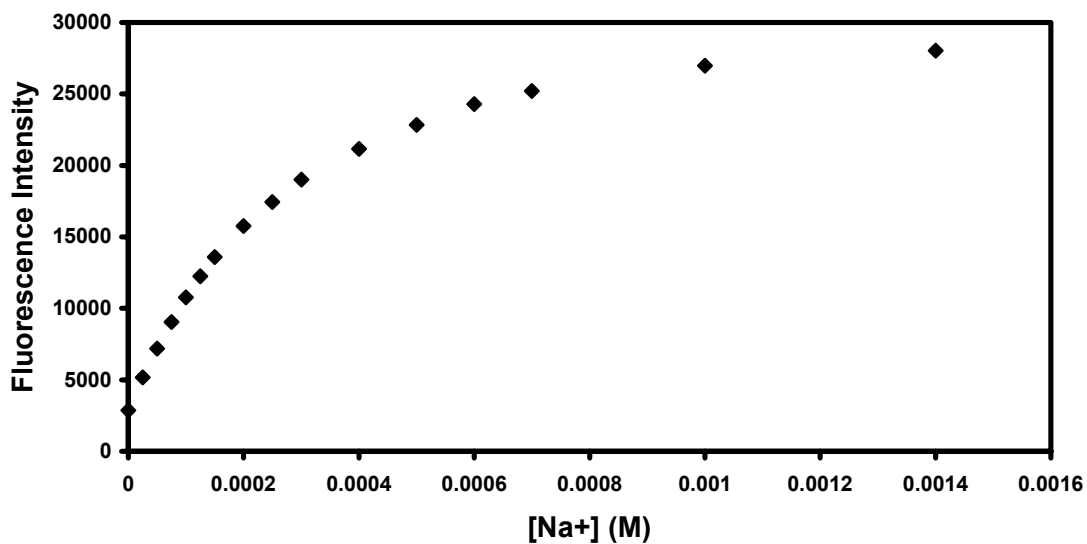


**Figure 11:** Fluorescence area increase of **A5** ( $1.22 \times 10^{-5}$  M) in DCM: MeOH (1:1) with added BTMAH ( $5.50 \times 10^{-7}$  M) as a function of  $[\text{Na}^+]$ , [0  $\mu\text{M}$  –1400  $\mu\text{M}$ ].

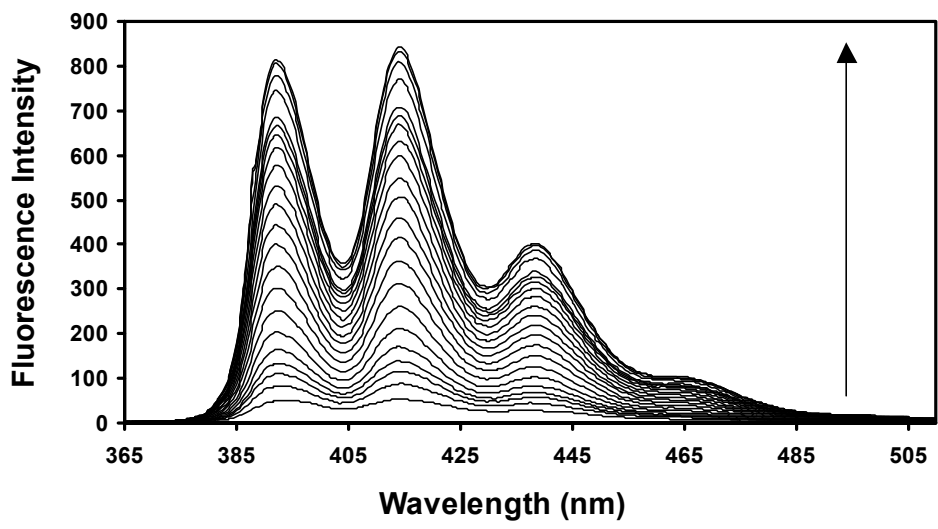


**Figure 12:** Fluorescence emission spectra ( $\lambda_{\text{ex}}$  365 nm) of A6 ( $1.10 \times 10^{-5}$  M) in DCM: MeOH (1:1) with added BTMAH ( $5.50 \times 10^{-7}$  M) as a function of  $[\text{K}^+]$ , [0  $\mu\text{M}$  –175.0  $\mu\text{M}$ ].

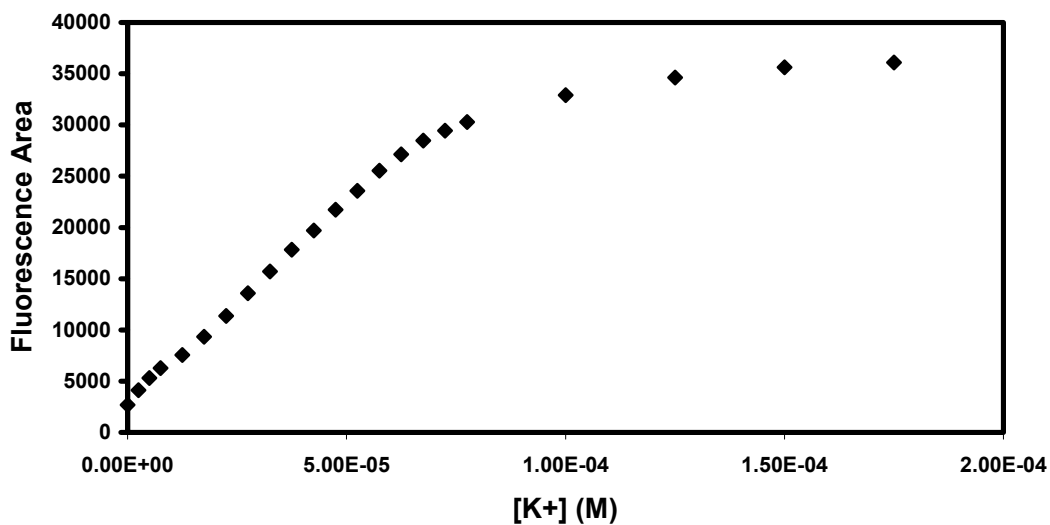


**Figure 13:** Fluorescence area increase of A6 ( $1.10 \times 10^{-5}$  M) in DCM: MeOH (1:1) with added BTMAH ( $5.50 \times 10^{-7}$  M) as a function of  $[\text{K}^+]$ , [0  $\mu\text{M}$  –175.0  $\mu\text{M}$ ].

Protonation of the nitrogen atom in the azacrown can potentially block the electron transfer process and for this reason, the organic base, benzyltrimethylammonium hydroxide (BTMAH), was added to minimize protonation.<sup>7,9</sup> In fact, the addition of base to solutions of **A6** in the absence of potassium ions causes a 4-fold decrease in the fluorescence intensity, consistent with this protonation effect. However, the addition of excess base caused an increase in fluorescence intensity.

Nevertheless, some fluorescence is still observed. It is difficult to unambiguously determine the origin of this fluorescence, i.e. whether it reflects the intrinsic rate constants for fluorescence and electron transfer in this molecule or whether there is a low background concentration of potassium, sodium or other cations present as impurities. Indeed, the intensity of the fluorescence emission in the presence of base and in the absence of added potassium is somewhat variable and it is possible to reduce this intensity by using rigorously cleaned glassware during sample preparation, suggesting that at least some of the effect is due to impurity ions.<sup>44,45</sup>

Upon testing, **A6** was found to have a fluorescence enhancement, FE, for  $K^+$  greater than 50. This finding is consistent with published data where for the same compound the F.E. was found to equal 47.<sup>3</sup>

## **II. 1,3 alternate calixarene[4]arene-crown-5 (I)**

### *i. Synthesis*

The synthesis of 1,3 alternate calixarene[4]arene-crown-5 (**I**) can be found in reference 46.

A structure of the molecule is given in **Figure 14**.

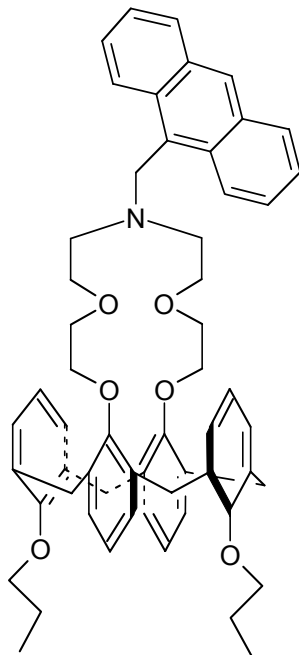


**Figure 14:** 1,3 alternate calixarene[4]arene-crown-5 (**I**)

### *ii. Fluorescence Data*

The aza-crowns, **P5**, **P6**, **A5**, **A6**, were model compounds for more complex fluoroionophores designed to exhibit higher cation selectivity. **A6** was synthesized as a model for **I** because it contains both the same chromophore/amine electron transfer system and based on molecular modeling, the electrostatic characteristics of the complexation sites are qualitatively similar in both compounds. The synthesis of **A6** also served as a baseline for determining whether selectivity and sensitivity of the azacrown moiety is enhanced by the incorporation of the calix[4]arene group. Thus, the aza-crown moiety was combined with a calixarene group and the resulting molecule was tested for cation response and selectivity. To provide a consistent comparison of **A6** to **I**, fluorescence spectra of **A6** were obtained in DCM, (shown in **Figure 15**).

The results obtained using **A6** in DCM show over a ca. 50-fold enhancement of the fluorescence intensity upon addition of potassium ions. [Figure 16]

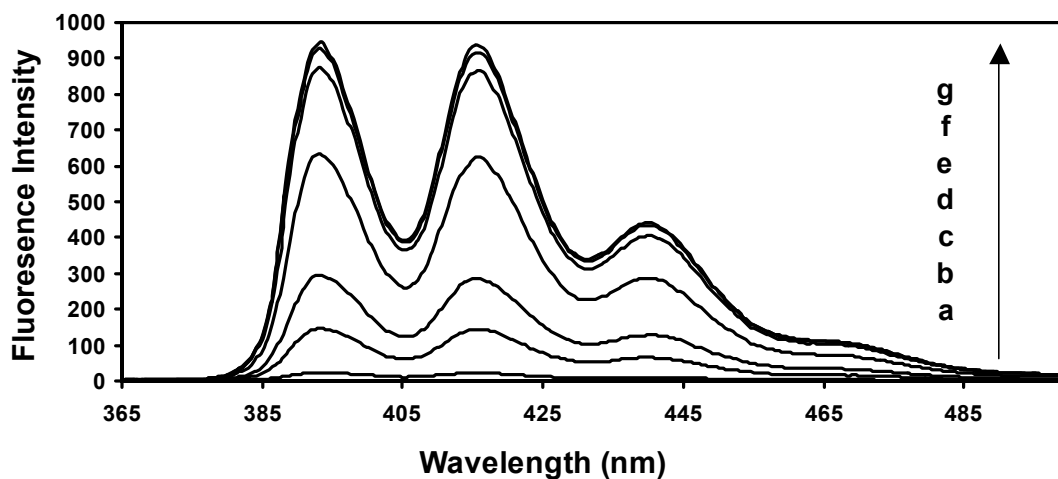


**Figure 15:** Fluorescence emission spectra ( $\lambda_{\text{ex}}$  355 nm) of **A6** ( $5.50 \times 10^{-6}$  M) in DCM with added BTMAH ( $8.75 \times 10^{-7}$  M) as a function of  $[\text{K}^+]$ , [0  $\mu\text{M}$  - 11.3  $\mu\text{M}$ ].

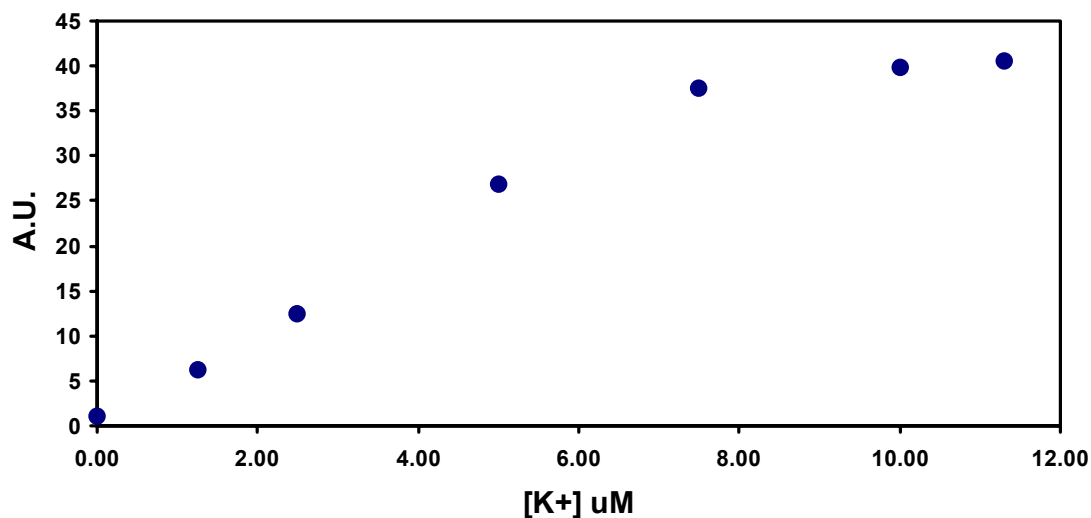


**Figure 16:** Fluorescence area increase of **A6** ( $5.50 \times 10^{-6}$  M) in DCM with added BTMAH ( $8.75 \times 10^{-7}$  M) as a function of  $[\text{K}^+]$ .

**Figure 17** shows the fluorescence spectra obtained for **I** in the absence and presence of added potassium acetate in dichloromethane solution. In order to compare directly the behavior of **A6** and **I**, the spectrum for **I** in the absence of potassium ions was normalized to that of **A6** to account for differences in sample absorbance at the excitation wavelength. As with **A6**, the fluorescence intensity of **I** in the presence of added base, increases dramatically with addition of potassium ions, although both the rate of increase as a function of ion concentration and the dynamic range for **I** is considerably less than for **A6**, (8.5-fold and 50-fold increases respectively).

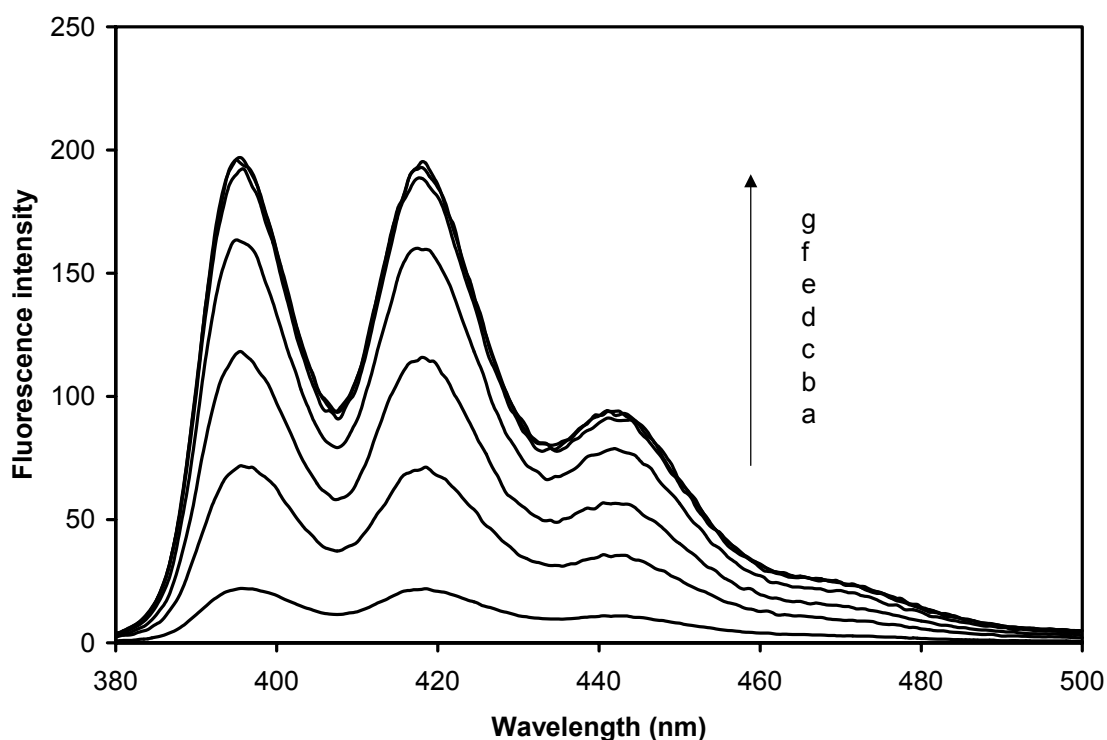


**Figure 17:** Fluorescence emission spectra ( $\lambda_{\text{ex}}$  355 nm) of **I** ( $1.1 \times 10^{-6}$  M) in dichloromethane with added BTMAH ( $1.0 \times 10^{-7}$  M) as a function of  $[\text{K}^+]$ . a: 0  $\mu\text{M}$ , b: .5  $\mu\text{M}$ , c: 1  $\mu\text{M}$ , d: 1.5  $\mu\text{M}$ , e: 2  $\mu\text{M}$ , f: 2.5  $\mu\text{M}$ , g: 3  $\mu\text{M}$ .

The reason for this reduced response of **I** compared to **A6** is unclear. One potential explanation is that the ion occupies a site in **I** relative to the electron lone pair on the azacrown nitrogen atom as well as to the anthryl fluorophore that is different than in **A6**. For example, if the most stable position of the ion in the complex is at a greater distance from the nitrogen lone pair in **I**, this could lead to a weaker electrostatic interaction and result in less effective interference with the electron transfer quenching process. Such an effect could conceivably be caused by an interaction between the ion and the  $\pi$ -systems of the phenyl rings of the calixarene group. The binding of cations through  $\pi$  interactions has been observed for other host-guest molecules<sup>47,48,49</sup> as well as the 1,3 alternate calix[4]arene-crown-5 used in the present study.<sup>50</sup> In fact, electrostatics calculations on the potassium ion-**I** complex point out significant changes in charge density in the calixarene phenyl rings upon complexation. Additionally, it was found that when the structure of **A6** complexed with potassium ion was minimized, a  $K^+ \cdots N$  distance = 3.00 Å was optimal whereas a  $K^+ \cdots N$  distance of 3.48 Å was observed for **I**. Therefore, a weaker interaction with the amine electron donor and consequently a reduction in the fluorescence response would be expected for **I** compared to **A6**.

### iii. Solvent Effects

Previous studies of analogous anthryl-benzocrown ether calixarenes indicated a considerable and complex solvent effect on the intensity of fluorescence in such compounds.<sup>16</sup> Specifically, addition of methanol to dichloromethane was observed initially to cause an increase in the fluorescence presumably due to complexation of the methanol with the oxygen atoms of the benzocrown ether, i.e., electron transfer was less efficient. With continued addition of methanol, the increase in polarity in turn increased the efficiency of electron transfer and led to a

decrease in the fluorescence. Given this reported medium effect and its potential importance in the operation of a sensor based on this molecular structure, we have investigated the effect of solvent on **I**, both in the absence and presence of added potassium ions. In the absence of ions, the addition of methanol to the dichloromethane solutions caused an increase in the fluorescence intensity at small methanol concentrations and then a decrease as the methanol concentration was increased further. This behavior is similar to that reported for the benzocrown systems.<sup>1</sup> It is likely here that at low methanol concentrations, the increase in fluorescence intensity is due to a hydrogen bond interaction between methanol and the azacrown nitrogen. The fact that the effect of small concentrations of added methanol is more pronounced in **I** than in the previously studied benzocrown compounds is consistent with the fact that the nitrogen lone pair is a more localized source of electrons for the fluorescence quenching process than the 1,2-dimethoxybenzo moiety within benzocrown ethers. However, at higher methanol concentrations the drop in fluorescence intensity observed can be ascribed to an increase in the efficiency of electron transfer due to an increase in solvent polarity. This polarity effect overshadows the hydrogen bonding effect.

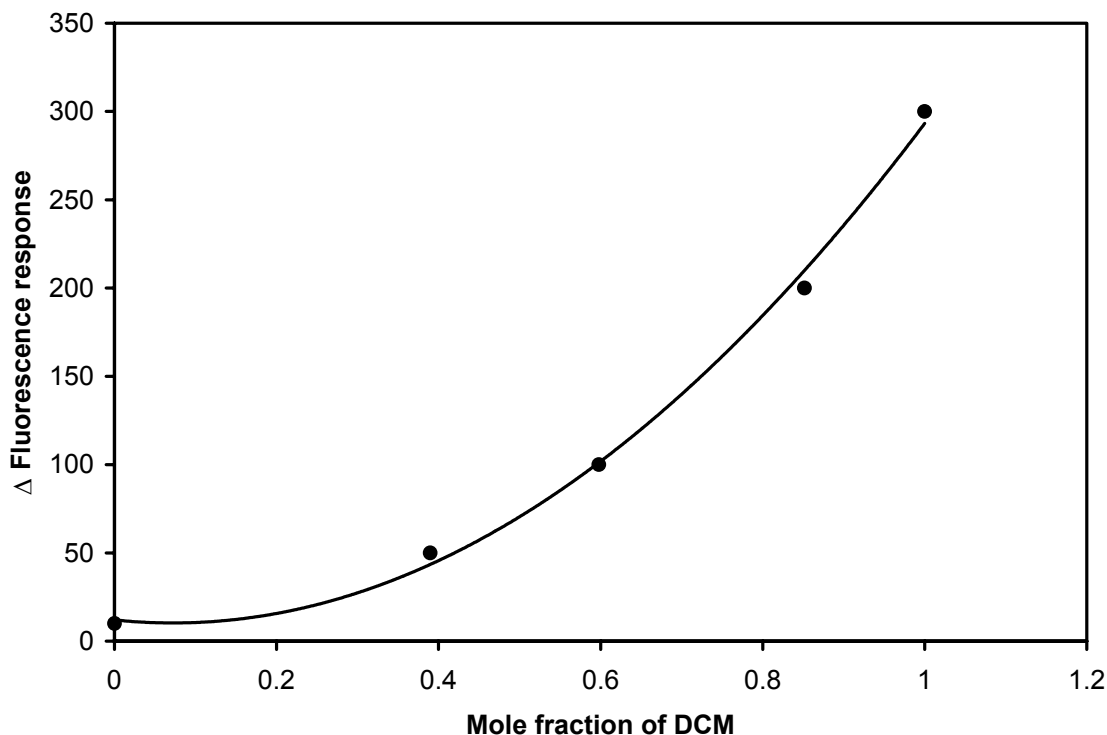


**Figure 18:** Delta fluorescence response to  $K^+$  of **I** as a function of the mole fraction of dichloromethane in methanol.

In the presence of added potassium ions, an additional effect of solvent is observed. **Figure 18** shows the delta response of **I** as a function of the mole fraction of dichloromethane in methanol. The delta response is determined from the slope of the fluorescence intensity versus ion concentration curve at a specific solvent composition. It is clear that as the mole fraction of methanol decreases, the delta response increases dramatically. We ascribe this behavior to a solvation effect in that, as the solvent polarity decreases with increased dichloromethane concentration, the potassium ions seek out a more energetically favorable solvation environment, namely the complexation site in **I**. This response to solvation is expected to have an important impact on the composition of the membrane that is eventually chosen to host **I** in sensor applications.

The anthryl azacrown-calix[4]arene, **I**, complexes with potassium ions in organic solution triggering a substantial increase in anthryl fluorescence emission through the disruption of the PET quenching process. Preliminary measurements indicate that the selectivity for potassium ions over other alkali metal cations particularly sodium and lithium for **I** is increased dramatically over that of the anthryl azacrown model compound, **A6**. These preliminary solution phase studies indicate a 1:1 complexation between **I** and the ion, suggesting that **I** could be sensitive to potassium in the normal physiological concentration range once incorporated into a sensor. Furthermore, the observed fluorescence response to changes in solvent polarity suggests that the sensor substrate composition will have an important impact on the efficiency of **I** as an ionophore and could allow further optimization of sensitivity and selectivity.

### **III. Bicyclic Peptide V**

#### *i. Design of Synthetic Route*

Bicyclic peptide **V** was designed based on molecular modeling using MOE. The modeling indicates that the use of **V** as a fluorionophore for ammonium cations should be more selective than that of the currently used standard, nonactin.

In order to construct bicyclic peptide **V**, several different possible synthetic routes that were examined. Ultimately, the core part of the molecule that needs to be constructed is the linear peptide with both side chains deprotected, shown in **Figure 19**.

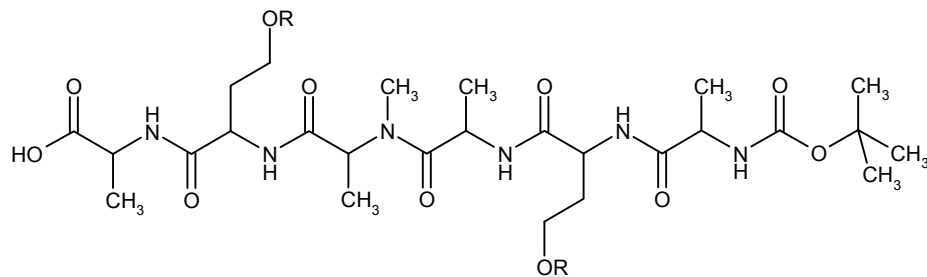


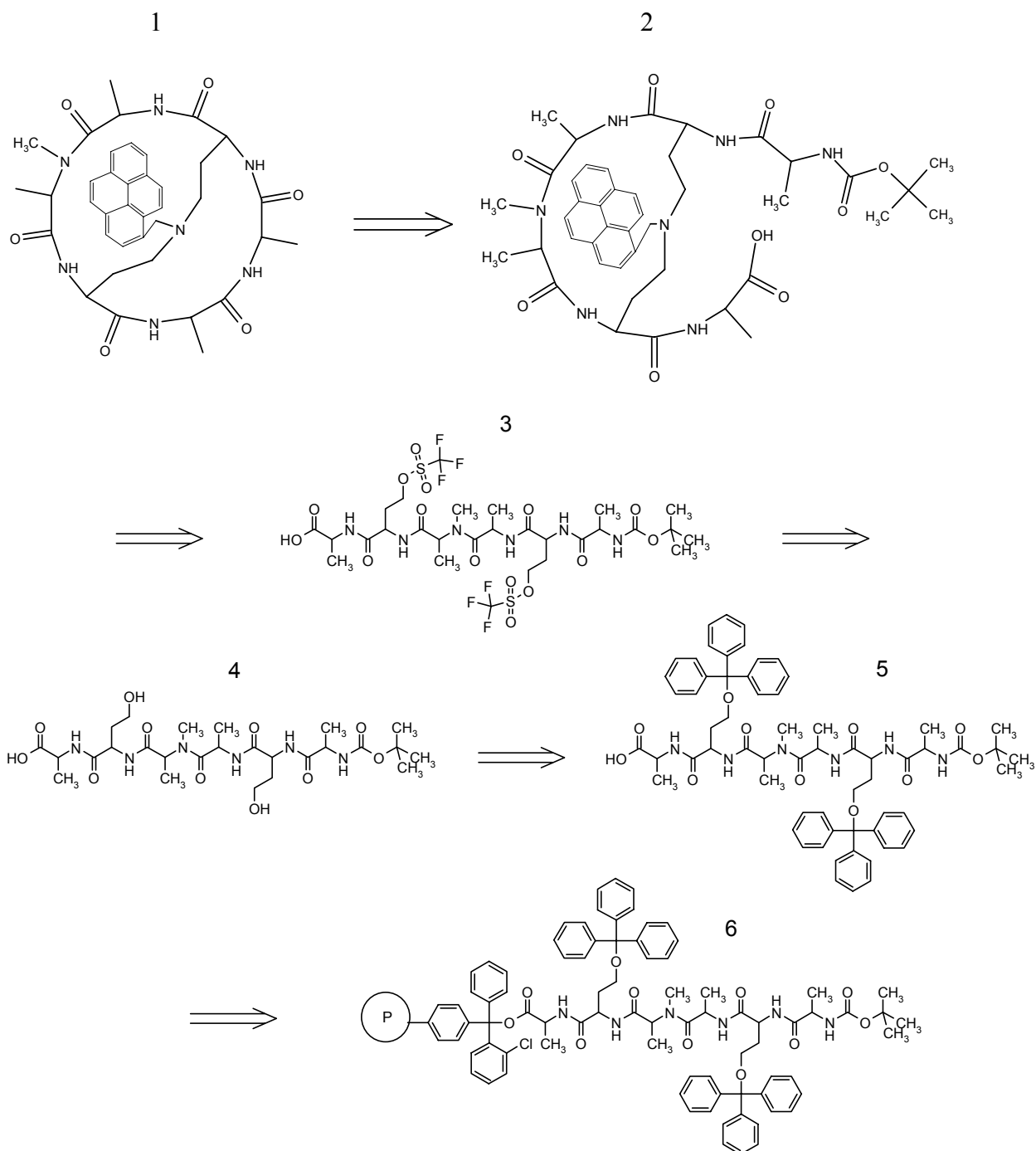
**Figure 19:** Open chain unprotected linear peptide.

Initially, we intended to synthesize the linear peptide with a end terminal Fmoc protecting group using a Wang Resin. However, it was determined that the Fmoc would be removed by the reagents used. Specifically, the use of base in subsequent steps would cleave the Fmoc group prior to the desired step. The option of using a terminal tBoc protecting group was then explored because it is stable under basic conditions. However, the use of tBoc precludes the use of a Wang Resin. Since 95% TFA is required to cleave the peptide from this resin, the tBoc group would be completely removed.

Questions arose as to whether cyclization of the main outer peptide ring would be a viable option. But, the deprotection of the alcohols could cause an unknown amount of cyclization between the side chains and the free amine or carboxylic acid. It was decided that the better option would be to attempt to cyclize the side chains first while leaving the amine protected by the tBoc group.

This decision then meant that a different resin would have to be employed, in which the cleavage conditions would not remove the tBoc protecting group. Various resins were explored, such as those that undergo photo cleavage and one that may be cleaved in NaOH. It was decided that the best alternative may be to use the 2-chloro-

trityl chloride resin, which cleaves in 5% TFA. Under this condition, the tBoc group should not be removed.



**Scheme 14:** Retrosynthetic analysis of bicyclic peptide (V)

## ii. Preliminary Synthesis

Decisions toward a synthetic route of constructing bicyclic peptide **V** were based on trial syntheses. The synthetic route was designed around the need for having a stable amine protecting group, while being able to activate the alcohols to facilitate the pyrenemethyl amine addition across the homo-serine side chains, as in **Scheme 14, Structure 3**. Initial attempts were directed toward activating the alcohol while still using a Fmoc protecting group on the residue. This would mean that either the Wang or the HMBA resins, which have been frequently used within our group and known to give good yields, could be employed and cleaved in strong acid without affecting the protecting group. A synthetic procedure that enabled the activation of the alcohol while not removing the end protecting group on the amine of the linear peptide was needed in order to prevent unwanted side reactions. In an attempt to find a method of activating the alcohols without removing the Fmoc, several trial syntheses were attempted. Syntheses tried and results obtained are described below.

Based on a procedure found in *Organikum*<sup>46</sup> Fmoc-Ser-OH (1.0 eq., 3.1mmol) was mixed with tosyl chloride (1.1 eq., 3.7 mmol) and DIPEA (1.6 eq., 4.9mmol) in DCM. After 4 ½ hours at room temperature, 3 g of ice were added along with HCl (2-3 mL). The organic layer was then washed with water and dried with Na<sub>2</sub>SO<sub>4</sub>, but yielded little evidence that the tosylation had taken place. The reaction was then re-run using 5 eq of DIPEA; however it was determined that these basic conditions removed the Fmoc group.

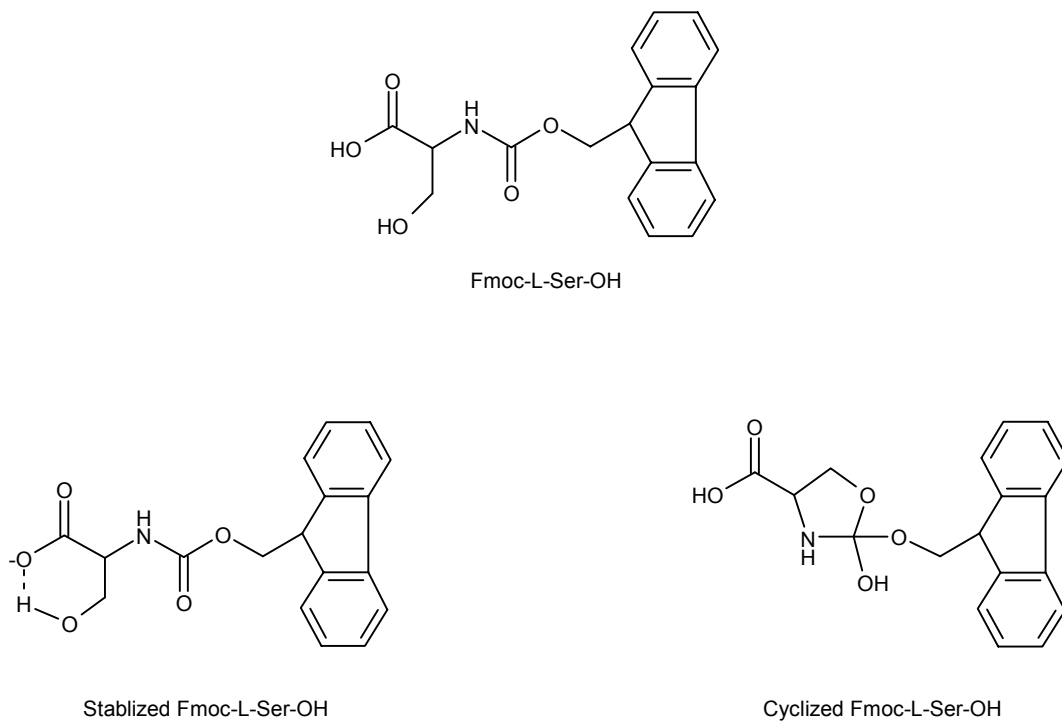


**Figure 20:** Cyclizations of Fmoc-L-Ser-OH under basic conditions to form either a six membered ring through stability or a cyclized five membered ring.

It is possible that once the base removes the proton on the carboxylic acid, the Fmoc-Ser-OH is stabilized by the formation of a six membered ring between the alcohol and the carboxylic acid, causing the alcohol of the serine to be much less reactive. The other possibility is that under basic conditions, the alcohol is able to attack the carbonyl and cyclizes to form a five membered ring, shown in **Figure 20**. To avoid these possible cyclizations, the methyl ester was formed and used in further reactions.

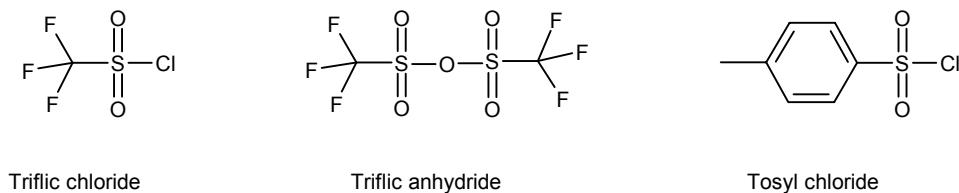


**Figure 21:** Structures of triflic chloride, triflic anhydride, and tosyl chloride.

Because a triflic group is a better leaving group than a tosyl group<sup>51</sup>, subsequent reactions were attempted to find an efficient method for triflating the alcohol. [Figure 21] Fmoc-Ser-O-Me (1 eq., 7.4mmol) and DIPEA (2eq, 14.8mmol) were stirred at  $-78^{\circ}\text{C}$  in DCM and triflic anhydride (1.1 eq., 8.1mmol) added dropwise over 1 hr. The organic layer was rinsed with water and then  $\text{NaHCO}_3$ . It was determined that the Fmoc was also removed during this reaction. The above reaction was repeated using Fmoc-Ser-O-Me (1.0 eq., 5.8mmol) and tosyl chloride (1.1 eq., 6.4 mmol) in DCM at room temperature and then cooled to  $0^{\circ}\text{C}$ . DIPEA (1.1 eq., 6.4mmol) was added dropwise over a  $\frac{1}{2}$  hour. After  $2\frac{1}{2}$  hours at room temperature, 50 g of ice were added along with HCl (20 mL). The organic layer was then washed with water and dried with  $\text{Na}_2\text{SO}_4$ . The Fmoc was once again removed under these basic conditions.

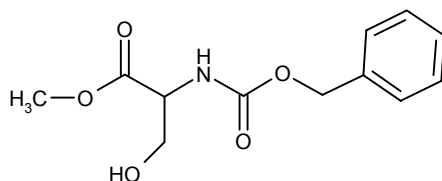


**Figure 22:** Structure of Bzl-L-Ser-OMe

The use of an N-protecting benzyl group was then employed. Bzl- Ser-O-Me (1.0 eq., 5.0mmol), **Figure 22**, was mixed with tosyl chloride (1.1 eq., 5.5mmol) and Et<sub>3</sub>N (2 eq., 10mmol) in chloroform. After 4 ½ hours at room temperature 3 g of ice were added along with HCl (2-3 mL). The organic layer was then washed with water and dried with Na<sub>2</sub>SO<sub>4</sub>. The products were not kept under inert conditions and based on TLC'S (3:1 DCM:Hexane), decomposition took place, therefore the reaction was repeated under inert conditions. Bzl- Ser-O-Me (1.0 eq., 36.7mmol) was mixed with tosyl chloride (1.1 eq., 40.4mmol) and Et<sub>3</sub>N (2 eq., 73.4mmol) in chloroform. After 4 ½ hours at room temperature, 3 g of ice were added along with HCl (2-3 mL). The organic layer was then washed with water and dried with Na<sub>2</sub>SO<sub>4</sub>. TLC plates were run in DCM:Hexane (4:1). Based on NMR, cyclization took place. Spectra obtained were identical to previous NMR spectra obtained when attempting to add an alkyl chain to the alcohol of Bzl- Ser-O-Me.

The next attempt made was to brominate the alcohol of Fmoc-Ser-OH. Fmoc-Ser-OH (3.1mmol, 1.0g) and PBr<sub>3</sub> (34mmol, 0.32mL) were refluxed over night in DCM. Organic layer was washed with water and 3N NaOH (5mL) to convert from an acid bromide to a carboxylic acid. TLC plates were run in DCM:EtOAc (19:1).

The decision was made to utilize an end tBoc protecting group, which is stable to basic conditions that are needed to activate the alcohol. This decision also meant that a very acid sensitive resin would need to be employed. Because the tBoc group is cleaved in 50% TFA, either a photolytically-cleaved resin, base-cleaved resin, or very acid-sensitive resin was required. Light sensitive resins are extremely expensive, and one resin that could be cleaved in base was found, but there is evidence that cleavage is inefficient based on a private communication with Advanced Chemtech. The decision

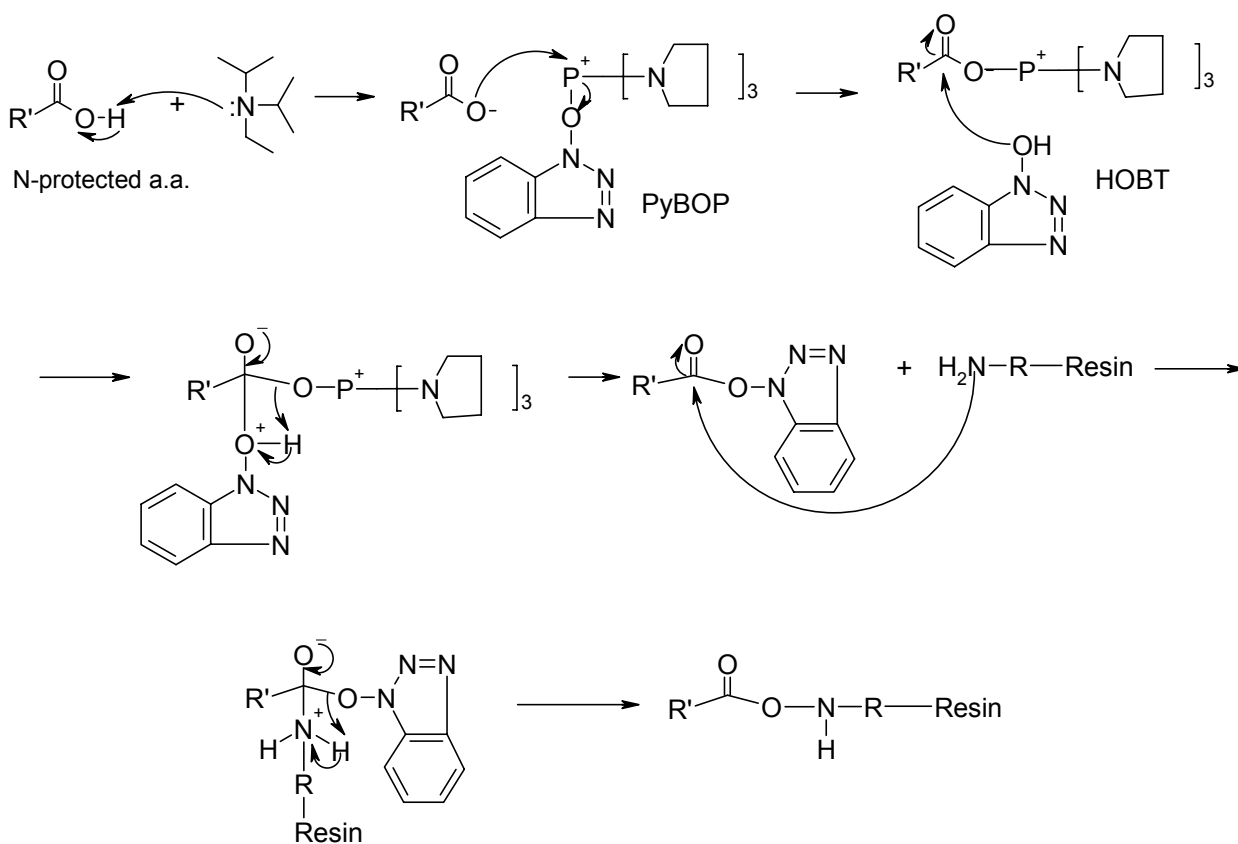
was made to attempt the synthesis of the linear peptide on the 2-chlorotrityl-chloride resin which cleaves in 5% TFA a condition that presumably would not remove the tBoc.

### iii. Synthesis

The linear peptide was loaded with Fmoc-Ala-OH using DIPEA and tested for its loading amount. By using a known amount of Resin-Ala-Fmoc(0.010g), the resin can be subjected to Fmoc deprotection conditions of (20% piperidine). The absorption spectra of the Fmoc in solution can then be measured and the concentration of Fmoc in solution calculated. The moles of Fmoc present indicate amount of loading on the resin. Both times that the resin loading was tested it was found to be above 95%.

The linear peptide was synthesized using solid phase Fmoc strategy. Some adaptations were made to the usual synthesis to facilitate better coupling yields. It was experimentally determined that a higher coupling yield was obtained when a slightly higher amount of PyBOP was used. This observation may be due to two possibilities; either the higher amount of PyBOP present increased the amount of activated esters formed thereby increasing the likelihood for amino acid coupling, or the PyBOP that was being used had previously been exposed to air/water and some of the chloride had been removed. The only other alteration that was made to the previously used strategy was the use of DCM along with DMF. Due to a shortage of DMF, the use of DCM was employed for coupling, and found to dramatically increase the amount of coupling, especially for the bulkier groups. When only DMF is used for the addition of the homoserine, the reaction mixture becomes thick and frothy. The use of DCM drastically increases the solubility of the mixture.

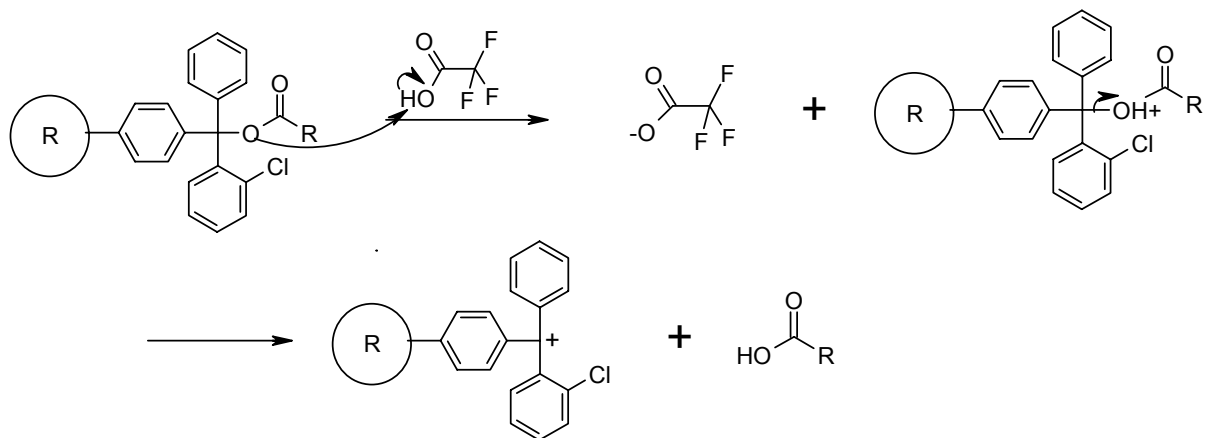
Coupling of each amino acid using a Fmoc strategy proceeds via the mechanism shown below in **Scheme 15**. Removal of the hydrogen from the acid to form the anion, leads to attack on PyBOP. An HOBT anion is then removed from the PyBOP to yield the activated ester of the amino acid. Nucleophilic attack of HOBT on the carbonyl causes the removal of the PyBOP ester, and enables the amine of the previous amino acid to attack the carbonyl and remove the HOBT, causing coupling to take place.



**Scheme 15:** Solid phase peptide coupling using PyBOP, HOBT, and DIPEA.

The Kaiser test, which indicates the presence of free amine, was used to insure proper coupling had taken place during each step. Some coupling steps were repeated twice to insure complete coupling because slightly negative Kaiser tests were obtained after single coupling. As the peptide became longer, and especially after the addition of each homo-serine, slightly negative Kaiser tests were obtained (light purple beads, rather than yellow). Based on later mass spectra, this is not due to any significant amount of incomplete coupling of any of the residues. According to Nova BioChem, larger, bulky groups are known to aggregate, thereby giving a slightly negative Kaiser test.<sup>52</sup>

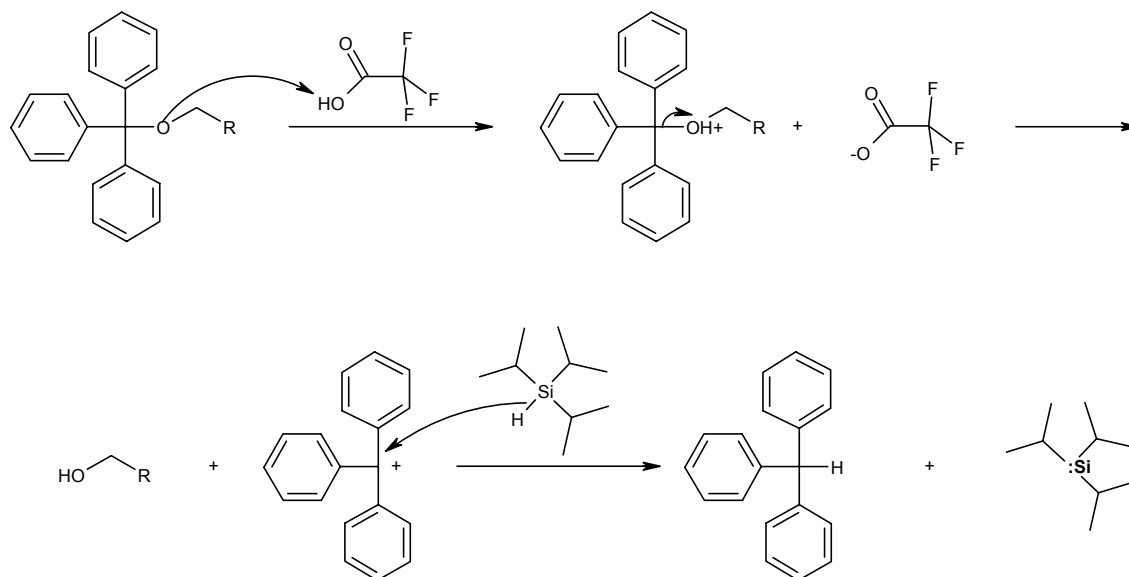
In a previous synthesis, the cleavage reagents used were AcOH: TFE: DCM (2:2:6) for 2 hours, which did not completely, if at all, cleave the peptide. Therefore, cleavage of the peptide was done following another Nova BioChem procedure to prevent the removal of the trityl groups. 1% TFA in DCM (42mLs) was bubbled through the peptide synthesizer for 5 minutes and then filtered into 10% pyridine in methanol to quench the reaction. [Scheme 16] Each fraction was collected and visualized using TLC (EtoAc:MeOH, 3:1). The first 2 fractions contained the majority of peptide present (2.020g); subsequent fractions contained a smaller amount of peptide (0.400g). A lower overall peptide yield was obtained than expected. This may be due to the fact that either incomplete loading took place initially, which is doubtful due to the high calculated loading yield from the Fmoc UV testing, or the peptide may be partially cleaved during coupling reactions or rinses. Because the trityl cation on the resin is extremely stable, i.e. the product of cleavage, it is possible that some unwanted cleavage took place.



**Scheme 16:** 2-Chlorotrityl Chloride resin cleavage using 1% TFA in DCM

The peptide was then precipitated from each cleavage mixture by rotoevaporation to 5% volume and then adding de-ionized water. A white gummy precipitate was immediately formed on the glass. The pH of the water was then tested to insure that acidic conditions were not present since they could lead to cleavage of the tBoc group. The major amount of precipitate from the first two cleavage batches was found to have a pH of about 6-7. a small amount of pyridine was added to insure acidic conditions were not present (to a pH of ~7). The minor fraction was found to have a pH of ~0-1, and therefore a significant amount of base was quickly added. This fraction of peptide was kept separate from the major fraction. Both fractions were cooled in the fridge overnight.

The deprotection of the trityl groups was done using 1% TFA in DCM 2.5 eq. Triisopropylsilane (TIS). TIS is used as a carbocation scavenger by acting as a hydride donor.<sup>53</sup> Cleavage of the trityl groups yields unprotected alcohols on the homo-serine residues along with tritylmethane, shown in **Scheme 17**.

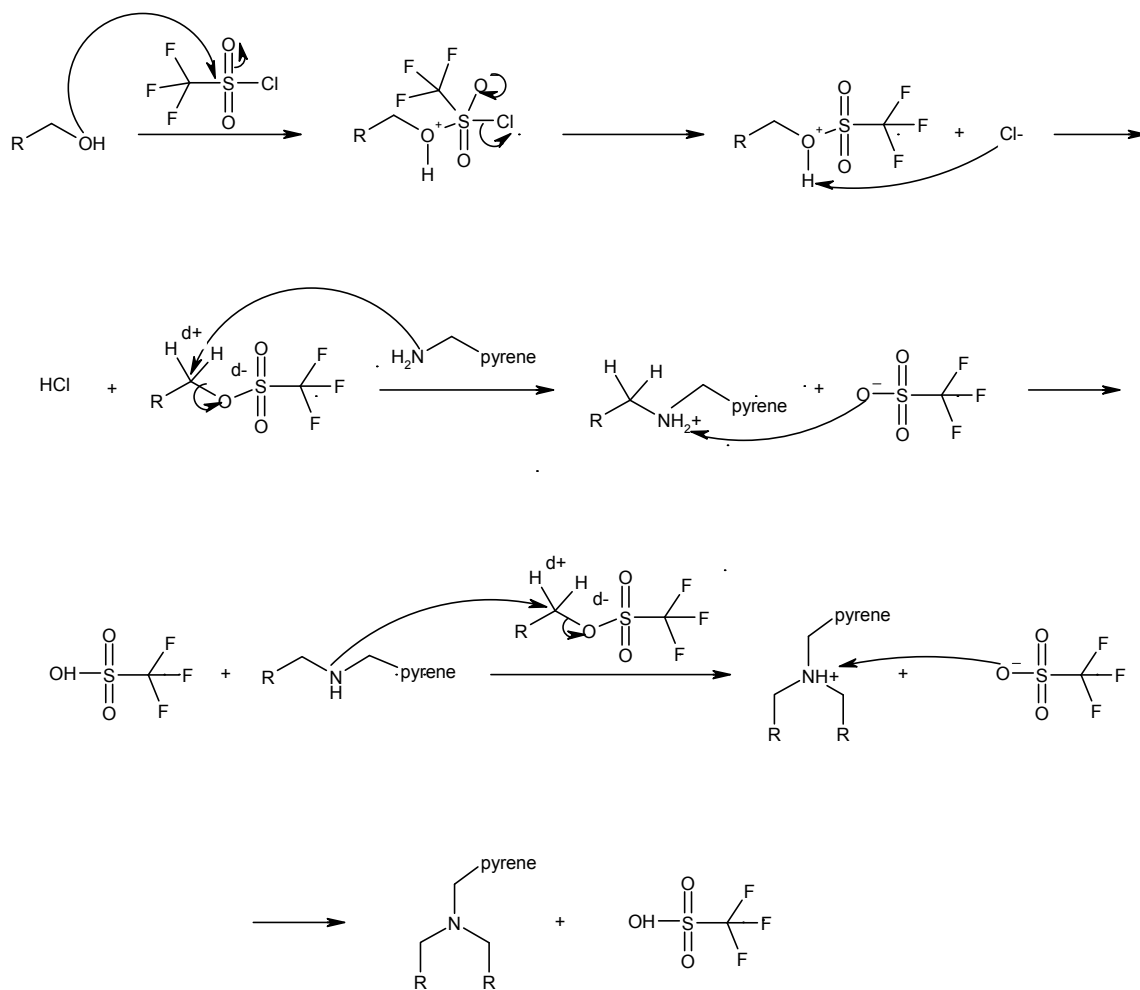


**Scheme 17:** Deprotection of alcohol using 1% TFA and 2.5 eq. TIS.

In order to form a tertiary amine connecting both homo-serine residues, reactivity of the alcohols would need to be increased. Several options were explored before the linear peptide was synthesized to provide a suitable leaving group for the amine addition via a  $S_N2$  mechanism. The utilization of the triflate leaving group was determined to be the most viable option to attain a reasonable product yield.

Once the linear peptide with the end tBoc group were synthesized, the addition of the amine was attempted. [Scheme 18] 2.2 eq. of triflic chloride was added to dropwise to the linear peptide and 3.0 eq. of  $\text{Et}_3\text{N}$  with cooling. After 1 hour at room temperature, the yellow solution was evaporated to yield a yellow oil. The oil was re-dissolved in acetonitrile to a volume of 350 mL and 1.0 eq. of 1-pyrenemethylamine were added along with 4.0 eq. of base. A low concentration was used (0.95mg/mL) to ensure that the reaction would be intermolecular rather than intramolecular. The reaction was carried

out overnight and the reaction mixture changed from cloudy orange to clear.



**Scheme 18:** Triflation and pyrene addition mechanism

Based on TLC, 3 spots were obtained in DCM:MeOH (10:1); one faint spot that barely moved, one at an  $R_f$  of 0.45, and one at an  $R_f$  of 1.0. All spots appeared under the UV lamp, and indicated the presence of the pyrene group. The middle spot

corresponded to the pyrene-containing starting material and the bottom spot might possibly be the linear peptide with one pyrene attached. Possibly, the top spot was the desired product. The crude NMR is shown in the appendix and integrates fairly well for the desired product.

A column was then run using the same solvent system and many more than three fractions were obtained, none of which (based on mass spec and NMR) contained the desired product. It is assumed that decomposition through photo-induced oxidation took place on the silica and decomposed the products. Since the structure has a very similar make-up to the aza-crown ether chromophore compounds, these compounds also underwent photo-oxidation.

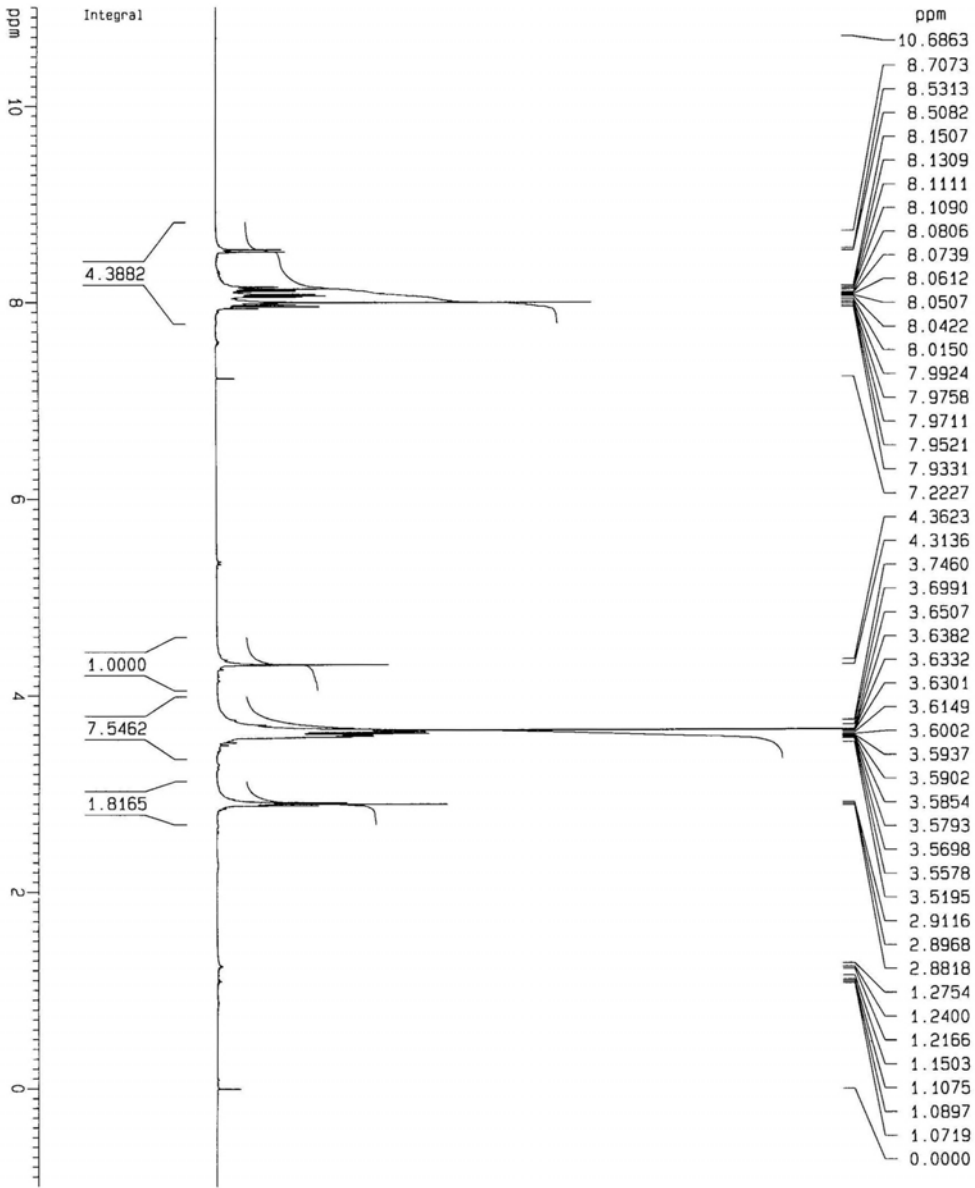
The linear peptide was successfully synthesized and the alcohols deprotected. The addition of the amine will be repeated using a similar procedure as above.<sup>54</sup> The products formed will then be recrystallized and not subjected to silica. If that product is obtained, the amino tBoc will then be removed using 50% TFA in DCM and cyclization of the peptide ring done. Fluorescence testing will then be performed on the bicyclic peptide to determine its selectivity and sensitivity toward complexing ammonium cations.

## Conclusions

Based on studies of **P6**, **P5**, **A6**, and **A5**, it can be concluded that photo-electron transfer from the amine group quenches the fluorescence of the chromophore in the absence of cations. Therefore, by monitoring fluorescence emission intensity it is possible to determine the concentration of cations in solution. 1,3 alternate calixarene[4]arene-crown-5 was synthesized and found to form a 1:1 complex and have selectivity for potassium over all other alkali metal cations including sodium and lithium. Our current molecule, **V**, is expected to behave similarly based on its molecular architecture, and is predicted to selectively bind ammonium cations over potassium cations. Future work will focus on completing the synthesis of molecule **V** and characterizing its photophysical properties in the presence of ammonium cations.

## Appendix A

Pyrenyl-aza-crown-5



Current Data Parameters  
 NAME pyzacs5  
 EXPNO 70  
 PROCNO 1

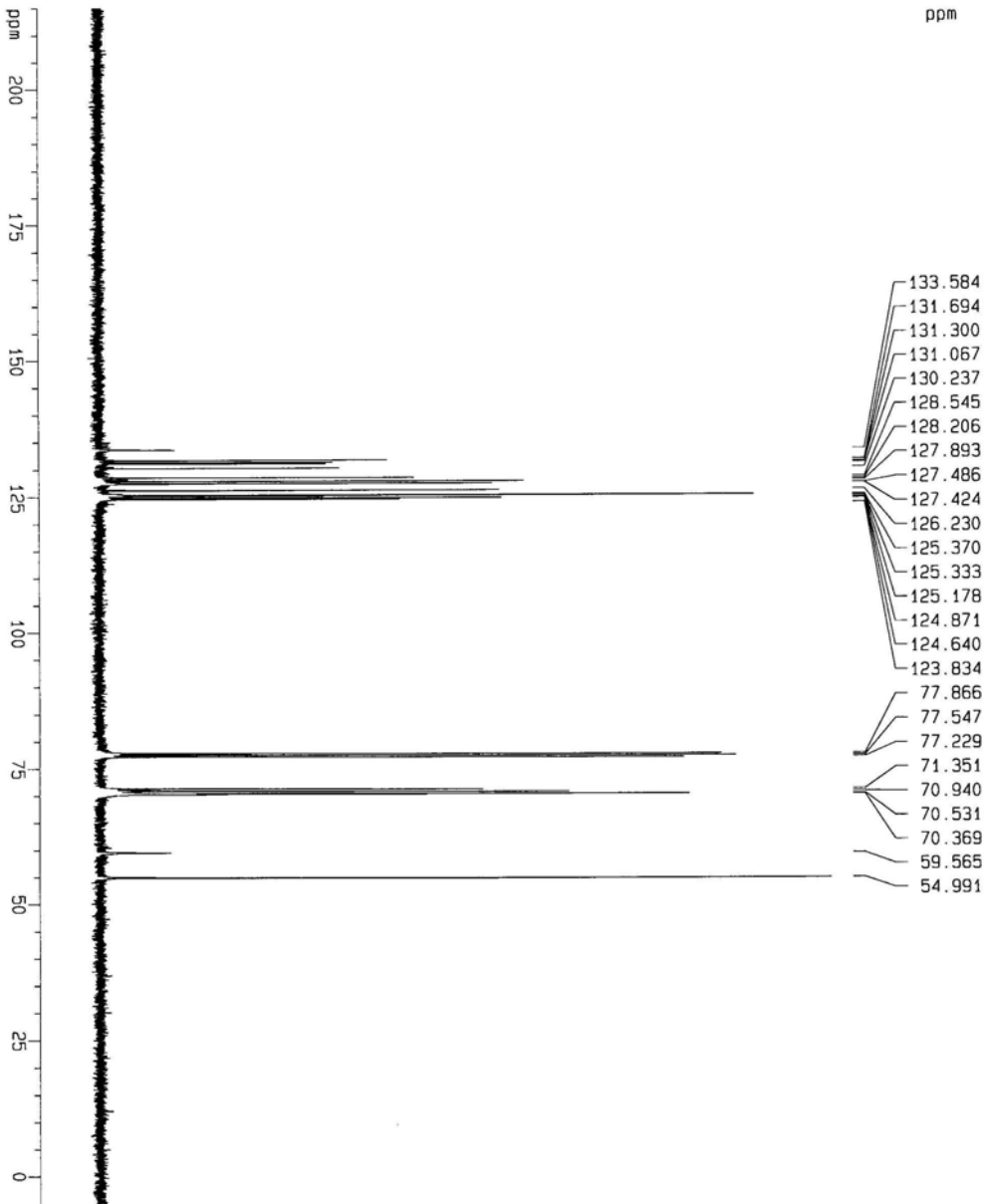
F2 - Acquisition Parameters  
 Date\_ 20010712  
 Time 17.24  
 INSTRUM spect  
 PROBM 5 mm Multinu  
 PULPROG zg30  
 TO 32768  
 SOLVENT CDCl3  
 NS 16  
 DS 2  
 SMH 8278.146 Hz  
 FIDRES 0.25629 Hz  
 AQ 1.9792372 sec  
 RG 35.9  
 DM 60.400 usec  
 DE 6.00 usec  
 TE 300.0 K  
 O1 1.00000000 sec

----- CHANNEL f1 -----  
 NUC1 1H  
 P1 9.00 usec  
 PL1 0.00 dB  
 SFO1 400.1324710 MHz

F2 - Processing parameters  
 SI 32768  
 SF 400.1300244 MHz  
 MDW EM  
 SSB 0  
 LB 0.30 Hz  
 GB 0  
 PC 1.00

1D NMR plot parameters  
 CX 20.00 cm  
 F1P 11.000 ppm  
 F1 4401.43 Hz  
 F2P -1.000 ppm  
 F2 -400.13 Hz  
 PPMCKM 0.50000 ppm/cm  
 HZCKM 240.07802 Hz/cm

Pyrenyl-aza-crown-5



Current Data Parameters  
 NAME pyzaccr5  
 EXPNO 71  
 PROCNO 1

F2 - Acquisition Parameters  
 Date\_ 20010712  
 Time 17.53

INSTRUM spect  
 PROBHD 5 mm Multinu  
 PULPROG zgpg30  
 TD 65536  
 SOLVENT CDCl3  
 NS 512  
 DS 4

SWH 25125.629 Hz  
 FIDRES 0.39387 Hz  
 AQ 1.3042184 sec  
 RG 4096  
 DW 19.900 usec  
 DE 6.00 usec  
 TE 300.0 K  
 D1 2.00000000 sec  
 d11 0.03000000 sec  
 d12 0.00002000 sec

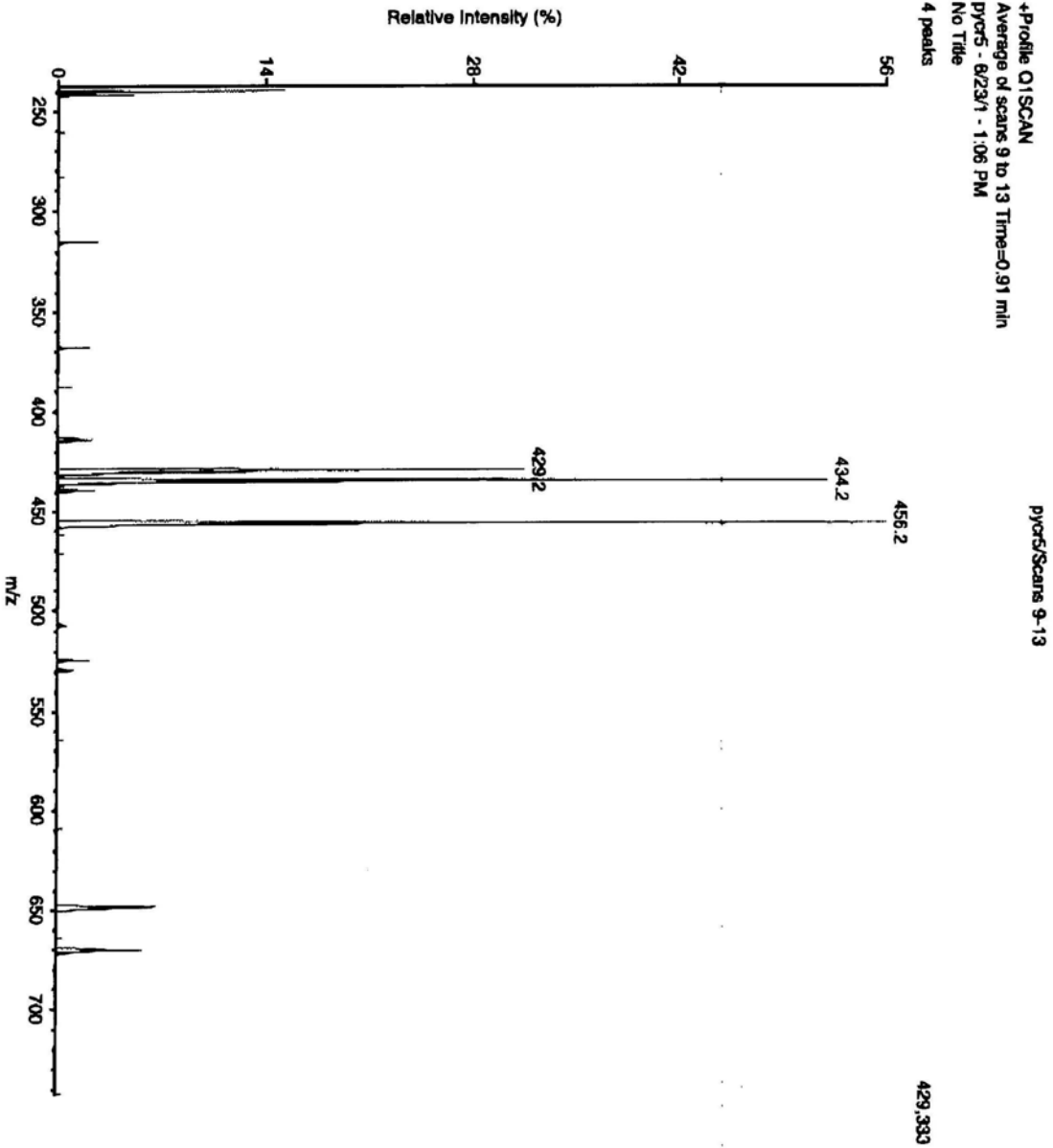
\*\*\*\*\* CHANNEL f1 \*\*\*\*\*  
 NUC1 13C  
 P1 10.70 usec  
 PL1 -1.00 dB  
 SF01 100.6237959 MHz

\*\*\*\*\* CHANNEL f2 \*\*\*\*\*  
 CPDPRG2 waltz16  
 NUC2 1H  
 PCHD2 80.00 usec  
 PL2 0.00 dB  
 PL12 20.00 dB  
 PL13 20.00 dB  
 SF02 400.1316005 MHz

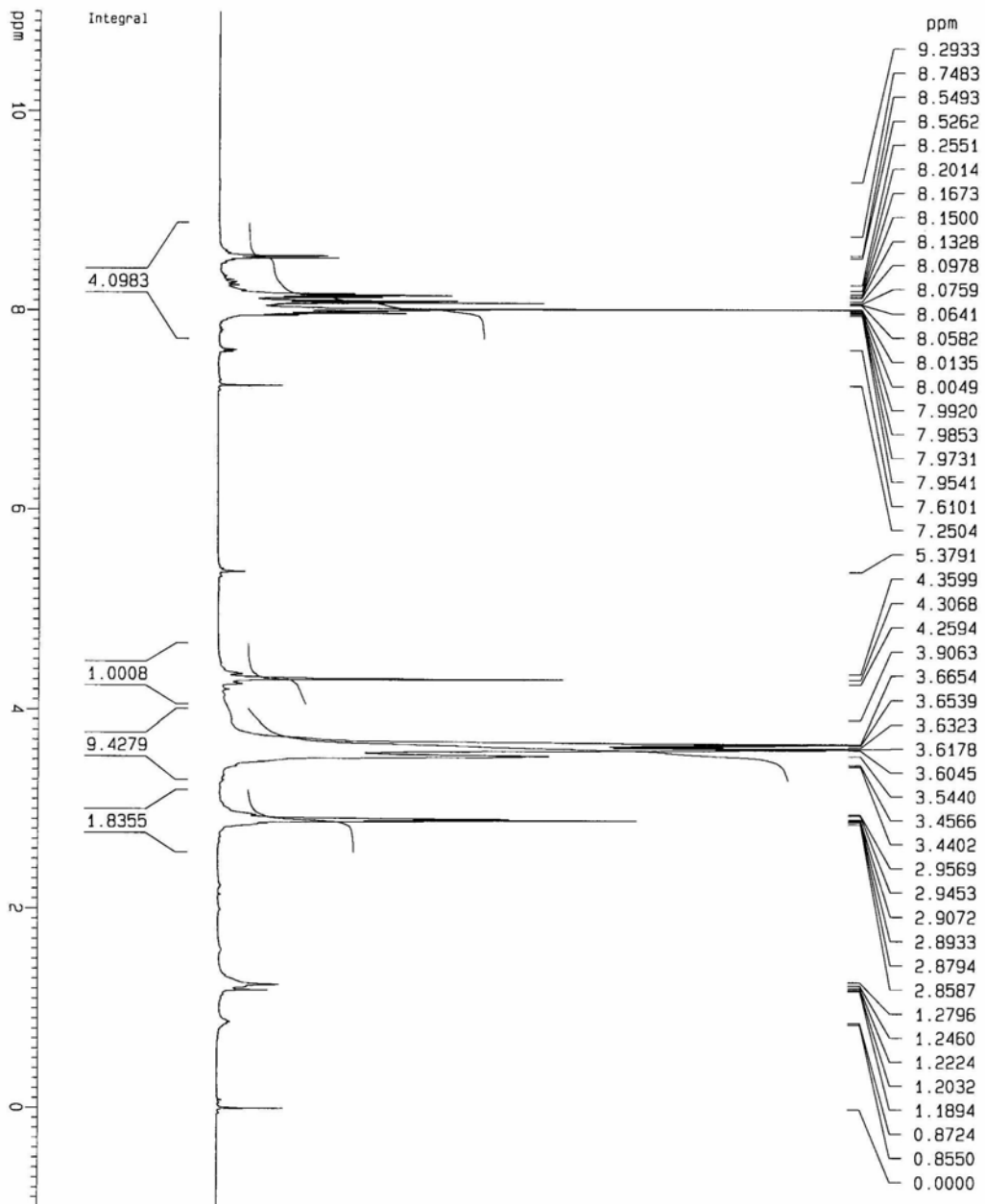
F2 - Processing parameters  
 SI 32768  
 SF 100.6127290 MHz  
 KW 0  
 SSB 0  
 LB 1.00 Hz  
 GB 0  
 PC 1.40

1D NMR plot parameters  
 CX 20.00 cm  
 F1P 215.000 ppm  
 F1 21631.74 Hz  
 F2P -53.000 ppm  
 F2 -503.06 Hz  
 PRPCK 11.00000 ppm/cm  
 HZCM 1106.73999 Hz/cm

DI 50  
 ISV 5000  
 IN 650  
 OR 120  
 R0 30  
 M1 1000  
 RE1 121.0000  
 DM1 0  
 F1 27.2  
 L7 -10  
 R2 -70  
 M3 1000  
 RE3 118  
 DM3 0.060  
 RX -30  
 R3 -70  
 L9 150  
 FP -50  
 MU -5000  
 CC 10  
 DI μA 2.08  
 CGT -4.0  
 IS v 5119.7  
 B-RAM -10,004.9



Pyrenyl-1-aza-crown-6



Current Data Parameters  
 NAME pyazacr6  
 EXPNO 10  
 PROCNO 1

F2 - Acquisition Parameters  
 Date\_ 20010927  
 Time 15.04

INSTRUM spect  
 PROBRD 5 mm Multinu  
 PULPROG zg30

TD 32768  
 SOLVENT CDCl3  
 NS 16

DS 2  
 SMH 8278.146 Hz  
 FIDRES 0.252629 Hz

AQ 1.9792372 sec  
 RG 35.9

DM 60.400 usec  
 DE 6.00 usec

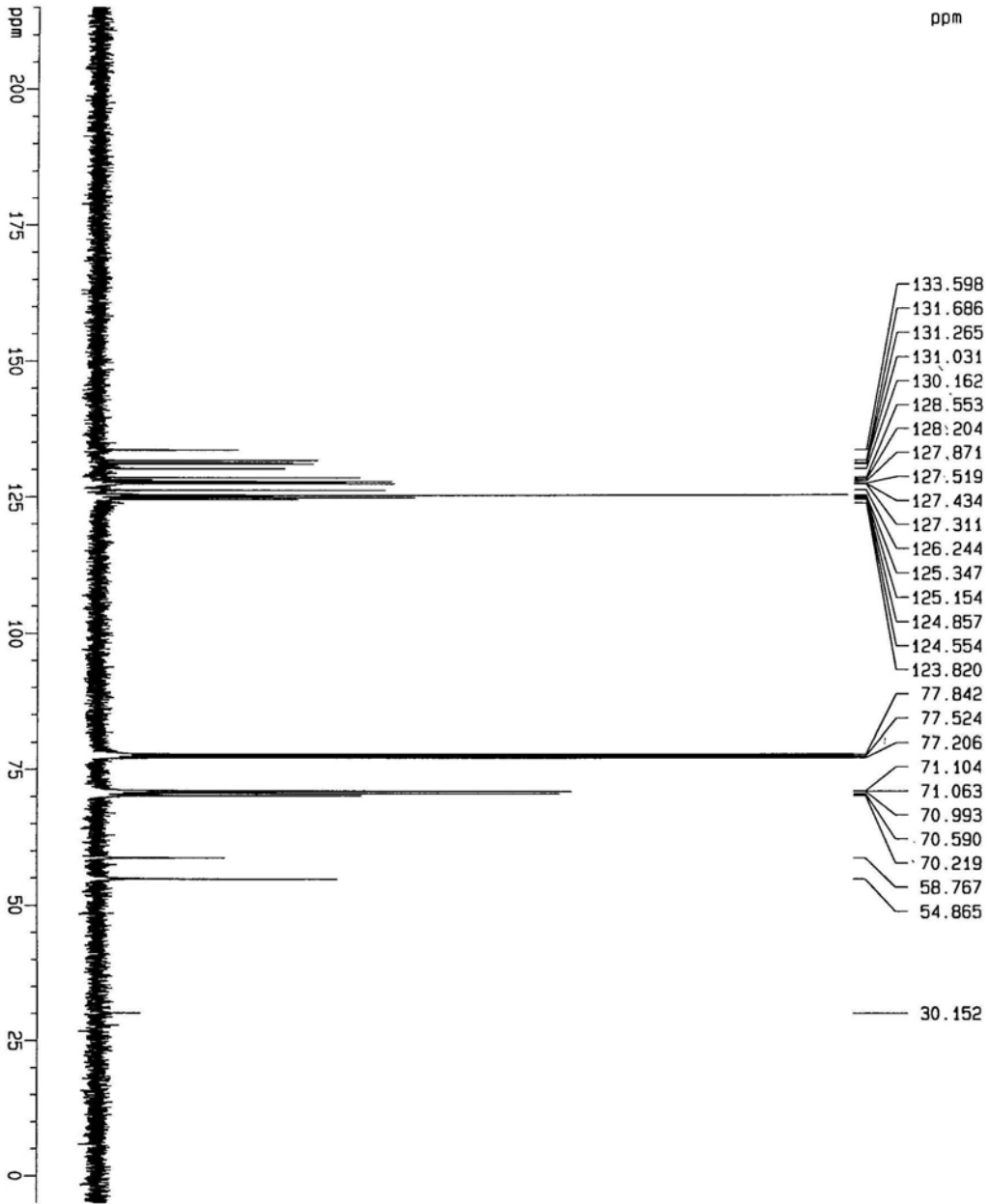
TE 300.0 K  
 D1 1.00000000 sec

\*\*\*\*\* CHANNEL f1 \*\*\*\*\*  
 NUC1 1H  
 P1 10.00 usec  
 PL1 0.00 dB  
 SF01 400.1324710 MHz

F2 - Processing Parameters  
 SI 32768  
 SF 400.1300133 MHz  
 MDW EM  
 SSB 0  
 LB 0.30 Hz  
 GB 0  
 PC 1.00

1D NMR plot parameters  
 CX 20.00 cm  
 F1P 11.000 ppm  
 F1 4401.43 Hz  
 F2P -1.000 ppm  
 F2 -400.13 Hz  
 PPMCM 0.50000 ppm/cm  
 HZCM 240.07800 Hz/cm

Pyrenyl- $\alpha$ -CROWN-6



Current Data Parameters  
NAME pyzarc6  
EXPNO 11  
PROCNO 1

F2 - Acquisition Parameters

Date\_ 20010927  
Time 15.33  
INSTRUM spect  
PROBHD 5 mm Nujlinu  
PULPROG zgpg30  
TD 65536  
SOLVENT CDCl3  
NS 512  
DS 4  
SMH 25125.629 Hz  
FIDRES 0.38387 Hz  
AQ 1.3042164 sec  
RG 8192  
DE 19.900 usec  
TE 300.0 K  
D1 2.00000000 sec  
d11 0.03000000 sec  
d12 0.00020000 sec

\*\*\*\*\* CHANNEL f1 \*\*\*\*\*  
NUC1 13C  
P1 8.70 usec  
PL1 0.00 dB  
SF01 100.62373569 MHz

\*\*\*\*\* CHANNEL f2 \*\*\*\*\*  
CPDPRG2 waltz16  
NUC2 1H  
PCPD2 107.00 usec  
PL2 0.00 dB  
PL12 23.00 dB  
PL13 23.00 dB  
SF02 400.1316005 MHz

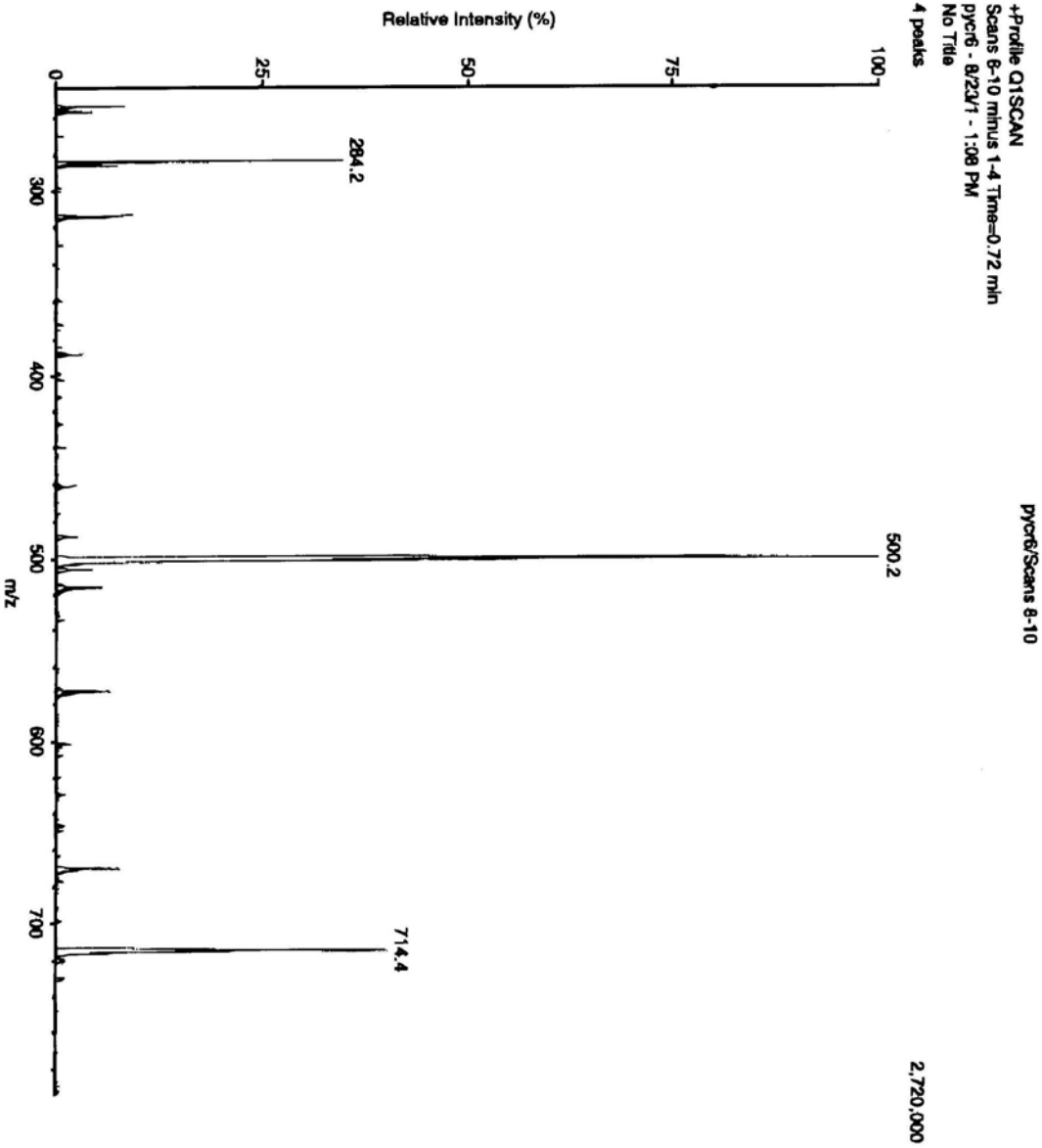
F2 - Processing parameters

SF 32768  
SF 100.6127290 MHz  
KDM 0  
SSB 0  
LB 1.00 Hz  
GB 0  
PC 1.40

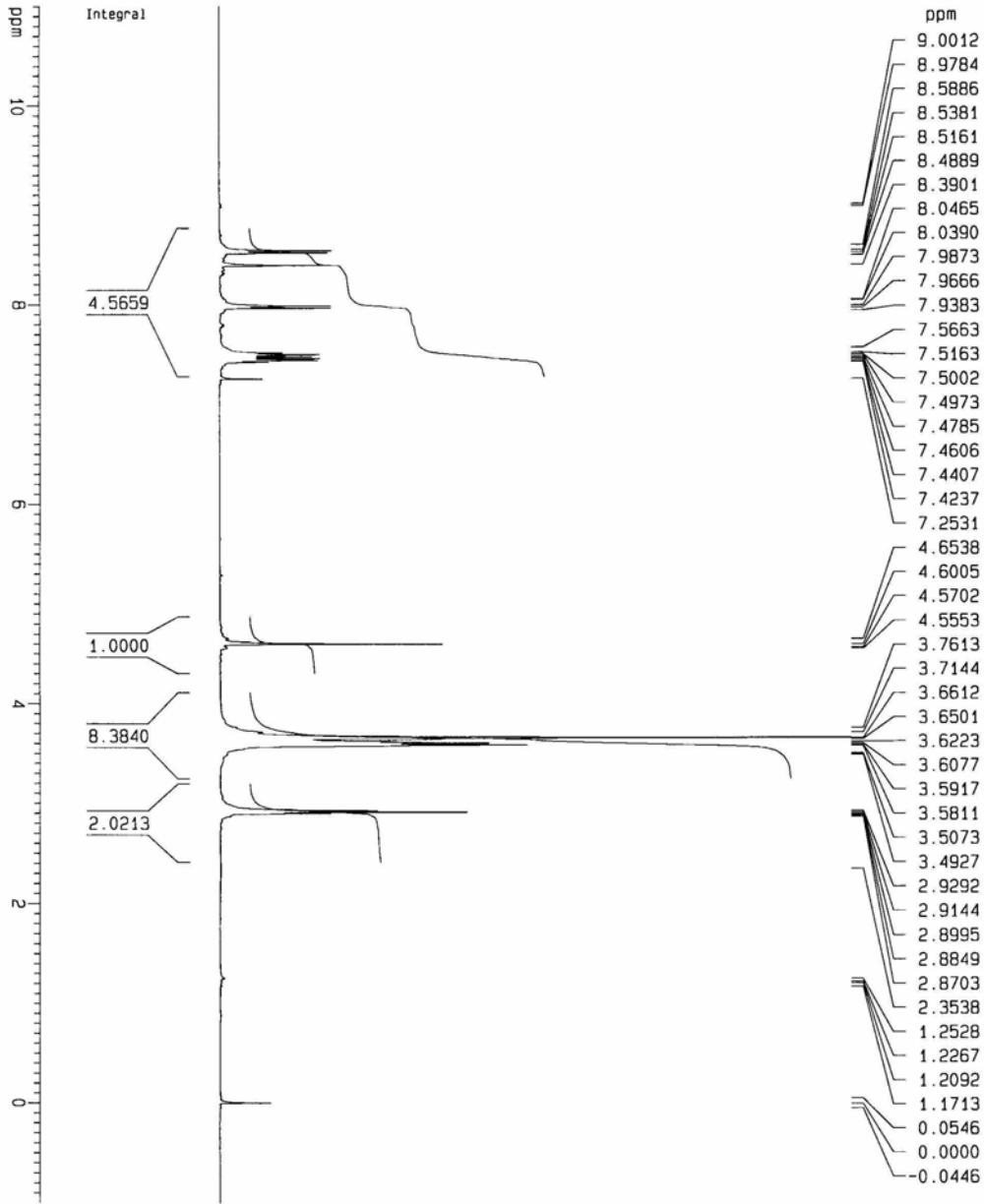
1D NMR plot parameters

CX 20.00 cm  
F1P 215.000 ppm  
F1 21631.74 Hz  
F2P -5.000 ppm  
F2 -503.06 Hz  
PPHCM 11.00000 ppm/cm  
HZCM 1106.73999 Hz/cm

DI 50  
 ISV 5000  
 IN 650  
 OR 120  
 R0 30  
 M1 1000  
 RE1 121.0000  
 DM1 0  
 R1 27.2  
 L7 -10  
 R2 -70  
 M3 1000  
 RE3 118  
 DM3 0.060  
 RX -30  
 R3 -70  
 L9 150  
 FP -50  
 MU -5000  
 CC 10  
 Di PA 5.007  
 CGT -1.3  
 IS V 5109.9  
 0-RAM -10.004.9



Anthryl-aza-crown-5



Current Data Parameters

NAME	anr5
EXPNO	20
PROCNO	1

F2 - Acquisition Parameters

Date_	20010910
Time	15.24
INSTRUM	spect
PROBHD	5 mm Multinu
PULPROG	zg30
TD	32768
SOLVENT	CDCl3
NS	16
DS	2
SMH	8278.146 Hz
FTDRES	0.252629 Hz
AQ	1.9792372 sec
RG	90.5
DM	60.400 usec
DE	5.00 usec
TE	300.0 K
D1	1.00000000 sec

===== CHANNEL f1 =====

NUC1	1H
P1	10.00 usec
PL1	0.00 dB
SFO1	400.1324710 MHz

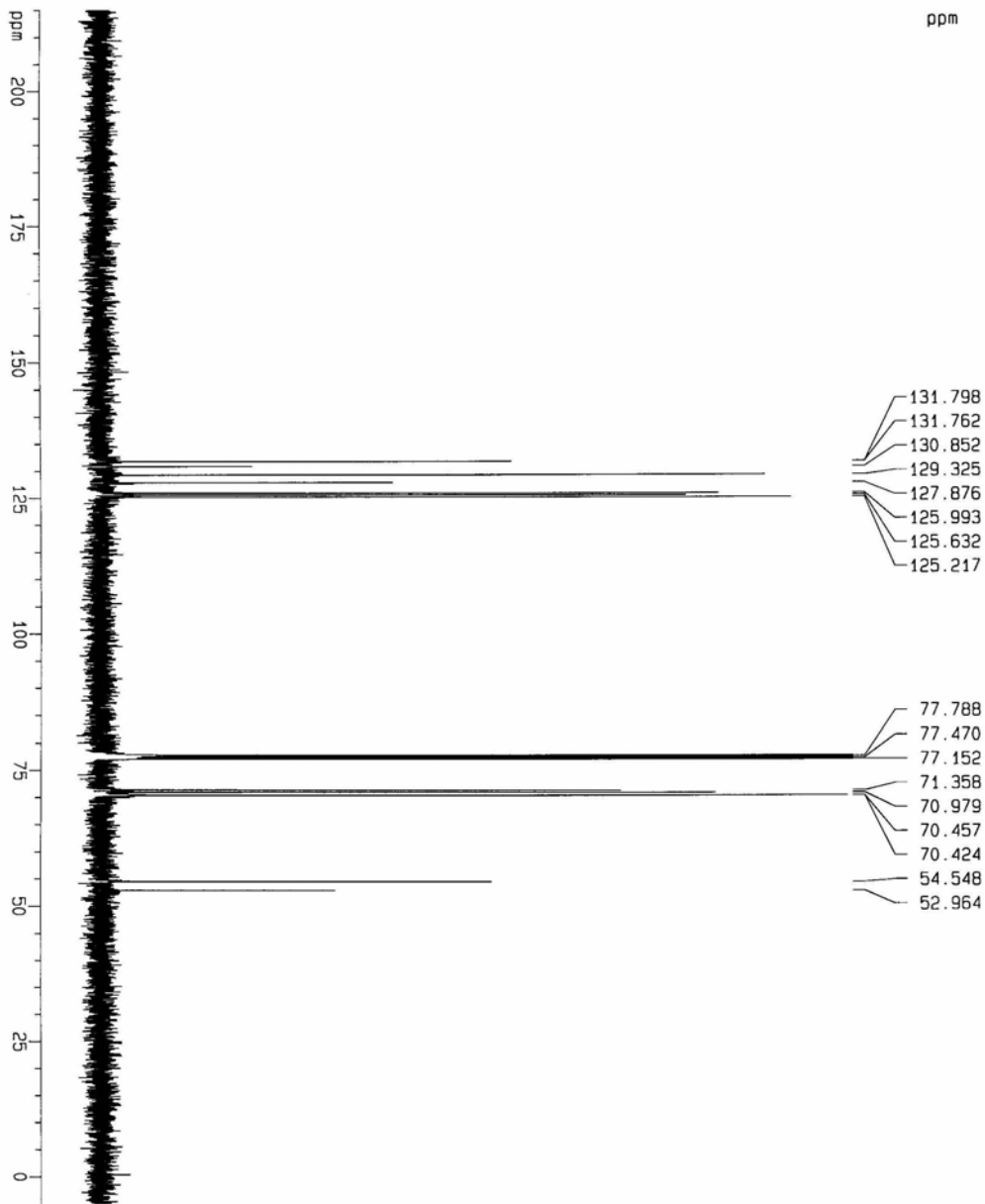
F2 - Processing parameters

SI	32768
SF	400.1300119 MHz
MWM	EM
SSB	0
LB	0.30 Hz
GB	0
PC	1.00

1D NMR plot parameters

CX	20.00 cm
F1P	11.000 ppm
F1	4401.43 Hz
F2P	-1.000 ppm
F2	-400.13 Hz
PPM/CM	0.60000 ppm/cm
HZ/CM	240.07800 Hz/cm

Anthr[1]-aza-CROWN-5



Current Data Parameters  
 NAME anthr5  
 EXPNO 21  
 PROCNO 1

F2 - Acquisition Parameters  
 Date\_ 20010910  
 Time 15.53

INSTRUM spect  
 PROBD 5 mm W/11nu  
 PULPROG zgpg30  
 TD 65536  
 SOLVENT CDCl3  
 NS 512  
 DS 4

SMH 25125.629 Hz  
 FIDRES 0.383387 Hz  
 AQ 1.3042184 sec  
 RG 8192

DE 19.900 usec  
 TE 300.0 K  
 O1 2.0000000 sec  
 d11 0.0300000 sec  
 d12 0.0000200 sec

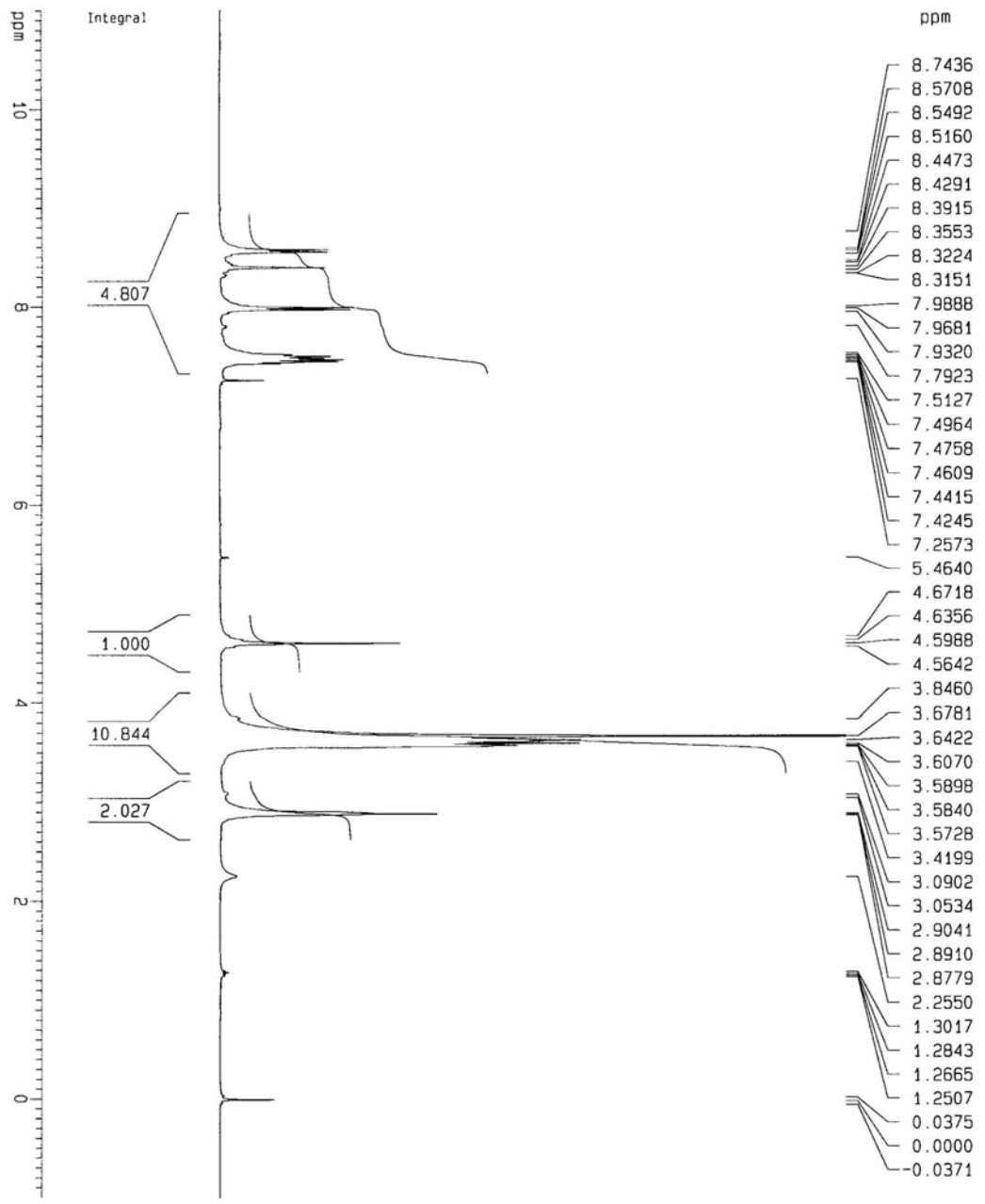
CHANNEL f1  
 NUC1 13C  
 P1 8.70 usec  
 PL1 0.00 dB  
 SF01 100.6237959 MHz

CHANNEL f2  
 CPDPRG2 waltz16  
 NUC2 1H  
 PCPD2 107.00 usec  
 PL2 0.00 dB  
 PL12 23.00 dB  
 PL13 23.00 dB  
 SF02 400.1316005 MHz

F2 - Processing parameters  
 SI 32768  
 SF 100.6127290 MHz  
 MDW EM  
 SSB 0  
 LB 1.00 Hz  
 GB 0  
 PC 1.40

1D NMR plot parameters  
 CX 20.00 cm  
 F1P 215.000 ppm  
 F1 21631.74 Hz  
 F2P -503.06 ppm  
 F2 11.00000 ppm/cm  
 HZCK 1106.73999 Hz/cm

Anthryl-aza-crown-6



Current Data Parameters  
 NAME ANTHRILAZACROW  
 EXPNO 10  
 PROCNO 1

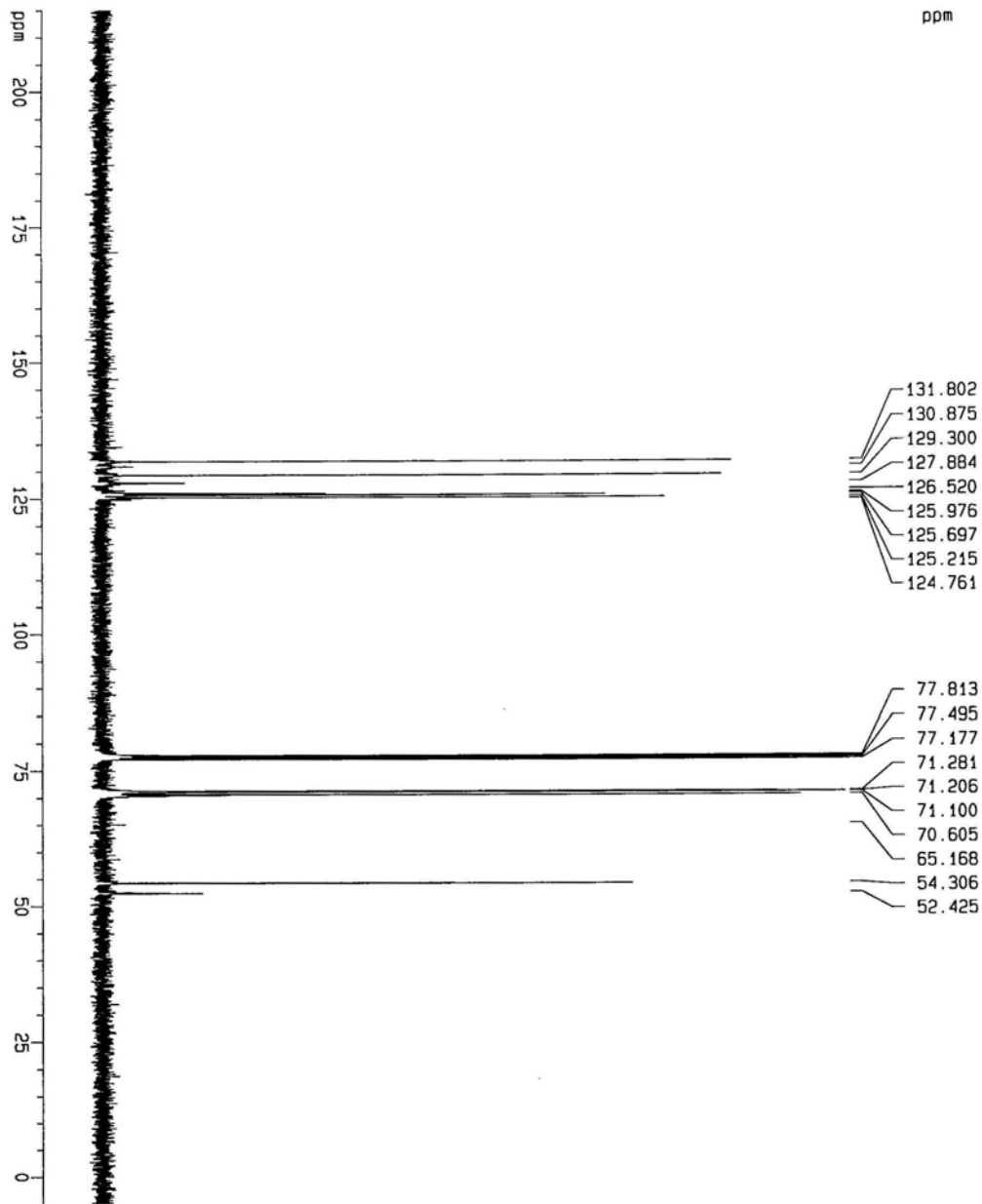
F2 - Acquisition Parameters  
 Date\_ 20010618  
 Time 15.25  
 INSTRUM spect  
 PROBHD 5 mm Multinu  
 PULPROG zg30  
 TD 32768  
 SOLVENT CDCl3  
 NS 16  
 DS 2  
 SMH 8278.146 Hz  
 FIDRES 0.259629 Hz  
 AQ 1.9792372 sec  
 RG 143.7  
 DM 60.400 usec  
 DE 6.00 usec  
 TE 300.0 K  
 D1 1.00000000 sec

===== CHANNEL f1 =====  
 NUC1 1H  
 P1 9.00 usec  
 PL1 0.00 dB  
 SF01 400.1324710 MHz

F2 - Processing parameters  
 SI 32768  
 SF 400.1300110 MHz  
 WDW EM  
 SSB 0  
 LB 0.30 Hz  
 GB 0  
 PC 1.00

1D NMR plot parameters  
 CX 20.00 cm  
 F1P 11.000 ppm  
 F1 4401.43 Hz  
 F2P -1.000 ppm  
 F2 -400.13 Hz  
 PPMCM 0.60000 ppm/cm  
 HZCM 240.07800 Hz/cm

Anthryl-9-za-crown-6



```

Current Data Parameters
NAME      anthryl-9za-cr
EXPNO    11
PROCNO   1

F2 - Acquisition Parameters
Date_    2010615
Time     18.46
INSTRUM  spect
PROBHD   5 mm Multinu
PULPROG  zgpg30
TD        65536
SOLVENT  CDCl3
NS        512
DS        4
SMH       25129.629 Hz
FIDRES    0.383387 Hz
AQ         1.3042164 sec
RG         4096
DE         19.900 usec
TE         300.0 K
D1         2.00000000 sec
d11        0.03000000 sec
d12        0.00002000 sec

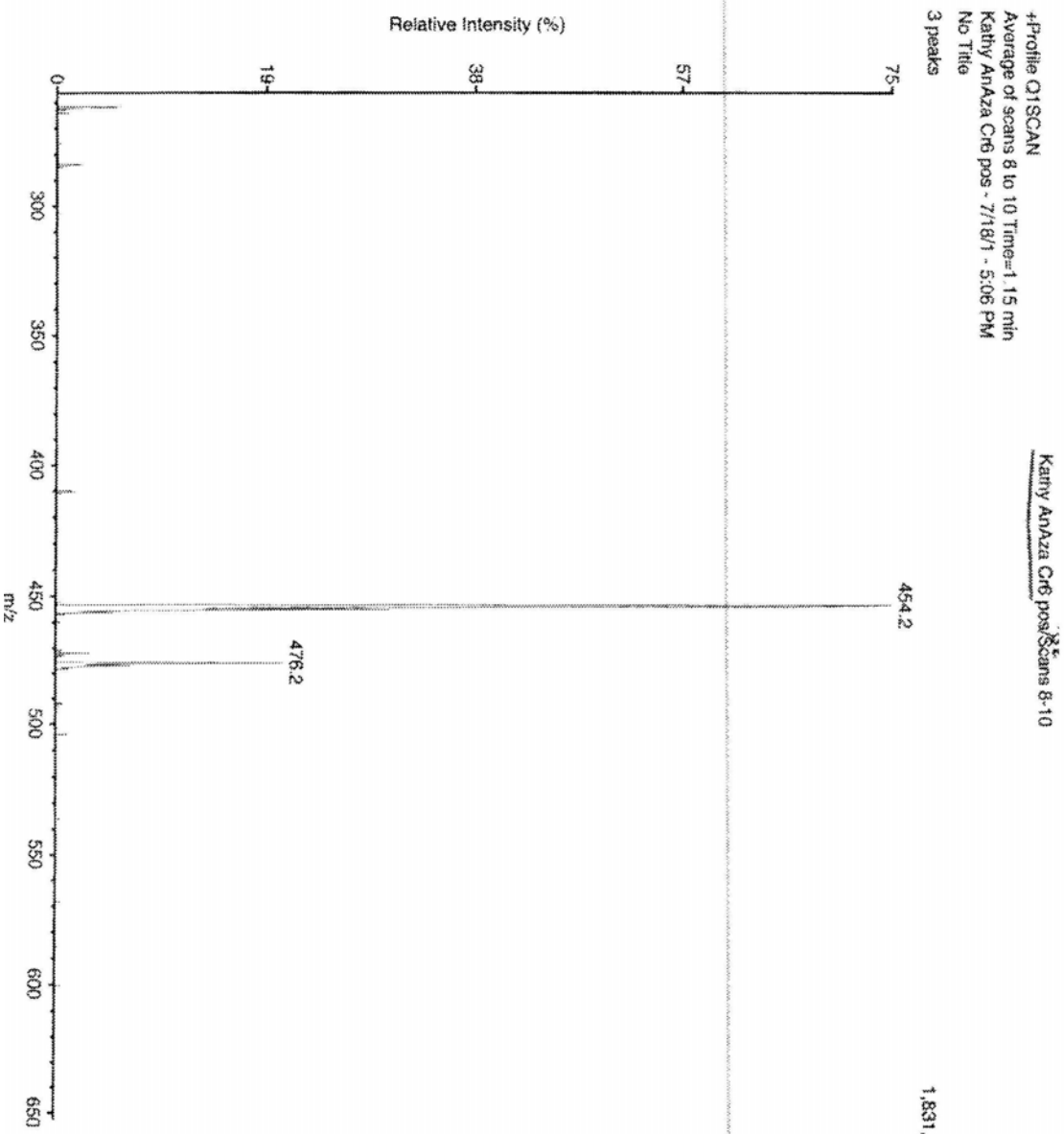
----- CHANNEL f1 -----
NUC1      13C
P1        10.70 usec
PL1       -1.00 dB
SFO1      100.6237959 MHz

----- CHANNEL f2 -----
CPOPRG2   waltz16
NUC2       1H
PCPD2      80.00 usec
PL2        0.00 dB
PL12       20.00 dB
PL13       20.00 dB
SFO2       400.1316005 MHz

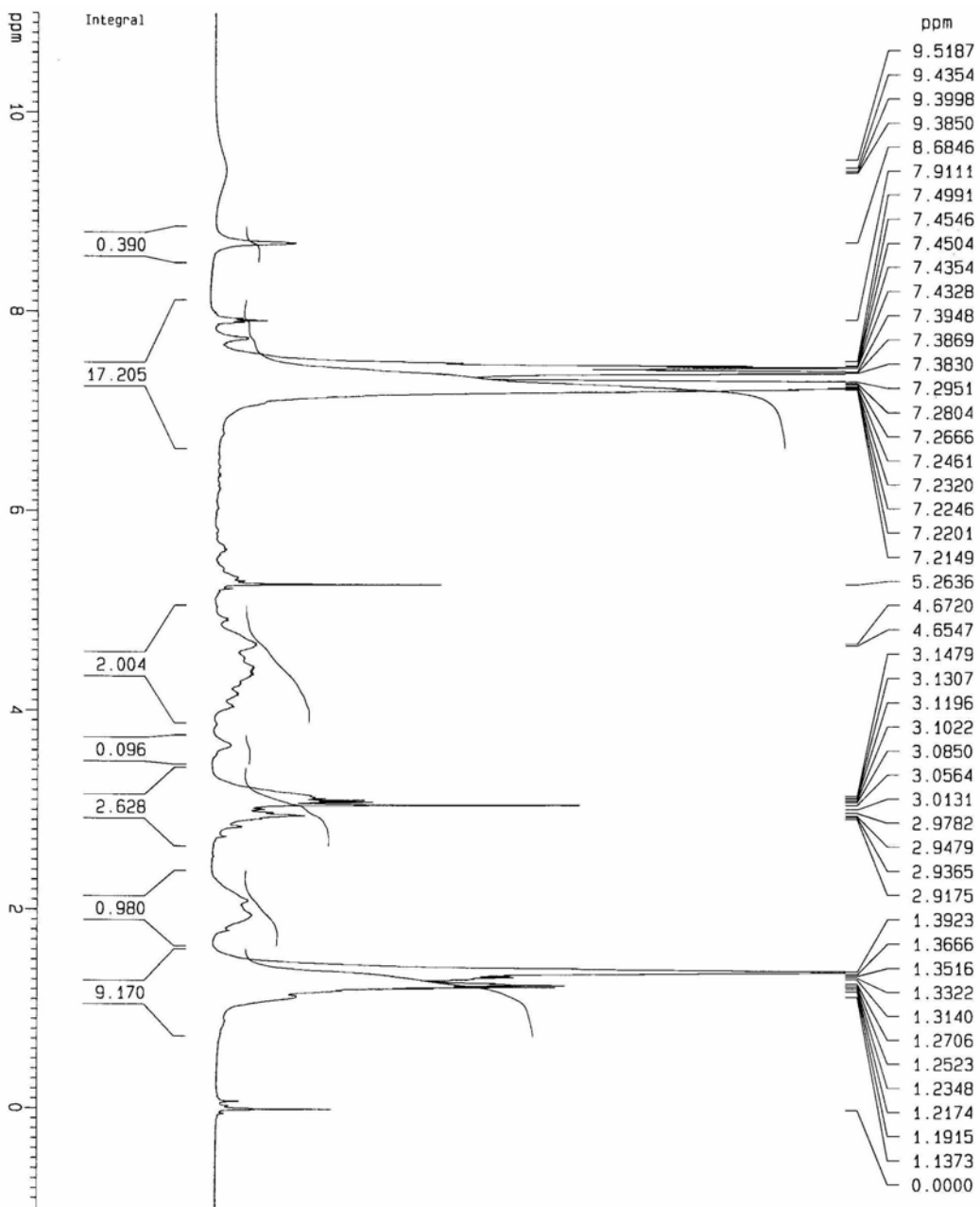
F2 - Processing parameters
SI         32768
SF         100.6127290 MHz
WDW        EM
SSB        0
LB         1.00 Hz
GB         0
PC         1.40

1D NMR plot parameters
CX         20.00 cm
F1P        215.000 ppm
F1         21631.74 Hz
F2P        -5.000 ppm
F2         -503.06 Hz
PPMCM      11.00000 ppm/cm
HZCM       1106.73999 Hz/cm
    
```

DI 50  
 ISV 5000  
 IN 650  
 OR 120  
 R0 30  
 M1 1000  
 RE1 121.0000  
 DM1 0  
 F1 27.2  
 L7 -10  
 R2 -70  
 M3 1000  
 RE3 118  
 DM3 0.060  
 RX -30  
 R3 -70  
 L9 150  
 FP -50  
 MU -5000  
 CC 10  
 DI  $\mu$ A 2.08  
 CGT -2.6  
 IS V 5090.4  
 B-RAM -10,004.9



Linear Peptide (tct) -tboc



Current Data Parameters  
 NAME 1impeprt-tboc  
 EXPNO 10  
 PROCNO 1

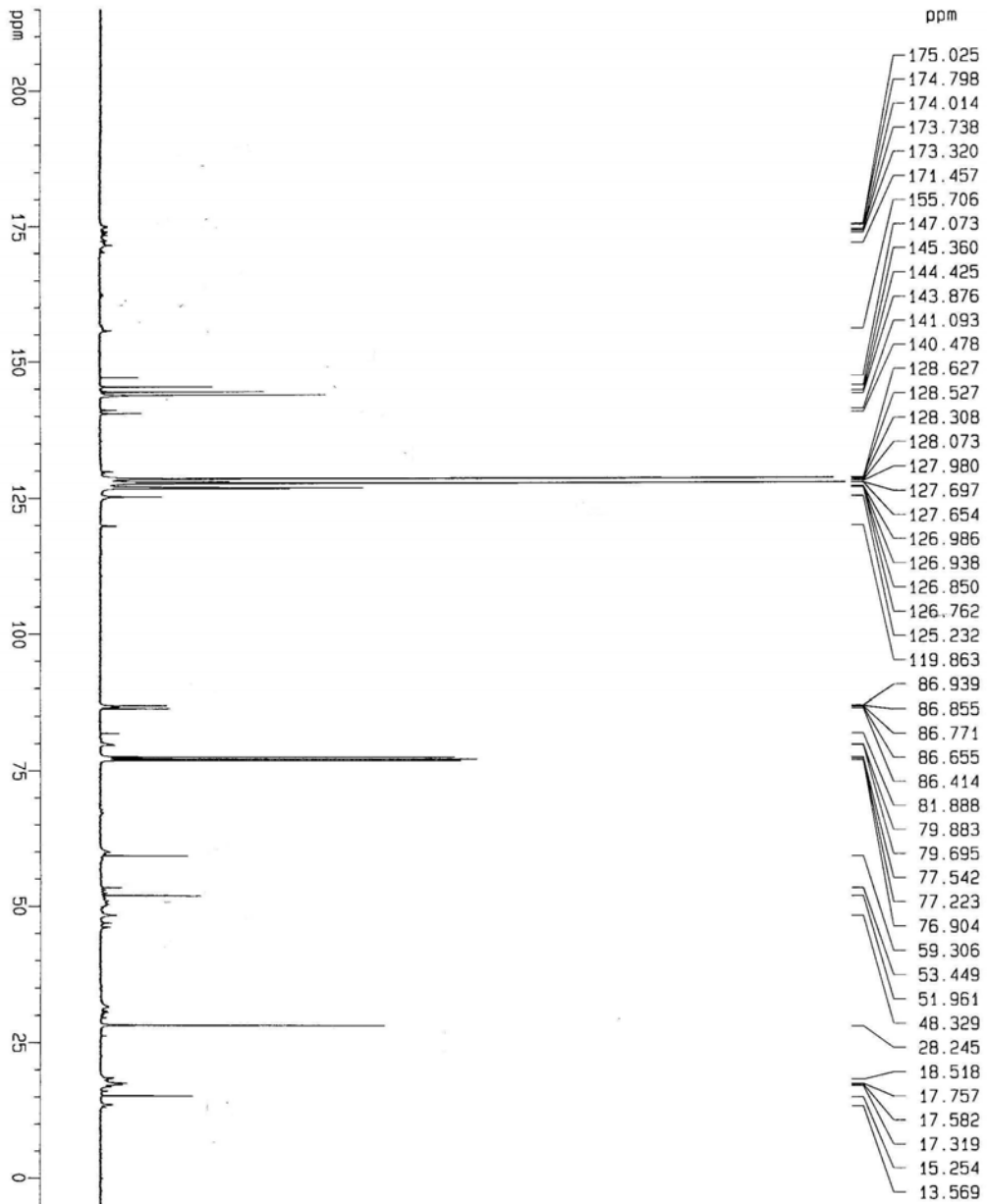
F2 - Acquisition Parameters  
 Date\_ 20020702  
 Time 2.47  
 INSTRUM spect  
 PROBRD 5 mm Multinu  
 PULPROG zg30  
 TO 32768  
 SOLVENT CDCl3  
 NS 16  
 DS 2  
 SMH 8278.145 Hz  
 FIDRES 0.252629 Hz  
 AQ 1.9792372 sec  
 RG 71.8  
 DM 60.400 usec  
 DE 6.00 usec  
 TE 300.0 K  
 D1 1.00000000 sec

\*\*\*\*\* CHANNEL f1 \*\*\*\*\*  
 NUC1 1H  
 P1 8.75 usec  
 PL1 0.00 dB  
 SF01 400.1324710 MHz

F2 - Processing parameters  
 SI 32768  
 SF 400.1300158 MHz  
 WDW EM  
 SSB 0  
 LB 0.30 Hz  
 GB 0  
 PC 1.00

10 NMR plot parameters  
 CX 20.00 cm  
 F1P 11.000 ppm  
 F1 4401.43 Hz  
 F2P -1.000 ppm  
 F2 -400.13 Hz  
 PPMCN 0.60000 ppm/cm  
 HZCN 240.07800 Hz/cm

Linear Peptide (trt)-tboc



```

Current Data Parameters
NAME      1:linpeptide-tboc
EXPNO     1
PROCNO    1

F2 - Acquisition Parameters
Date_     20090702
Time      7.34
INSTRUM   spect
PROBHD    5 mm MUltinu
PULPROG   zgpg30
TD         65536
SOLVENT   CDCl3
NS         5000
DS         4
SMH        25125.629 Hz
FIDRES    0.363387 Hz
AQ         1.3042164 sec
RG         4096
DM         19.900 usec
DE         6.00 usec
TE         300.0 K
D1         2.00000000 sec
d11        0.03000000 sec
d12        0.00002000 sec

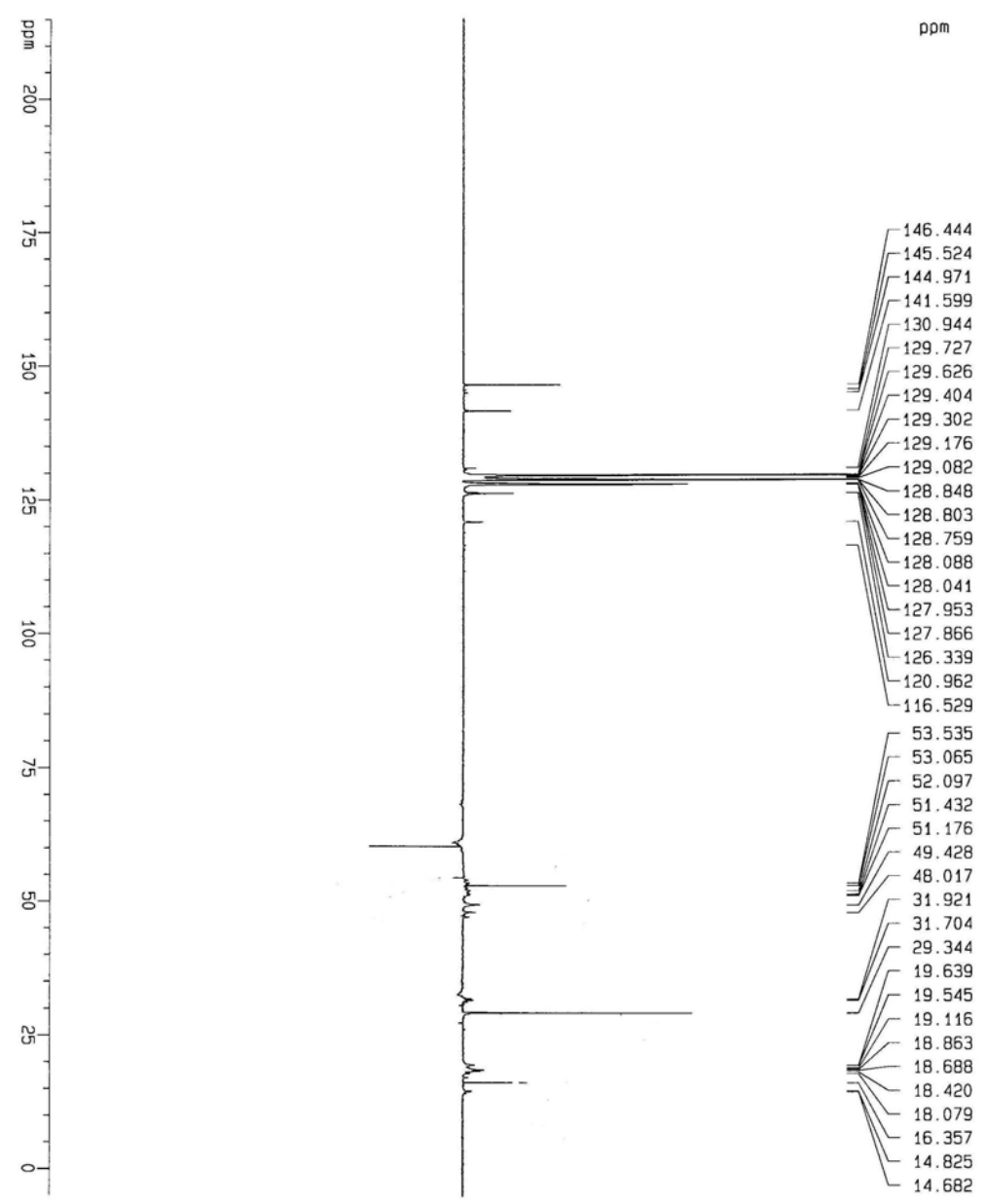
===== CHANNEL f1 =====
NUC1       13C
P1         8.70 usec
PL1        0.00 dB
SF01       100.6237959 MHz

===== CHANNEL f2 =====
CPDPRG2   waltz16
NUC2       1H
PCPD2     107.00 usec
PL2        0.00 dB
PL12      23.00 dB
PL13      23.00 dB
SF02       400.1316005 MHz

F2 - Processing parameters
SI         32768
SF         100.6127851 MHz
WDW        EM
SSB        0
LB         1.00 Hz
GB         0
PC         1.40

10 NMR plot parameters
CX         20.00 cm
F1P        215.000 ppm
F1         21631.75 Hz
F2P        -503.06 Hz
F2         -503.06 Hz
PPHCK      11.00000 ppm/cm
HZCK       1106.74000 Hz/cm
    
```

Linear Peptide (trt)-tboc



```

Current Data Parameters
NAME      1:linear-trt-tboc
EXPNO    12
PROCNO   1

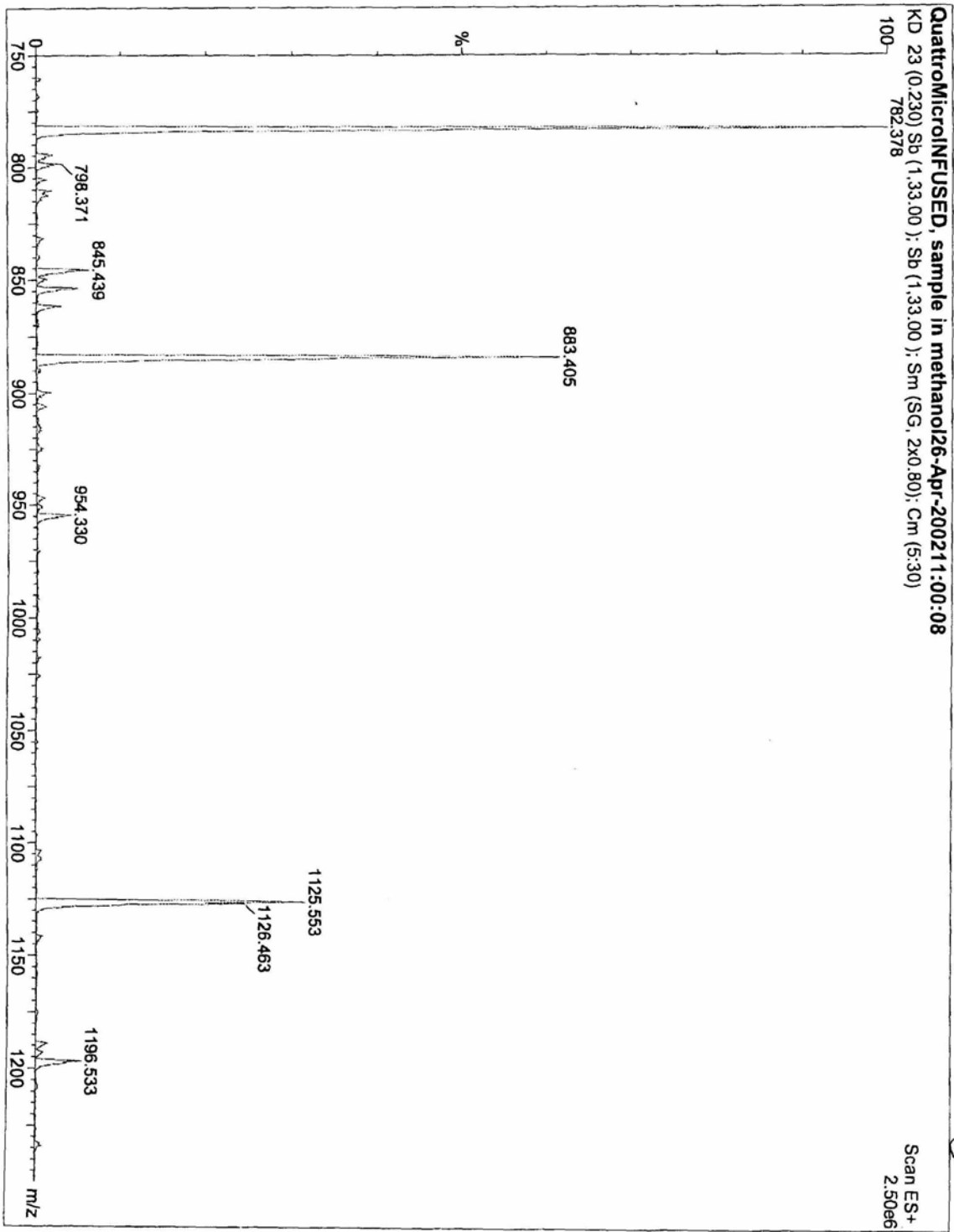
F2 - Acquisition Parameters
Date_    20020702
Time     9:56
INSTRUM  spect
PROBHD   5 mm Multinu
PULPROG  zgpg13s
TD        65536
SOLVENT  CDCl3
NS        2500
DS        4
SMH       23980.814 Hz
FIDRES   0.365918 Hz
AQ        1.3664756 sec
RG         8192
DM        20.850 usec
DE         6.00 usec
TE        300.0 K
CONST1   145.0000000
D1        2.0000000 sec
D2        0.00344828 sec
d12       0.0002000 sec
DELTA    6386.18261719 sec

***** CHANNEL f1 *****
NUC1      13C
P1        8.70 usec
D2        17.40 usec
PL1       0.00 dB
SFO1      100.6227898 MHz

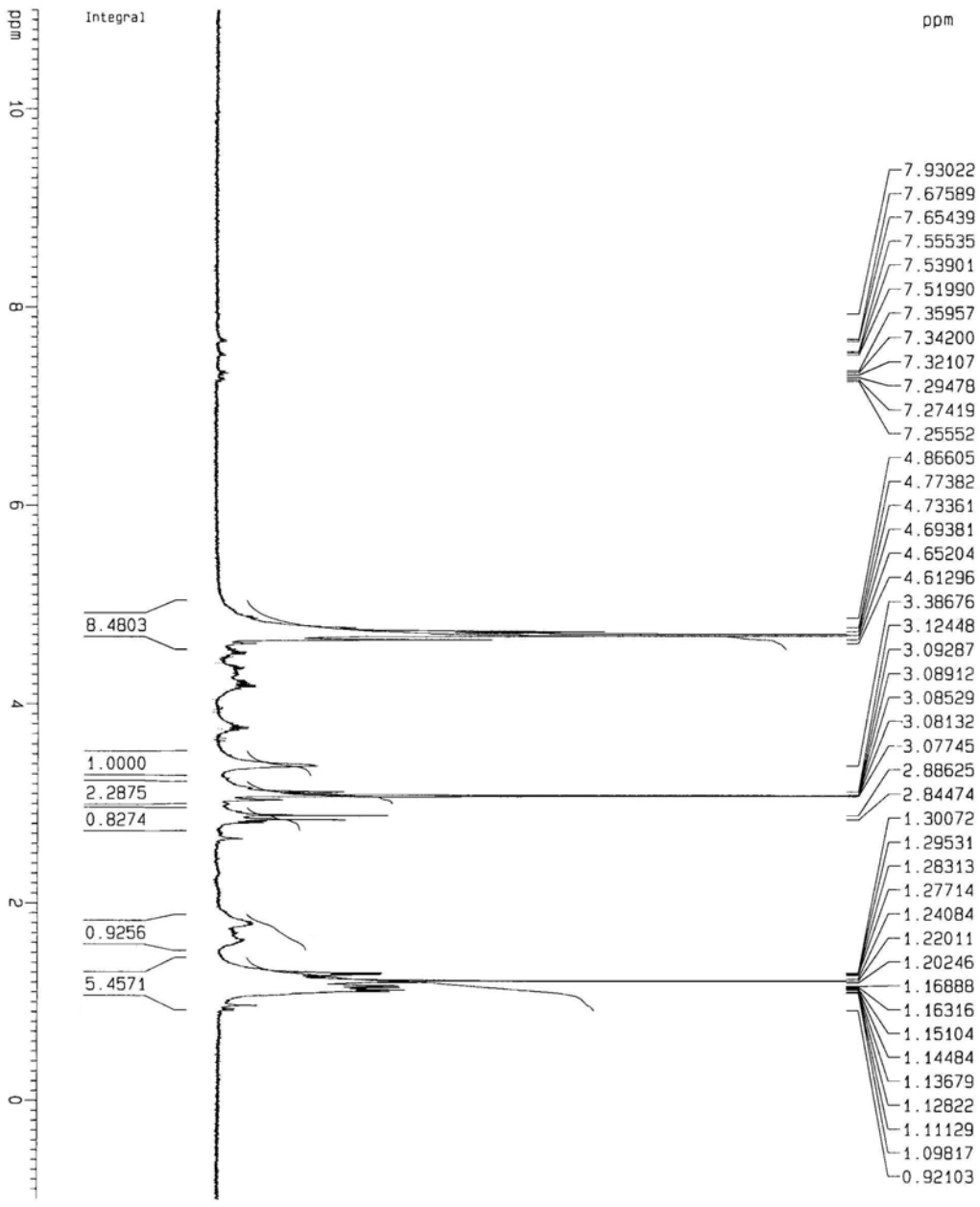
***** CHANNEL f2 *****
OPDRPG2   waltz16
NUC2      1H
P3        8.70 usec
P4        17.40 usec
PCPD2     107.00 usec
PL2       0.00 dB
PL12      23.00 dB
SFO2      400.1316005 MHz

F2 - Processing parameters
SI        32768
SF        100.6126746 MHz
MCK       EM
SSB       0
LB        1.00 Hz
GB        0
PC        1.40

1D NMR plot parameters
CX        20.00 cm
F1P       2191.000 ppm
F1        21631.73 Hz
F2P       -5.000 ppm
F2        -503.06 Hz
PPH2CH    11.00000 ppm/cm
HZCX      1105.73938 Hz/cm
    
```



Linear Peptide-tboc



- 7.93022
- 7.67589
- 7.65439
- 7.55535
- 7.53901
- 7.51990
- 7.35957
- 7.34200
- 7.32107
- 7.29478
- 7.27419
- 7.25552
- 4.86605
- 4.77382
- 4.73361
- 4.69381
- 4.65204
- 4.61296
- 3.38676
- 3.12448
- 3.09287
- 3.08912
- 3.08529
- 3.08132
- 3.07745
- 2.88625
- 2.84474
- 1.30072
- 1.29531
- 1.28313
- 1.27714
- 1.24084
- 1.22011
- 1.20246
- 1.16888
- 1.16316
- 1.15104
- 1.14484
- 1.13679
- 1.12822
- 1.11129
- 1.09817
- 0.92103

Current Data Parameters  
 NAME 1inpeptboc  
 EXPNO 10  
 PROCNO 1

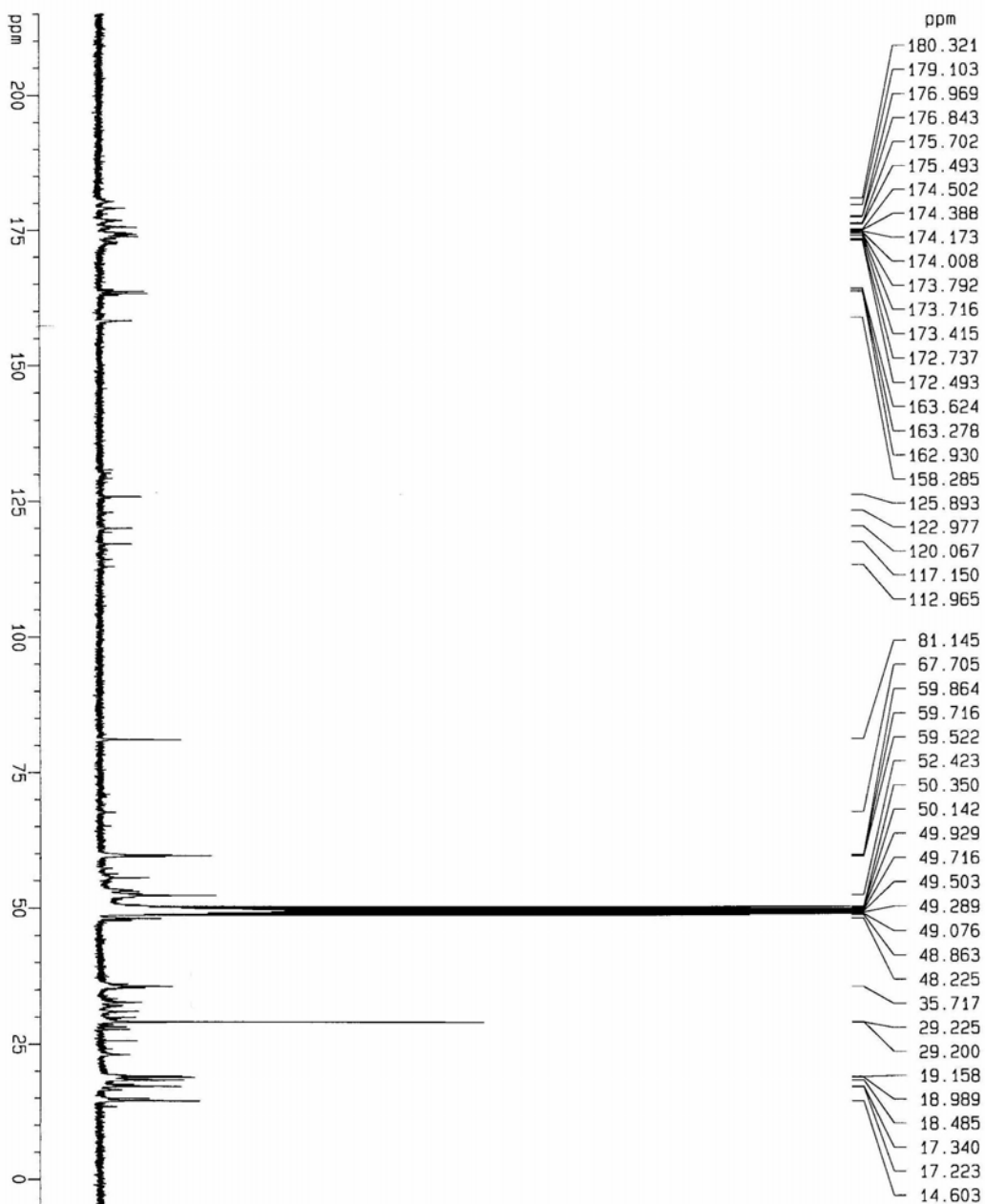
F2 - Acquisition Parameters  
 Date\_ 20020506  
 Time 7.44  
 INSTRUM spect  
 PROBHD 5 mm Multinu  
 PULPROG zg30  
 TD 32768  
 SOLVENT MeOH  
 NS 16  
 DS 2  
 SMH 8278.146 Hz  
 FIDRES 0.252629 Hz  
 AQ 1.9792372 sec  
 RG 574.7  
 DM 60.400 usec  
 DE 6.00 usec  
 TE 300.0 K  
 D1 1.00000000 sec

\*\*\*\*\* CHANNEL f1 \*\*\*\*\*  
 NUC1 1H  
 P1 8.75 usec  
 PL1 0.00 dB  
 SF01 400.1324710 MHz

F2 - Processing parameters  
 SI 32768  
 SF 400.1300976 MHz  
 MDM EM  
 SSB 0  
 LB 0.30 Hz  
 GB 0  
 PC 1.00

10 NMR plot parameters  
 CX 20.00 cm  
 F1P 11.000 ppm  
 F1 4401.43 Hz  
 F2P -1.000 ppm  
 F2 -400.13 Hz  
 PPMCM 0.60000 ppm/cm  
 HZCM 240.07806 Hz/cm

Linear Peptide - tbc2



Current Data Parameters  
 NAME 1\lncpeptide2  
 EXPNO 21  
 PROCNO 1

F2 - Acquisition Parameters  
 Date\_ 20020525  
 Time 3.13  
 INSTNUM spect  
 PROBHD 5 mm Multinu  
 PULPROG zgpg30  
 TD 65536  
 SOLVENT MeOH  
 NS 5000  
 DS 4  
 SMH 25125.629 Hz  
 FIDRES 0.383387 Hz  
 AQ 1.3042164 sec  
 RG 16394  
 DW 19.900 usec  
 DE 6.00 usec  
 TE 300.0 K  
 D1 2.00000000 sec  
 d11 0.03000000 sec  
 d12 0.00002000 sec

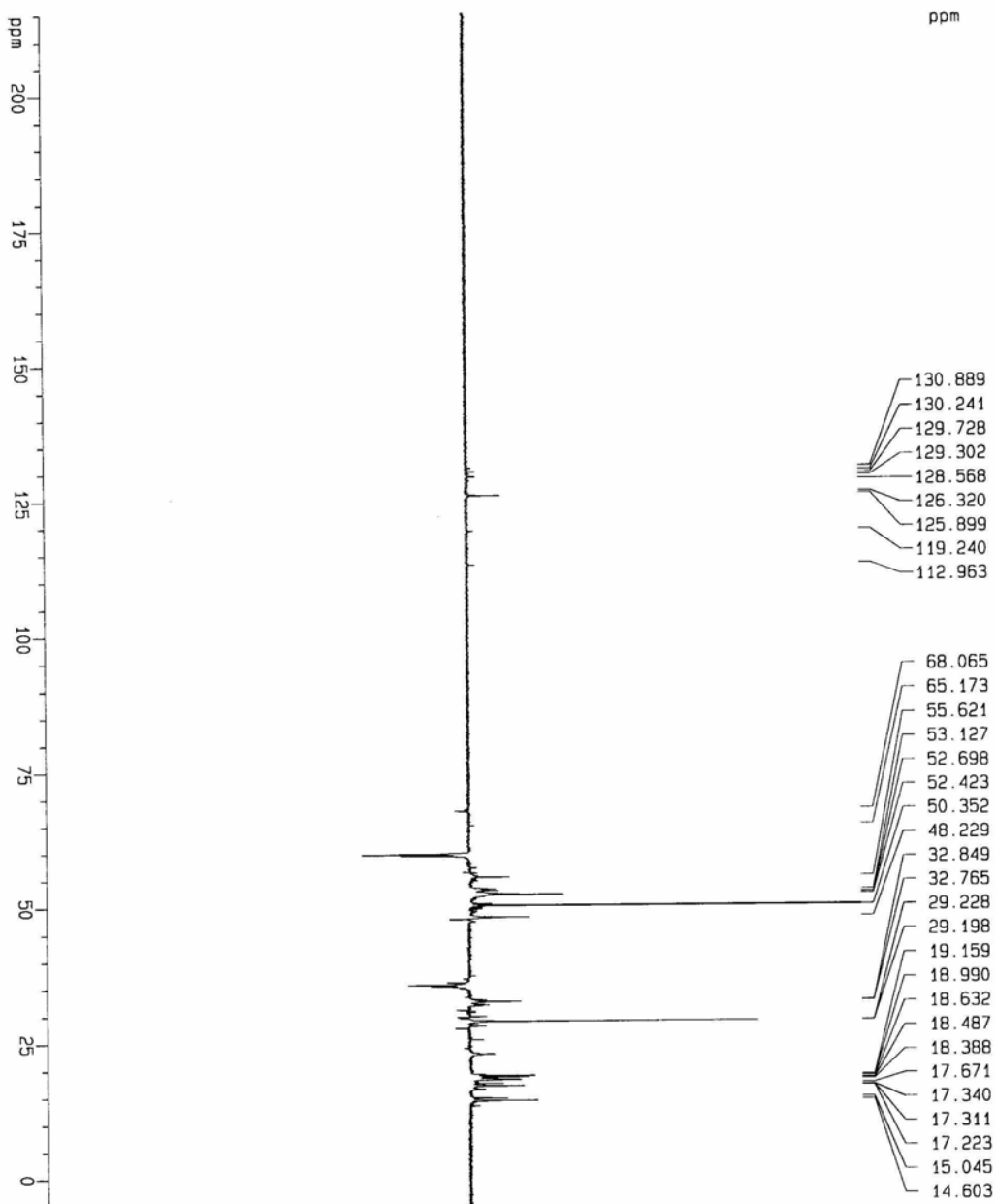
\*\*\*\*\* CHANNEL f1 \*\*\*\*\*  
 NUC1 13C  
 P1 8.70 usec  
 PL1 0.00 dB  
 SF01 100.6237959 MHz

\*\*\*\*\* CHANNEL f2 \*\*\*\*\*  
 CPDPRG2 waltz16  
 NUC2 1H  
 PCPD2 107.00 usec  
 PL2 0.00 dB  
 PL12 23.00 dB  
 PL13 23.00 dB  
 SF02 400.1316005 MHz

F2 - Processing parameters  
 SI 32768  
 SF 100.6125861 MHz  
 MDM EM  
 SSB 0  
 LB 1.00 Hz  
 GB 0  
 PC 1.40

1D NMR plot parameters  
 CX 20.00 cm  
 F1P 215.000 ppm  
 F1 21631.71 Hz  
 F2P -5.000 ppm  
 F2 -503.06 Hz  
 PPMCK 11.00000 ppm/cm  
 HZCK 1106.73940 Hz/cm

Linear Peptide -tboc 2



```

Current Data Parameters
NAME          1linear.tboc2
EXPNO         22
PROCNO        1

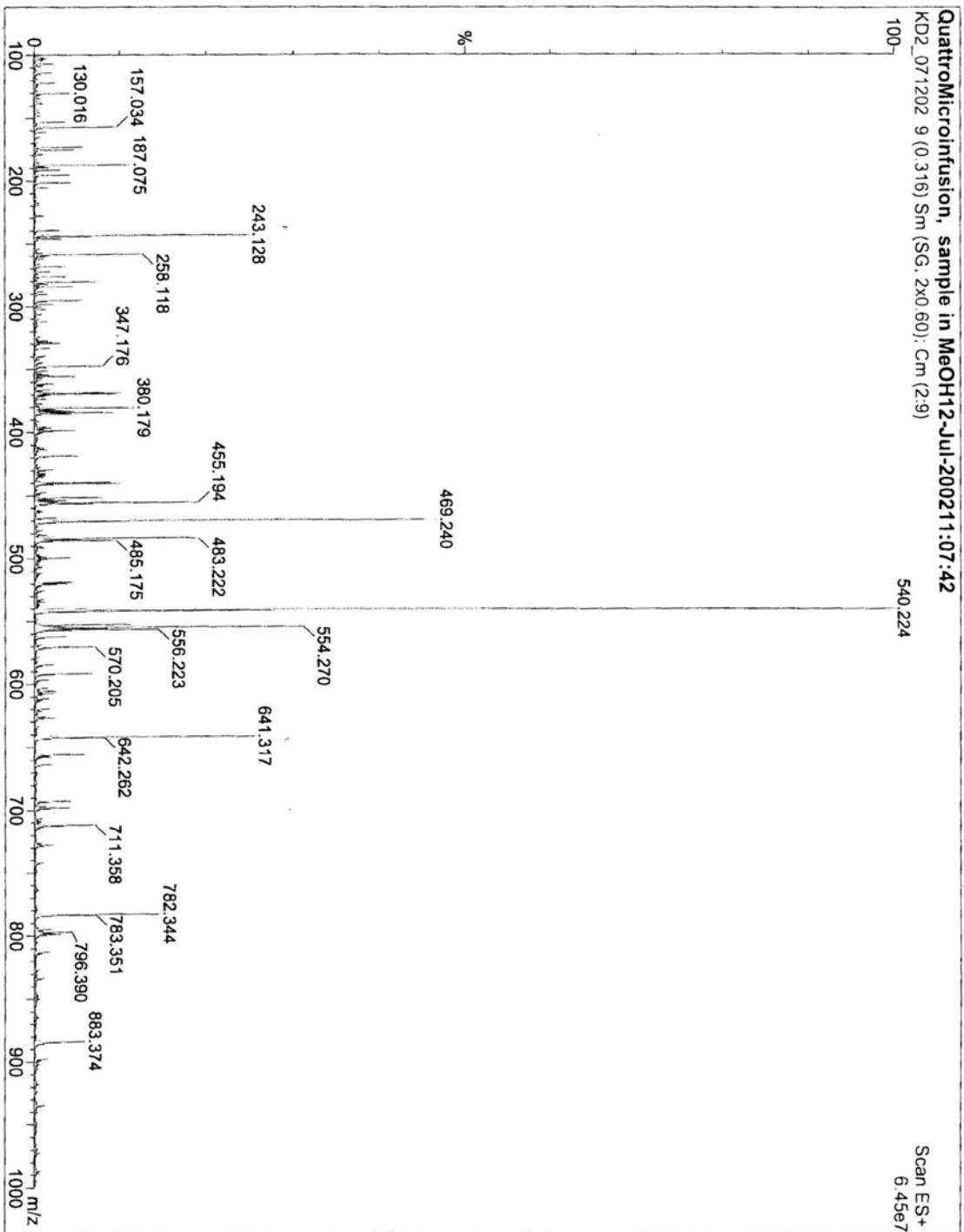
F2 - Acquisition Parameters
Date_         20020505
Time          7.57
INSTRUM      spect
PROBHD       5 mm Multinu
PULPROG      zgpg30
TD            65536
SOLVENT      MeOH
NS            5000
DS            4
SMH           23980.814 Hz
FIDRES       0.365918 Hz
AQ           1.3664756 sec
RG           2580.3
DM           20.850 usec
DE           6.00 usec
TE           300.0 K
DENSITY      145.0000000
D1           2.00000000 sec
d2           0.00344828 sec
d12         0.00002000 sec
DELTA       6386.1826119 sec

***** CHANNEL f1 *****
NUC1         13C
P1           8.70 usec
P2           17.40 usec
PL1          0.00 dB
SF01         100.627898 MHz

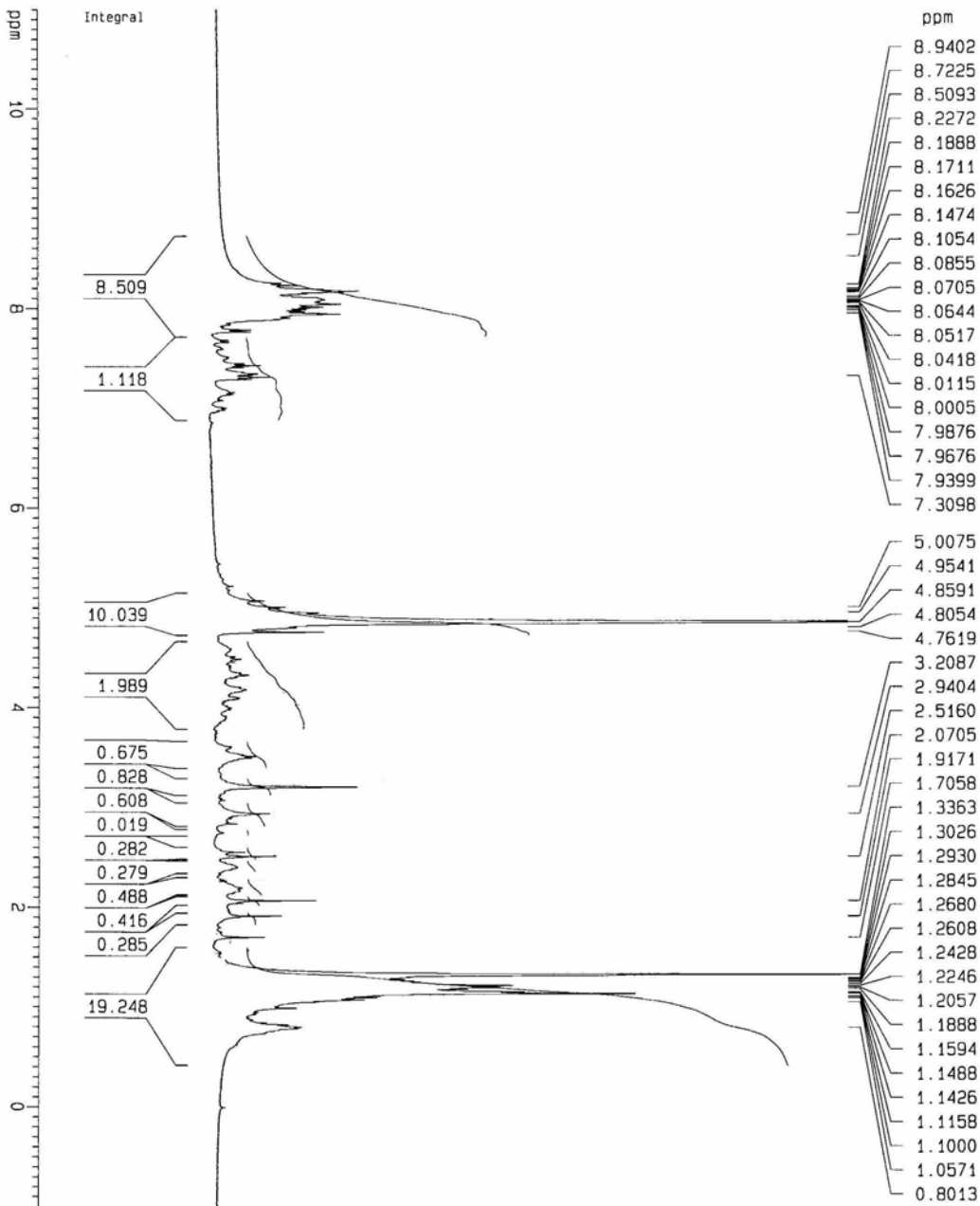
***** CHANNEL f2 *****
CPDPRG2      waltz16
NUC2         1H
P3           8.70 usec
P4           17.40 usec
PCPD2        107.00 usec
PL2          0.00 dB
PL12         23.00 dB
SF02         400.1316005 MHz

F2 - Processing parameters
SI           32768
SF           100.6125861 MHz
KCH          EM
SSB          0
LB           1.00 Hz
GB           0
PC           1.40

1D NMR plot parameters
CX           20.00 cm
F1P         215.000 ppm
F1          21631.71 Hz
F2P         -5.000 ppm
F2          -503.06 Hz
PPMCH       11.00000 ppm/cm
HZCM        1106.73840 Hz/cm
    
```



Linear peptide - lboc- py 1



Current Data Parameters  
 NAME 1  
 EXPNO 20  
 PROCNO 1

F2 - Acquisition Parameters  
 Date\_ 20020514  
 Time 19.47

INSTRUM spect  
 PROBRD 5 mm Multinu  
 PULPROG zg30  
 TD 32768  
 SOLVENT MeOH  
 NS 16  
 DS 2  
 SMH 8278.146 Hz  
 FIDRES 0.252629 Hz  
 AQ 1.9792372 sec  
 RG 161.3  
 DM 60.400 usec  
 DE 5.00 usec  
 TE 300.0 K  
 D1 1.00000000 sec

==== CHANNEL f1 =====  
 NUC1 1H  
 P1 8.75 usec  
 PL1 0.00 dB  
 SF01 400.1324710 MHz

F2 - Processing parameters  
 SI 32768  
 SF 400.1300487 MHz  
 WDM EM  
 SSS 0  
 LB 0.30 Hz  
 GB 0  
 PC 1.00

1D NMR plot parameters  
 CX 20.00 cm  
 F1P 11.000 ppm  
 F1 4401.43 Hz  
 F2P -1.000 ppm  
 F2 -400.13 Hz  
 PPMCM 0.50000 ppm/cm  
 HZCM 240.07802 Hz/cm

## References

---

- <sup>1</sup> Yoshida, Katsuhira; Mori, Takayoshi; Watanabe, Shigeru; Kawai, Hideki; Nagamura, Toshihiko. *J. Chem. Soc., Perkin Trans. 2* **1999**, 393.
- <sup>2</sup> Shih, Ying-Tai; Huang, Hsuan-Jung. *Analy. Chim. Acta.* **1999**, 392, 143.
- <sup>3</sup> Bissell, Richard A.; de Silva, A. Prasnanna; Gunaratne, H. Q. Nimal; Lynch, P.L. Mark; Maguire, Glenn E. M.; *Chem. Soc. Rev.* **1992**, 187.
- <sup>4</sup> Bissell, Richard A.; Calle, Emilio; de Silva, A. Prasanna; et al. *J. Chem. Soc. Perk.* **1992**, 2, 1559.
- <sup>5</sup> Kubo, Kanji; Kato, Nobuo; Sakurai, Tadimitsu; *Bull Chem.. Soc. of Japan.* **1997**, 70, 3041.
- <sup>6</sup> Kubo, Kanji; Ishige, Ryoichi; Kato, Nobuo; Yamamoto, Emi; Sakurai, Tadimitsu; *Heterocycles.* **1997**, 45, 12, 2365.
- <sup>7</sup> Ji, Hai-Feng; Dabestani, Reza; Brown, Gilbert M.; Hettich, Robert L. *Photochemistry and Photobiology.* **1999**, 69, 5, 513.
- <sup>8</sup> de Silva, A.P.; de Silva, S.A. *J. Chem. Soc., Chem Commun.* **1989**, 1183.
- <sup>9</sup> de Silva, A. Prasnanna; de Silva, Saliya A.; *J. Chem. Soc. Chem. Commun.* **1986**, 1709.
- <sup>10</sup> Kubo, Kanji; Ishige, Ryoichi; Kubo, Junko; Sakurai, Tadimitsu. *Talanta* **1999**, 48, 181.
- <sup>11</sup> A. Casnati, A. Pochini, R. Ungaro, C. Bocchi, F. Ugozzoli, R. J. M. Egberink, H. Struijk, R. Lugtenberg, F. de Jong and D. N. Reinhoudt, *Chem. Eur. J.* **1996**, 2, 436.
- <sup>12</sup> A. Casnati, A. Pochini, R. Ungaro, F. Ugozzoli, F. Arnaud, S. Fanni, M.-J. Schwing, R. J. M. Egberink, F. de Jong and D. N. Reinhoudt, *J. Am. Chem. Soc.* **1995**, 117, 2767.
- <sup>13</sup> H.-F. Ji, R. Dabestani, G. M. Brown and R. L. Hettich, *J. Chem. Soc. Perkin Trans.* **2001**, 2, 585.
- <sup>14</sup> H.-F. Ji, R. Dabestani, G. M. Brown and R. L. Hettich, *Photochem. Photobiol.* **1999**, 69, 513.
- <sup>15</sup> H.-F. Ji, G. M. Brown and R. Dabestani, *Chem. Commun.* **1999**, 609.
- <sup>16</sup> H.-F. Ji, R. Dabestani, G. M. Brown and R. A. Sachleben, *Chem. Commun.* **2000**, 833.
- <sup>17</sup> H.-F. Ji, R. Dabestani, R. L. Hettich and G. M. Brown, *Photochem. Photobiol.* **1999**, 70, 882.

- 
- <sup>18</sup> H.-F. Ji, R. Dabestani and G. M. Brown, *J. Am. Chem. Soc.* **2000**, 122 , 9306.
- <sup>19</sup> J. S. Kim, W. K. Lee, K. No, Z. Asfari and J. Vicens, *Tet. Lett.* **2000**, 41, 3345
- <sup>20</sup> J. S. Kim, O. J. Shon, J. W. Ko, M. H. Cho, I. Y. Yu, J. Vicens, *J. Org. Chem.* **2000**, 65, 2386.
- <sup>21</sup> J. S. Kim, O. J. Shon, W. Sim, S. K. Kim, M. H. Cho, J.-G. Kim, I.-H. Suh and D. W. Kim, *J. Chem. Soc. Perkin Trans.* **2001**, 1, 31.
- <sup>22</sup> K. Kubo, R. Ishige, N. Kato, E. Yamamoto and T. Sakurai, *Heterocycles.* **1997**, 45, 2365.
- <sup>23</sup> K. Yoshida, T. Mori, S. Watanabe, H. Kawai and T. Nagamura, *J. Chem. Soc. Perkin Trans.* **1999**, 2, 393.
- <sup>24</sup> J.S. Kim, I. Y. Yu, J. H. Pang, J. K. Kim, K. W. Lee, and W. Z. Oh, *Microchem. J.* **1998**, 58, 225.
- <sup>25</sup> Pederson, C. J.; Lehn, J. M.; Cram, D. J. *Resonance* . **2001**, 6, 6, 71.
- <sup>26</sup> Kremer, L.N.; Spicer, L.D. *J. Am. Chem. Soc.* **1975**, 97, 17, 5022.
- <sup>27</sup> Dietrich, Bernard; Kintzinger, Jean-Pierre; Lehn, Jean-Marie; Metz, Bernard; Zahidi, Assou. *J. Phys. Chem.* **1987**, 91, 6600.
- <sup>28</sup> Krakowiak, K.E.; Bradshaw, J.S. *J. Org. Chem.* **1995**, 60, 7070.
- <sup>29</sup> Graf, E.; Kintzinger, J.P.; Lehn, J.M.; LeMoigne, J. *J. Am. Chem. Soc.* **1982**, 104, 1672.
- <sup>30</sup> Jon, Sang Yong; Kim, Jeongho; Kim, Sang-Hyun Park; Jeon, Woo Sung; Heo, Jeongsuk; Kim, Kimoon. *Angew. Chem. Int. Ed.* **2001** 40, 11, 2116.
- <sup>31</sup> Draxler, Sonja; Lippitsch, Max E.. *Applied Optics.* **1996**, 35, 21, 4117-4123.
- <sup>32</sup> Suzuki, K.; Siswanta, D.; Otsuka, T.; Amano, T.; Ikeda, T.; Hisamoto, H.; Yoshihara, R.; Ohba, S. *Anal. Chem.* **2000**, 72, 2200.
- <sup>33</sup> Furlan, Ricardo L. E; Ng, Yiu-Fai; Cousins, Graham R. L.; Redman, James E.; Sanders, Jeremy K.M.. *Tetrahedron* .**2002**, 58, 771.
- <sup>34</sup> Zanotti, G.C.; Campbell, B.E.; Easwaran, K.R.K.; Blout, E.R. *Int. J. Peptide Protein Res.* **1988**, 32, 527.
- <sup>35</sup> Zanotti, G.C.; Paolillo, L.; Barbato, G.; Fraternali, F.; D'Alagni, M. *Peptides.* **1990**, 499.

- 
- <sup>36</sup> Cursi, E.; Giralt, E.; Andreu, D. *Peptide Res.* **1995**, 8, 62.
- <sup>37</sup> Benco, John S.; Nienaber, Hubert A.; McGimpsey, W. Grant. *Anal. Chem.* **2002**, *under review*.
- <sup>38</sup> Benco, John S.; Nienaber, Hubert A.; Dennen, Katherine; McGimpsey, W. Grant. *J. Photochem. & Photobio. A: Chemistry.* **2002**, 6098, 1.
- <sup>39</sup> Petrov, N. Kh.; Kuhnle, W.; Fiebig, T.; Staerk, H.; *J. Phys Chem. A.* **1997**, 101, 7043.
- <sup>40</sup> Dabestani, Reza; Ellis, Keith J.; Sigman, Micheal E.; *J. of Photochem. and Photobio.. A: Chemistry.* **1995**, 86, 231.
- <sup>41</sup> Reyes, Celso A.; Medina, Myriam; Crespo, Carlos; et. al.; *Environ. Sci. Technol.* **2000**, 34, 415.
- <sup>42</sup> Sigman, Micheal E.; Schuler, Peter F.; Ghosh, Mriganka M.; Dabestani, Reza; *Environ. Sci. Technol.* **1998**, 32, 3980.
- <sup>43</sup> Murov, Steven L.; Carmichael, Ian; Hug, Gordon L.; Handbook of Photochemistry. Second ed. New York. Marcel Dekker, Inc. p. 6, 270, 271
- <sup>44</sup> E. Bakker, P. Bühlmann, and E. Pretsch, *Chem. Rev.* **1997**, 97, 3083.
- <sup>45</sup> Benco, H. A. Nienaber, W. Grant McGimpsey, *Sensors and Actuators B.* **2002**, *In Press*.
- <sup>46</sup> (Autorencollectiv) Organikum; 16. Auflage; VEB Deutscher Verlag der Wissenschaften Berlin, **1986**, 559.
- <sup>47</sup> P.J. Dijkstra, J.A., Brunink, K.E. Bugge, D.N. Reinhoudt, S. Harkema, R. Ungaro, F. Ugozzoli, E. Ghidini, *J. Am. Chem. Soc.* **1989**, 111, 7567.
- <sup>48</sup> E. Ghidini, F. Ugozzoli, R. Ungaro, S. Harkema, A.A. El-Fadl, D.N. Reinhoudt, *J. Am. Chem. Soc.* **1990**, 112, 6979.
- <sup>49</sup> W.F. Nijenhuis, E.G. Buitenhuis, F. de Jong, E.J.R. Sudholter, D.N. Reinhoudt, *J. Am. Chem. Soc.* **1991**, 113, 7963.
- <sup>50</sup> Z. Brzozka, B. Lammerink, D.N. Reinhoudt, E. Ghidini, R. Ungaro, *J. Chem. Soc. Perkin Trans. 2.* **1993**, 1037.
- <sup>51</sup> Yang, Chuluo; Wong, Yiu Tung; li, Zaoying; Krepinsky, Jiri J.; Jia, Guochen. *Organometallics.* **2001**, 20, 5220.

---

<sup>52</sup> NovaBiochem Catalog and Handbook. **1999**, p. S 44.

<sup>53</sup> Blanchette, Mary; Baker, Mary Lou; Guindon, Cathy A.; *Tet. Lett.* **1989**, 30, 21, 2739.

<sup>54</sup> Pickersgill, Fraser I.; Rapoport, Henry; *J. Org. Chem.* **2000**, 65, 4048.